

University of South Florida

NASA Student Launch
Centennial Challenge MAV Project

Critical Design Review

15 January 2016



Society of Aeronautics and Rocketry

15219 Plantation Oaks Drive, Apt 4.
Tampa, FL, 33647

Table of Contents

Table of Contents

1) Summary of CDR Report

1.1 Team Summary

1.2 Launch Vehicle Summary

2) Changes Made Since PDR

2.1 Vehicle Criteria

2.2 AGSE Criteria

3) Launch Vehicle Criteria

3.1 Design and Verification of Launch Vehicle

3.1.1 Applicable Calculations

3.1.1a Center of Pressure

3.1.1b Airflow Considerations

3.1.1c Center of Gravity

3.1.1d Drag

3.1.1e Thrust

3.1.1.f Kinematics

3.1.2 Stability

3.1.3 Fabrication

3.1.3a Motor Mount: Centering Rings

3.1.3b Motor Mount: Fins

3.1.3c Motor Mount: Eye Bolts and Motor Retainer

3.1.3d Route the Aft Tube Fin Slots

3.1.3e Altimeter Bay

3.1.3f Altimeter Bay Integration

3.1.3g Payload Bay

3.1.3h Nose cone

3.1.3i Rail Buttons

3.2 Subsystems

3.2.1 Nosecone

3.2.2 Payload Bay

3.2.3 Motor

3.2.4 Fins

3.2.5 Propulsion Bay/ Fin Can

3.2.6 Motor Retention

3.2.7 Altimeter and Electronics Bay

3.3 Recovery

3.3.1 Design Overview

3.3.2 Parachute Sizing and Selection

3.3.3 Bulkheads and Connective Elements

- 3.3.4 Altimeter Wiring
 - 3.3.5 Kinetic Energy and Descent Velocities
 - 3.3.6 Drift Calculations
 - 3.4 Mission Performance Predictions
 - 3.4.1 Performance Criteria
 - 3.4.2 Launch Vehicle Characteristics
 - 3.4.3 Motor Selection
 - 3.4.4 OpenRocket Simulations
 - 3.4.5 Mass Statement
 - 3.4.6 Launch Requirements and Solutions
 - 3.5 Interfaces and Integration
 - 3.5.1 Payload Bay System
 - 3.6 Subscale Flight Verification and Results
 - 3.6.1 Testing Plan
 - 3.6.2 Launch Vehicle Characteristics
 - 3.6.3 Simulations
 - 3.6.4 Testing Report and Post Flight Review
 - 3.7 Safety
 - 3.7.1 Safety Officer Responsibilities
 - 3.7.2 Team Safety Procedures
 - 3.7.3 Launch Procedures
- 4) AGSE/Payload Criteria
- 4.1 Systems Overview
 - 4.1.1 System Timeline
 - 4.2 Payload Capture and Containment
 - 4.2.1 Overview
 - 4.2.2 Design
 - 4.2.2a Base Structure
 - 4.2.2b Shoulder Joint (2nd Degree of freedom)
 - 4.2.2c Elbow Joint (3rd Degree of freedom)
 - 4.2.2d Wrist Joint (4th & 5th Degree of freedom)
 - 4.2.2e Gripper Assembly
 - 4.2.2g Wheel
 - 4.2.2h Suspension System
 - 4.2.2i Body
 - 4.2.2j Environmental Concerns
 - 4.2.3 Fabrication
 - 4.2.4 Mechanics of Solids
 - 4.2.4a Material Properties
 - 4.2.4b Mechanical Torque
 - 4.2.5 Arm Modeling and Schematics
 - 4.2.5a Base Structure
 - 4.2.5b Shoulder to Elbow

- 4.2.5c Elbow to Wrist
- 4.2.5d Gripper Assembly
- 4.2.5e Completed Robotic Arm
- 4.2.7 Challenges and Verification Plan
 - 4.2.7a Challenges
 - 4.2.7b Verification Plan
- 4.2.8 Payload Containment
- 4.2.9 Payload Modeling
- 4.3 Launch Platform
 - 4.3.1 Vehicle Erection System Overview
 - 4.3.2 Design of Vehicle Erection System Components
 - 4.3.2.a Worm Gear Set and Motor Selection
 - 4.3.3 Ignition Station
 - 4.3.4 Fabrication
- 4.7 Electronics Systems
 - 4.7.1 Overview
 - 4.7.2 Components
 - 4.7.2.a Raspberry Pi and Accompanying Software
 - 4.7.2.b Master PC and Computer Vision
 - 4.7.2.c Subsystem Communication
 - 4.7.2.d Rover Controls and Navigation
 - 4.7.3 Challenges and Verification Plan
 - 4.7.4 Schematics
- 5) Project Plan
 - 5.1 Budget Plan
 - 5.2 Funding Plan
 - 5.3 Timeline
 - 5.4 Educational Engagement
- 6) Conclusion
- 7) Appendix I – Risk Assessment

1) Summary of CDR Report

1.1 Team Summary

Institution: *The University of South Florida*

Organization: *USF Society of Aeronautics and Rocketry (SOAR)*

Location: 15219 Plantation Oaks Drive, Apt 4.
Tampa, FL, 33647

Mentor: Rick Waters

Launch Certification: Level 3 Certified TRA #: 8543

1.2 Launch Vehicle Summary

The launch system was designed and built in order to meet every requirement specified by the competition committee. A variety of factors including overall cost, weight, performance, fabrication and testing were considered when planning and constructing the launch vehicle and the ground support counterpart. In order to ensure mission success and launch safety strict procedures were maintained throughout the duration of the fabrication and testing stages. The vehicle and launch system were manufactured using materials that were readily available to the organization. The launch vehicle will be fabricated using materials such as G-12 and G-10 fiberglass, kraft phenolic tubing, polystyrene PS and a variety of other manufacturing materials. A brief vehicle overview can be seen in table 1.2.1 listed below.

Table 1.2.1 List of launch vehicle attributions

Vehicle Overall Mass (lbs)	22.82
Vehicle Length (in)	138.6
Vehicle Diameter (in)	4.00
Recovery System	Dual deployment (RRC3 altimeter)
Vehicle Motor Selected	CS L910s

2) Changes Made Since PDR

2.1 Vehicle Criteria

Throughout the course of the past few months and through the development of our subscale rocket we have determined several important changes to our launch vehicle in order to ensure a successful launch. The changes made since the PDR are as follows:

- The overall lengths of the airframes have been adjusted to reflect, 48 inches each for the fore and aft, as well as 24 inches for the payload. The extended fore airframe will allow more room for our selected parachute while the expanded payload bay will comfortably fit our payload containment system for the AGSE competition as well as an electronics bay.
- Our motor choice has changed from the L1112 to the Cesaroni L910. We found that in regards to our fiberglass airframe OpenRocket was not giving us an accurate measurement for mass, upon confirming all masses we have recalculated to determine that the L910 is the best motor to help us reach our target altitude.
- Our altimeter bay was been significantly extended to 16 inches to allow us more room to work with the involved electronics without fear of wires contacting by accident or the space ultimately being too small.
- We have selected the large Cert-3 parachute for our main parachute and have confirmed it fits in our 4" rocket diameter and have designed to allow it at least the minimum 17" length required.
- Our fin shape has been slightly modified to account for our new motor in regards to key specifications and the 1/8" thickness, bearing in mind issues due to fin flutter.
- Our payload bay has been modified to hold a linear actuator and power systems for expansion. It is subdivided into two sections, as well as a third section to host additional electronics such as our incorporated TeleGPS.

2.2 AGSE Criteria

The changes made to the AGSE system since the Preliminary Design Review were largely arrived at by two separate avenues, the first being optimization and refinement of the existing design, while the next was resolving compatibility issues that arose in the process of design finalization. The design in its current state is nearing the polished standard expected of competitors in the NASA Student Launch Initiative, however our team will certainly continue to face and overcome obstacles.

Over the course of the past several months the design for our AGSE has matured significantly, from concept to it's current design. To reach this point of satisfaction we had to research and model the systems and subsystems we sought to integrate. We had refine the material design of the rover body to align the center of mass at the differential gear box, performing torque calculations as functions of the varying position of the arm. Refinements were also made to the suspension system of the rover, progressing from what would have been a relatively less efficient model to a sleek, aesthetically pleasing and functionally improved design for the Rocker-Bogie system. This redesign centered mostly on the joint between the Rocker and the Bogie. The original model had the Rocker encompassing the Bogie at the joint, severely restricting the possible angles of incline. However, the current design allows for unrestricted angular motion, while maintaining the structural integrity of the previous model. Additionally, the desired dimensions on the arm increased relative to our initial estimations, while many of the rover dimensions shrank, reflecting the critical need to interact with the robot's environment, rather than fabricating an unnecessarily large rover platform.

Compatibility issues between design components attempted to be minimized through foresight of future issues and coordination between research efforts, however features our design still managed to be incompatible with the vision of our team. Take the servos intended for directional control of the rover as an example. In an ambitious attempt to model the NASA exploration rovers, we intended, in our preliminary design, to have the outer four wheel hubs of the rover attached to servos whose torque would change the trajectory. The deciding factor came in our software architecture, while we could implement independent libraries for control of these servos, their use did not align with the overarching goal of using a Robot Operating System (ROS) network. The ROS network simplifies greatly the setup of a robotic system, providing many prepackaged kernels used in the development of such a system, however the directional servos proved currently incompatible with the ROS local navigation stack. In a cost/benefit analysis of system simplicity and elegance, we decided to forgo the servos to retain the ROS network. The rover system will now implement the differential drive algorithms provided by ROS.

Compatibility issues also arose from the previous design for electrical integration of the embedded microcontroller, the Raspberry Pi. Several revisions to the electrical systems had to be made to reach the state at which we currently stand. The lack of PWM GPIO pins on the Raspberry Pi, led to the inevitable implementation of the Adafruit Servo Driving Board. The demand for the odometry information by the ROS network, for robot localization in the global mapping, required motors with encoder feedback, which in turn increased the demand for the quantity of GPIO pins on the Raspberry Pi. This was mitigated by the addition of an integrated circuit for expanding the number of GPIO pins on a Raspberry Pi by sacrificing the SPI pins to the IC.

3) Launch Vehicle Criteria

3.1 Design and Verification of Launch Vehicle



Figure 3.1.1: Model of Completed Rocket in Solidworks

While designing the launch vehicle the team focused largely on system reliability and structural simplicity. Previous competition experiences proved that simplicity often triumphed over complexity. The team integrated several structural features that proved successful from previous launch vehicles into the present vehicle design. This will be the first year that *USF SOAR* is competing in the NSL so many entirely new designs as well as modifications to pre-existing designs were made in order to maximize overall mission success. In order to generate a feasible vehicle design the team performed calculations using several of the equations listed in section 3.1.1 in order to output fundamental vehicle measurement requirements. These measurements were applied to simulators such as Open Rocket and Rocksim and the resulting data was analyzed.

The launch vehicle itself will be composed up of a fiberglass airframe and fins, a mechanized containment bay (to house the payload) and a dual deployment recovery system. The team chose to use a dual deployment recovery system as the recovery system method because of the system's reliability and increased safety. As a redundancy, two altimeters will be integrated into the launch vehicle system in order to ensure vehicle and observer safety. Each section will be joined together by kraft phenolic tube couplers. All static sections of the launch vehicle will be joined together using a thirty minute epoxy adhesive or plastic rivet fasteners.

During the launch vehicle's flight, several criteria points must be met in order for the launch to be considered successful:

1. The launch vehicle achieves apogee between 5,000 and 5,400 feet.
2. At apogee, the drogue parachute is successfully ejected.
3. Between 500 and 600 feet AGL, the nosecone and payload bay are separated from the rest of the vehicle, and the main parachute and payload parachutes are successfully ejected.
4. No portion of the vehicle or payload sustains any major damage during flight or landing.

3.1.1 Applicable Calculations

“The most important characteristic of a model rocket is its stability” - James and Judith Barrowman, 1966

The Barrowmans submitted a document in 1966, and another in 1967, that laid a firm foundation for the calculations of rocket stability, through the relative positions of the Center of Gravity (C_g) and the Center of Pressure (C_p).

3.1.1a Center of Pressure

A model rocket will fly straight into the oncoming airflow, however when there is an imbalance in the forces acting on the rocket the vehicle will have translational motion, similarly an imbalance in the torques, or moments, will cause rotational motion. Given a thrust misalignment, a fin incorrectly placed or a gust of wind, the rocket may tilt from its original orientation. In this event the vehicle will fly at a new angle, changing the aerodynamics of its path. The angle of attack, α , is the angle between the centerline of the launch vehicle and the vertical component of its velocity.

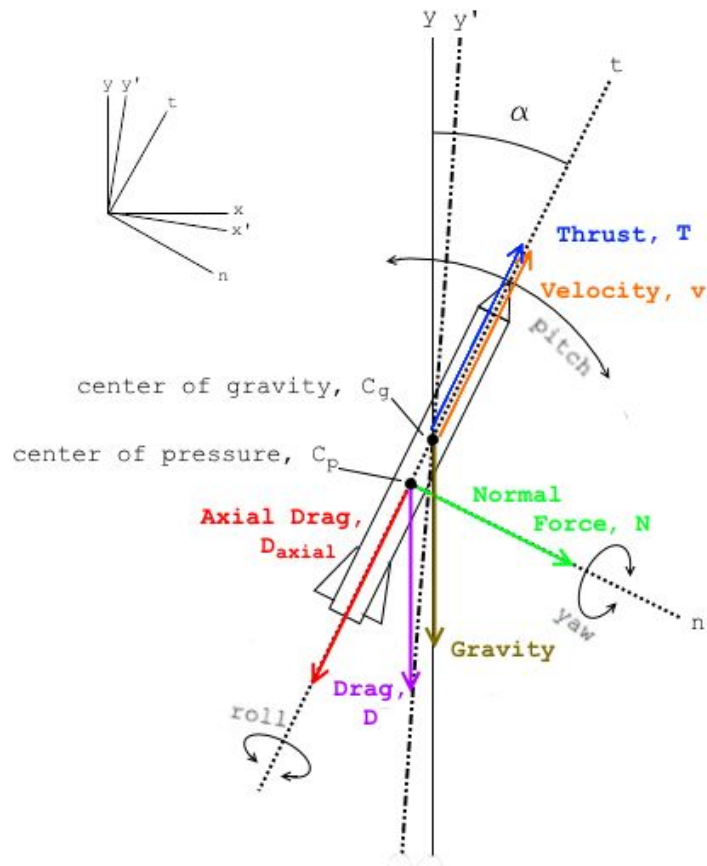


Figure 3.1.1a. 1: Rocket force diagram.

A stable rocket is one which continuously corrects its course to return to $\alpha = 0$ (zero). If the angle of attack increases too much, the C_p will move upwards and potentially overtake the C_g , which will negate the corrective motions of the stable rocket, thus making the rocket unstable.

Each component of the rocket has its own normal forces acting perpendicular the the surface; however, they can be summed up and expressed as acting through the center of pressure, C_p . If the C_p is located one to two calibers (max body diameters) aft of the center of gravity, C_g , the rocket will act to correct its trajectory by producing a moment. The stability margin is the distance between the C_p and C_g in calibers.

The center of pressure, C_p , is the point on the body where the normal force is the only force that produces a pitching moment. It is the point where there is as much normal force ahead as behind; a balancing point separate from the center of gravity. In order to develop the equation for C_p , we must first consider the relevant coefficients. Our plan of derivation:

1. Find Normal Force Coefficient
2. Identify Pitching Moment Coefficient
3. Moving Pitching Moment Coefficient
4. Set to 0 (zero) to find Center of Pressure location, x
5. Use l'Hopital to find Center of Pressure (Barrowman's Method)

The normal force for an axially symmetric body in subsonic flow:

$$N(x) = \rho v_0 \frac{\partial}{\partial x} [A(x)w(x)]$$

Where,

$A(x)$:= cross-sectional area of the body

$w(x)$:= local downwash

ρ := density

v_0 := free airstream velocity

$w(x)$ as a function of α :

$$w(\alpha) = v_0 \sin(\alpha)$$

The normal force $N(x)$ at position x produces a pitching moment at the nose tip:

$$m_{pitch}(x) = xN(x)$$

1. The normal coefficient C_N :

$$C_N(x) = \frac{N(x)}{.5\rho V_0^2 A_{reference}} = \frac{2\sin(\alpha)}{A_{reference}} \frac{dA(x)}{dx}$$

$$C_N = \frac{N}{.5\rho V_0^2 A_{reference}} = \frac{2\sin(\alpha)}{A_{reference}} \int_0^l \frac{dA(x)}{dx} dx = \frac{2\sin(\alpha)}{A_{reference}} [A(l) - A(0)]$$

Where,

l := length of rocket

$A_{reference}$:= area of base of the nose cone

2. Pitch moment coefficient C_m :

$$C_m(x) = \frac{m_{pitch}(x)}{.5\rho V_0^2 A_{reference} d} = \frac{xN(x)}{.5\rho V_0^2 A_{reference} d}$$

$$C_m = \frac{2\sin(\alpha)}{A_{reference} d} \int_0^l x \frac{dA(x)}{dx} dx = \frac{2\sin(\alpha)}{A_{reference} d} [lA(l) - \int_0^l A(x) dx]$$

Where,

d := diameter at a specific point

3. How to move the pitch moment coefficient to another point:

$$C_{m\ new} * d = C_m * d - C_N \Delta x$$

Where,

$\Delta x :=$ distance from nosecone along centerline of vehicle

4. Finding location of C_p by setting $C_{m\ new}$ to 0 (zero), and solving for x :

$$\begin{aligned} C_{m\ new} * d &= C_m * d - C_N \Delta x \\ 0 &= C_m * d - C_N \Delta x \\ x &= \frac{C_m * d}{C_N} \end{aligned}$$

Where,

$x :=$ distance of C_p from nosecone tip on centerline

This equation is valid only for when the angle of attack, α , is greater than zero.

$$\lim_{\alpha \rightarrow 0} C_m = 0, \text{ and } \lim_{\alpha \rightarrow 0} C_N = 0$$

5. Using l'Hopital's Rule and Barrowman's Method to simplify finding C_p :

$$x = \frac{\frac{\partial C_m}{\partial \alpha}}{\frac{\partial C_N}{\partial \alpha}} * d |_{\alpha=0} = \frac{C_{ma}}{C_{Na}} * d$$

Barrowman's method is based on normal force coefficients and is only valid in the linear regime. At small α , C_N and C_m can be approximated as linear with α , therefore

	For $\alpha > 0$	For $\alpha = 0$
Normal force coefficient derivative =	$C_{Na} = \frac{C_N}{\alpha}$	$C_{Na} = \frac{\partial C_N}{\partial \alpha} _{\alpha=0}$
Pitch moment coefficient derivative =	$C_{ma} = \frac{C_m}{\alpha}$	$C_{ma} = \frac{\partial C_m}{\partial \alpha} _{\alpha=0}$

The Barrowman Method uses the coefficient derivatives to determine C_p . The first element in applying this methods is to observe that the normal force contribution of a straight, constant diameter body tube is zero. Only the nose, any body diameter transition sections, and fins contribute to the normal force of the rocket. However, the launch vehicle used in the NSLI has no body transition sections, and thus treatment of such is unnecessary. Calculations are performed with the normal force coefficients. All centers of pressure are referenced to datum zero, which is located at the tip of the nose cone.

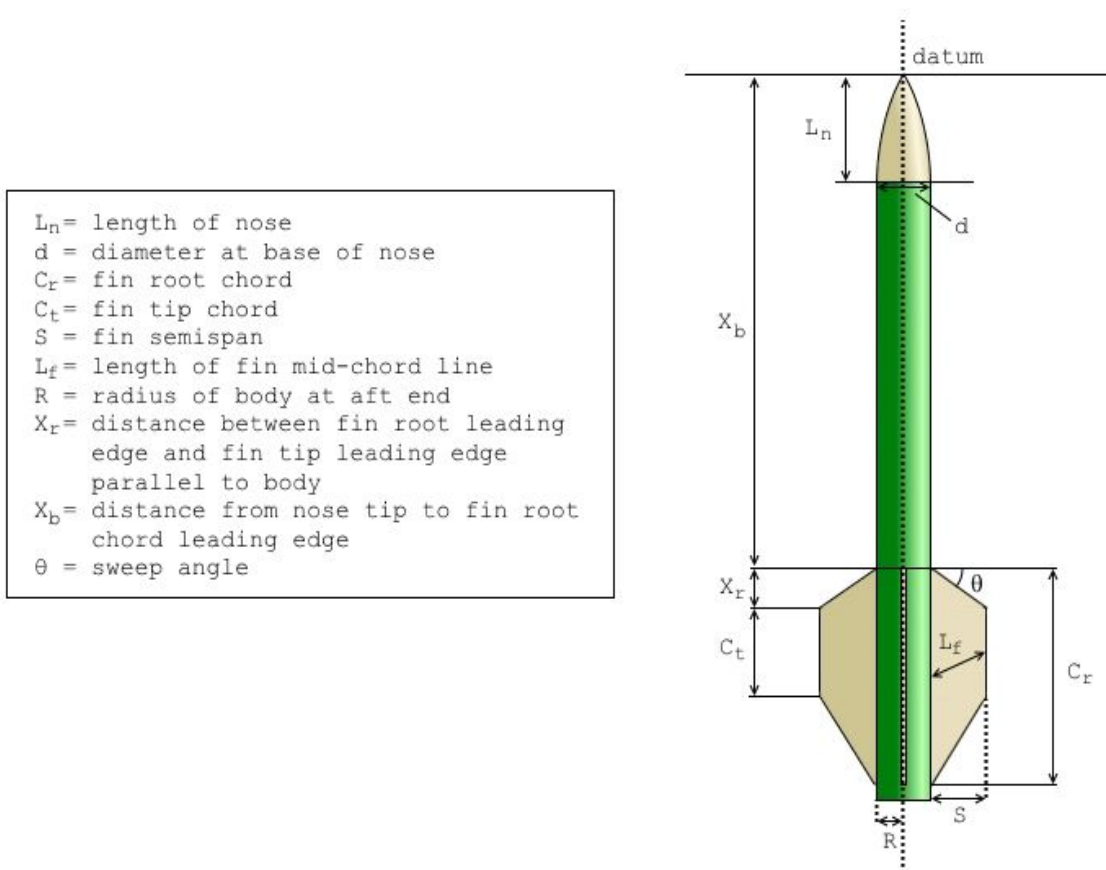


Figure 3.1.1a. 2: Diagram of rocket with legend.

The equations used for calculating the center of pressure of the nose cone depends on the type of curvature the nose cone exhibits. The nose used for this competition has ogive geometry. The shape of an ogive nose cone is formed from a quarter section of a circle with “ogive radius” ρ , like in Figure 4. By rotating the shaded region of the figure about the centerline, the resulting volume of revolution is the nose cone, having a radius of R at its base. The body of the rocket will be tangent to the ogive shape at its base. The distance from the tip of the nose to the center of pressure is X_n . The radius of the nose’s base, the ogive radius, and the length L_n of the nose are related in the following way:

$$\rho = \frac{R^2 + L_n^2}{2R}.$$

L_n must be less than or equal to ρ . When the two are equal, the nose is a hemisphere. The Barrowmans calculated that the normal force coefficient acting on the center of pressure of the nose is the same, regardless of its shape. So $(C_{Na})_n = 2$.

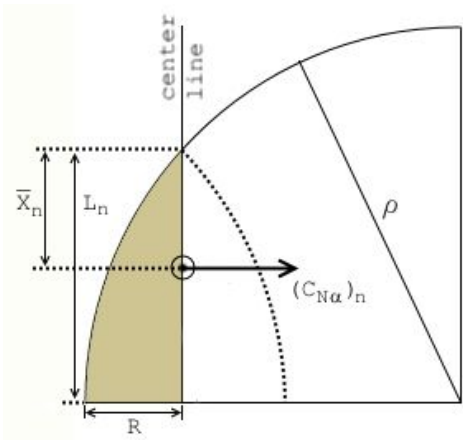


Figure 3.1.1a.3: Geometry of an ogive nose cone, including location of center of pressure.

The location of the center of pressure, however, depends greatly on the shape of the nose itself. One can calculate the location of the center of pressure of an ogive nose cone by dividing the volume of the nose itself by the area at its base, where the volume is given by the following formula:

$$V = \pi [L_n \rho^2 - \frac{L_n^3}{3} - (\rho - R)\rho^2 \arcsin(\frac{L_n}{\rho})] .$$

Doing so will yield the distance from the base of the nose to the center of pressure. Subtracting this value from L_n will finally result in X_n , the distance from the tip to the center of pressure. The generic result of this calculation is cited as $0.466L_n$ when $L_n > 6R$.

The normal force coefficient $(C_N)_f$ acting on the center of pressure of the fins is calculated using this formula:

$$(C_N)_f = \left[1 + \frac{R}{S+R} \right] \left[\frac{4N(S_d)^2}{1 + \sqrt{1 + \left(\frac{2L_f}{Cr+C_t} \right)^2}} \right]$$

where the variables involved are the same as those defined in Figure 3, N is the number of fins, and L_f can be calculated using the Pythagorean Theorem:

$$L_f = \sqrt{S^2 + \left(.5C_t - .5C_r + \frac{S}{\tan \theta} \right)^2} .$$

The distance from the tip of the nose cone to the center of pressure of the fins is given by:

$$X_f = X_b + \frac{X_r}{3} \frac{(Cr+2C_t)}{(Cr+C_t)} + \frac{1}{6} \left[(Cr + C_t) - \frac{Cr*C_t}{(Cr+C_t)} \right] .$$

The normal force coefficient acting on the center of pressure of the entire rocket is simply the summation of the normal force coefficients of the nose, transition sections (of which there are none), and the fins:

$$(C_N)_{total} = (C_N)_n + (C_N)_f .$$

The distance from the tip of the nose cone to the center of pressure of the rocket can be calculated in a way which is analogous to the calculation of center of gravity:

$$X = \frac{(C_N)_n * X_n + (C_N)_f * X_f}{(C_N)_{total}} .$$

In order for this center of pressure calculation to be valid, seven criteria must be satisfied:

1. The angle of attack, α , must be less than 10° .
2. The speed of the rocket's flight must be subsonic.
3. The airflow around the body must be smooth and cannot change rapidly.
4. The rocket must be thin compared to its length.
5. The nose of the rocket must come smoothly to a point.
6. The rocket must be an axially symmetric body.
7. The fins must be thin, flat planes.

Our rocket does satisfy these criteria.

3.1.1b Airflow Considerations

The airflow around the body of a rocket can be approximated as acting in layers, or lamina.

These layers each have different velocity. The lamina most adjacent to the surface of the rocket can be said to have zero velocity relative to the rocket and remains with the surface, this lamina is the boundary layer. The boundary layer grows in thickness as the air travels down the length of the launch vehicle. After the boundary layer each new layer has a higher velocity than the last until free stream velocity is reached. This type of orderly airflow is deemed laminar, while disorderly airflow is deemed turbulent.

At some point a transition occurs and the laminae begin to mix. The boundary layer becomes turbulent and grows in thickness rapidly. The skin friction resistance caused by a turbulent boundary layer is much greater than a laminar boundary layer. The point at which the flow becomes turbulent is the point at which there exists a local critical Reynolds number (R_N). The Reynolds number, in our application, denotes a ratio between the inertial (resistant to motion) forces and the viscous (analogous to fluid friction) forces, as such, it is a dimensionless ratio. We shall use the Reynolds number to determine if the airflow is laminar, turbulent, or transitory.

$$R_N = \frac{\text{density} * \text{velocity} * \text{length}}{\text{viscosity}}$$

$$R_{N \text{ critical}} = \frac{V_0 * x}{\mu}$$

Where,

V_0 := free airstream velocity

x := distance along body from nose to tip

μ (mu) := kinematic viscosity of air ($\sim 1.615 * 10^{-4}$ ft²/s)

And,

$$R_{N \text{ critical}} = \sim 500,000$$

Many aerodynamic parameters vary with changing velocity. One important aerodynamic parameter is the Mach number, which is the free airstream velocity divided by the local speed of sound. In subsonic flight all airflow occurs below the speed of sound ($M < 0.8$). At very low Mach numbers we can treat air as an incompressible fluid ($\nabla \cdot V = 0$). The SOAR rocket will be safely under the local speed of sound.

$$Mach = M = \frac{V_{stream}}{s}$$

Where,

V_{stream} := free airstream velocity

s := local speed of sound

Recalling that V is representative of the fluid airflow, and that in our model the air is treated as incompressible, we have then that the density can be treated as constant ($\nabla \rho = 0$) and can be accordingly removed from Euler's continuity equation. Taking note that this simplification is not suited for more complex modelling, particularly with rockets travelling near or above the local speed of sound.

Steady Form Continuity

$$\nabla \cdot \rho V = 0$$

Incompressible Form Continuity

$$\nabla \cdot V = 0$$

Accordingly, Euler's Steady Form momentum equations can also be factored and simplified,

Steady Form, Two Dimensional

$$X - \text{momentum: } \frac{\partial(\rho u^2)}{\partial x} + \frac{\partial(\rho uv)}{\partial y} = - \frac{\partial P}{\partial x} \quad Y - \text{momentum: } \frac{\partial(\rho uv)}{\partial x} + \frac{\partial(\rho v^2)}{\partial y} = - \frac{\partial P}{\partial y}$$

Incompressible Form Continuity

$$X - \text{momentum: } u \frac{\partial(u)}{\partial x} + v \frac{\partial(u)}{\partial y} = - \frac{1}{\rho} \frac{\partial P}{\partial x} \quad Y - \text{momentum: } u \frac{\partial(v)}{\partial x} + v \frac{\partial(v)}{\partial y} = - \frac{1}{\rho} \frac{\partial P}{\partial y}$$

Where, P := Pressure

ρ := Density

u := x-component of velocity

v := y-component of velocity

3.1.1c Center of Gravity

According to Barrowman, we can calculate the Center of Gravity of our vehicle in only five steps,

1. Determine the weight of each individual component.
2. Find the Center of Gravity for each component.
 - a. Cylindrical objects (body tubes, engines, couplers, etc.) have C_g at their midpoints.
 - b. Nosecones have C_g at one-third their total length, from the wide end.
 - c. The parachute, shock cord, and lines have C_g at the middle of their length when packed into the body tube.
3. Measure the distance between the nose tip and the center of gravity of each component.
4. Sum the weights of the individual components to get the total body weight.

$$W_{Body} = \sum_i W_i$$

5. Use the formula: $X_{CgT} = \frac{\sum_i (W_i (X_{Cg})_i)}{W_{Body}}$

Where, X_{CgT} := Location of vehicle's Center of Gravity

$(X_{Cg})_i$:= Distance from datum zero to C_g of the i^{th} component

W_i := Weight of the i^{th} component

3.1.1d Drag

Drag resists the motion of the vehicle relative to the air. At subsonic speeds, drag is produced by skin friction, pressure distribution around the components, or parasitic drag from launch lugs on the rocket. Drag increases proportionally to the angle of attack, α , and has a minima when $\alpha = 0$. It is therefore important to use C_p to calculate the stability margin. Having a large enough margin will keep the rocket self-correcting, reducing drag. However, if the margin is too large, on a windy day the rocket will consistently arc overhead instead of flying vertically. This is termed weather-cocking. To avoid it, the standard is to ensure the stability margin is at least equal and preferably a little larger than the greatest diameter of the rocket, or a caliber. "One caliber stability" means that the C_p is one maximum body diameter behind the C_g .

Drag Equation:

$$D = \frac{1}{2} C_D \rho V_0^2 A_{reference}$$

Drag Coefficient:

$$C_D = \frac{D}{.5 \rho V_0^2 A_{reference}}$$

And,

$$C_{D0} = C_{A0}$$

Where,

$A_{reference}$:= Area of nosecone base

ρ := density

The C_D is used to describe how the shape of the rocket and its angle influence drag. It is a dimensionless quantity and anything that moves in air has a C_D . At $\alpha = 0$, the total drag coefficient (C_D) and axial drag coefficient (C_A) coincide, but at any other angle, they are considered separately. When $C_{D0} = C_{A0}$ it is called Zero Lift Drag Coefficient, and it has several parts. Each rocket component will contribute some drag to the calculation.

- Base Drag, C_{DB} , is only considered in the coasting phase, because at launch the base pressure is equal to the atmospheric, so there is no pressure inequivalence.

$$C_{DB\ booster} = 0$$

$$C_{DB\ coasting} = \frac{0.029}{\sqrt{C_{D\ Nosecone} + C_{D\ Body}}}$$

- Skin friction drag arises from the contact of the body and fins with the airflow. The area in contact is the reference area, and it is called the wetted area.

$$C_{skin\ friction} = \frac{D_{friction}}{.5 \rho V_0^2 A_{wetted}}$$

It is a function of the Reynolds number and surface roughness. For a turbulent flow with a smooth surface with a surface roughness completely imbedded in a lamina:

$$R_N\ critical = 51 \left(\frac{R_s}{L} \right)^{-1.039}$$

Where, R_s := approximate height of the surface in micrometers

If Reynolds number is below 100,000:

$$C_{skin\ friction} = 0.0148$$

If it is above 100,000, but below R_N critical:

$$C_{skin\ friction} = \frac{1}{1.5 \ln R_N - 5.6}$$

If it exceeds the critical value:

$$C_{skin\ friction} = 0.032 \left(\frac{R_{NS}}{L}\right)^{0.2}$$

- Fin drag is a large component of rocket aerodynamics and a full treatment requires many equations, several among them are:

Taper Ratio:

$$\lambda_t = \frac{C_t}{C_r} = \frac{tip\ chord}{root\ chord}$$

Aspect Ratio:

$$AR = \frac{wingspan^2}{surface\ area\ of\ fins\ and\ connection} = \frac{b^2}{S}$$

Thickness Ratio:

$$\frac{t}{c} = \frac{thickness}{chord}$$

$$C_{DOFins} = \frac{D_{fins}}{(\frac{1}{2})dv^2 * planform\ area}$$

$$C_{DOFins} = 2 * C_{skin\ friction} (1 + 2(\frac{t}{c}))$$

- Nose cone drag exists, but is much smaller than skin friction drag. For subsonic flights ($M < 0.8$) we can approximate this coefficient as zero.

$$C_{D\ Nose} + C_{D\ Body} = 1.02 C_{skin\ friction} (1 + \frac{1.5}{(\frac{d}{l})^{3/2}}) \frac{Wetted\ Surface\ Area}{Area\ of\ Body}$$

- Parasitic drag is what develops from having one or two launch lugs attached to the body of the rocket. It may be modeled as a solid cylinder, instead of a hollow cylinder.

$$C_{D\ Launch\ Lug\ max} = 1.2 \frac{Surface\ area\ of\ lug}{Surface\ area\ of\ body\ tube}$$

The Total Drag Coefficient (C_D) is obtained by scaling all of the relevant drag coefficients to a common reference area and making a summation:

$$C_{D0} = \sum_T \frac{A_{Total}}{A_{reference}} (C_D)_{Total}$$

Where, $\alpha = 0$

When $\alpha \neq 0$, $C_{D0} \neq C_{A0}$. More area interacts with the airflow, the pressure gradients change and vortices at the fins develop. The axial drag coefficient (C_A) must be considered separately. All of these are valid for small α , usually less than 10° , but with an upper limit of around 17° .

For, $\alpha = 0^\circ$

$$C_A = 1$$

For, $\alpha = 17^\circ$

$$C_A = 1.3$$

3.1.1e Thrust

The calculation of thrust is a vital step in the understanding of rocketry. As such, it has an important place in the design of SOAR's launch vehicle. We know,

$$F = ma = m \frac{dv}{dt}.$$

However, this is relatively general, so we need a more thorough analysis of rocket thrust.

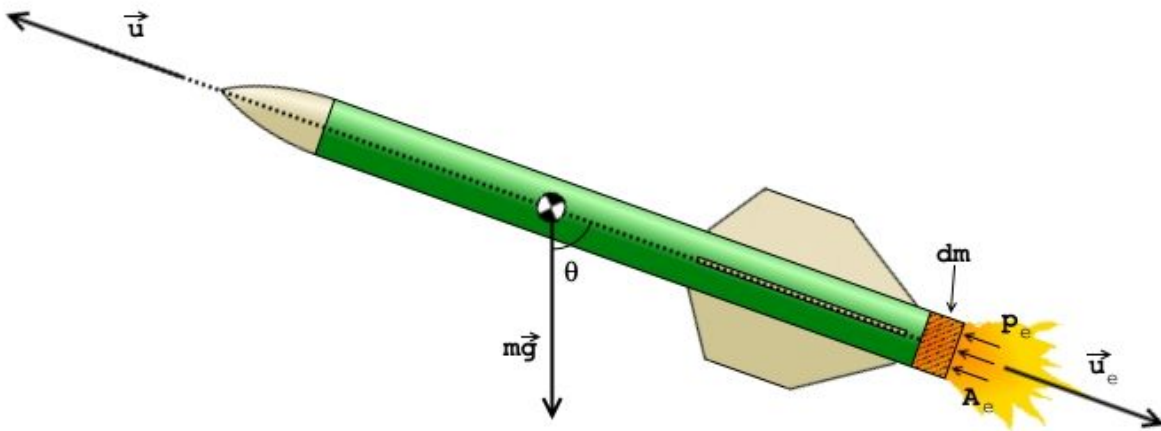


Figure 3.1.1e.1: Diagram of rocket in-flight.

We have

$$\frac{d}{dt}(m_b v + \int \rho(u + v)dV) = (P_{out} - P_{atm})A_e + F_{Drag} - F_{Gravity} + \dot{m}(u_e + v),$$

where

$$\frac{d}{dt}(m_b v + \int \rho(u + v)dV) := \text{Rate of change in vehicle momentum}$$

$$(P_{out} - P_{atm})A_e + F_{Drag} - F_{Gravity} := \text{External forces}$$

$$\dot{m}(u_e + v) := \text{Momentum flow through outlet}$$

And,

$$(u + v) := \text{velocity components relative to ground}$$

Treating the mass flow through the outlet,

$$\dot{m} = \frac{d(\text{mass total})}{dt} = \rho_{exit} u_{exit} A_{exit}$$

Substituting,

$$F_{int} = -\frac{d}{dt}(\int \rho(u)dV)$$

$$F_{thrust} = (P_{out} - P_{atm})A_e + \dot{m}u_e$$

$$\text{Acceleration } a = \frac{F_{thrust} + F_{drag} + F_{int}}{\text{mass}_{total}} - g$$

$$\frac{dv}{dt} = a; \frac{d(x, y, z)}{dt} = v,$$

Also, because propellant provides such a large portion of the total mass, the changing mass due to propellant loss must be considered,

$$\text{Empty Mass} = M_{empty} = \text{Payload mass} + \text{structural mass}$$

$$\begin{aligned} \text{Full Mass} = M_{full} &= \text{Payload mass} + \text{structural mass} + \text{propellant mass} \\ &= \text{Empty mass} + \text{propellant mass} \end{aligned}$$

$$\text{Structural Coefficient} = \epsilon = \frac{\text{structural mass}}{(\text{propellant mass} + \text{structural mass})}$$

$$\text{Payload Ratio} = \lambda = \frac{\text{payload mass}}{(\text{full mass} - \text{empty mass})}$$

$$\begin{aligned} \text{Propellant Mass Ratio} = MR &= \frac{\text{full mass}}{\text{empty mass}} \\ &= 1 + \frac{\text{propellant mass}}{\text{empty mass}} \\ &= \frac{1+\lambda}{1+\epsilon} \end{aligned}$$

3.1.1.f Kinematics

Now to calculate the burnout altitude and velocity, along with coasting distance and coasting time. It will be helpful to first define a few variables which will keep the calculations more tidy:

$$k = \frac{1}{2}\rho C_D A,$$

$$q = \sqrt{\frac{T-mg}{k}}, \text{ and}$$

$$x = \frac{2kq}{m} = 2\frac{\sqrt{(T-mg)k}}{m},$$

where ρ is the air density, C_D is the drag coefficient calculated in a section above, $m = m_r + m_e - .5m_p$ is the average mass of the rocket during its upward travel, g is the acceleration of gravity, T is the thrust calculated above, and A is the cross-sectional area of the body of the rocket. The amount of time t for which the motor will burn is the motor impulse divided by the thrust:

$$t = \frac{I}{T}.$$

The velocity at burnout is

$$v = q \frac{1 - \exp(-xt)}{1 + \exp(-xt)}.$$

The altitude y_B at burnout is

$$y_B = \frac{-m}{2k} \ln\left(\frac{T-mg-kv^2}{T-mg}\right).$$

The vertical distance y_C for which the rocket will coast after burnout is

$$y_C = \frac{m}{2k} \ln\left(\frac{mg+kv^2}{mg}\right),$$

where m is now equal to $m_r + m_e - m_p$, because all of the propellant has been expelled from the rocket during the coast to apogee. So the altitude at apogee is $y_B + y_C$. The time spent coasting can also be represented neatly by first defining helpful variables:

$$q_a = \sqrt{\frac{mg}{k}}, \text{ and } q_b = \sqrt{\frac{gk}{m}}.$$

Now the coasting time t_C can be found using:

$$t_C = \frac{\arctan(v/q_a)}{q_b}.$$

3.1.2 Stability



Figure 3.1.2.1: Diagram of Rocket showing the Center of Pressure and Center of Gravity

As can be seen from figure 3.1.2.1 above our team has determined the center of pressure and gravity of our launch vehicle in order to ensure that our design is stable. The center of gravity is located at 92.512 inches from the nosecone and our center of pressure is located at 114 inches from the nosecone. This gives us a stability of 5.38 calibers, well above the necessary 2 calibers.

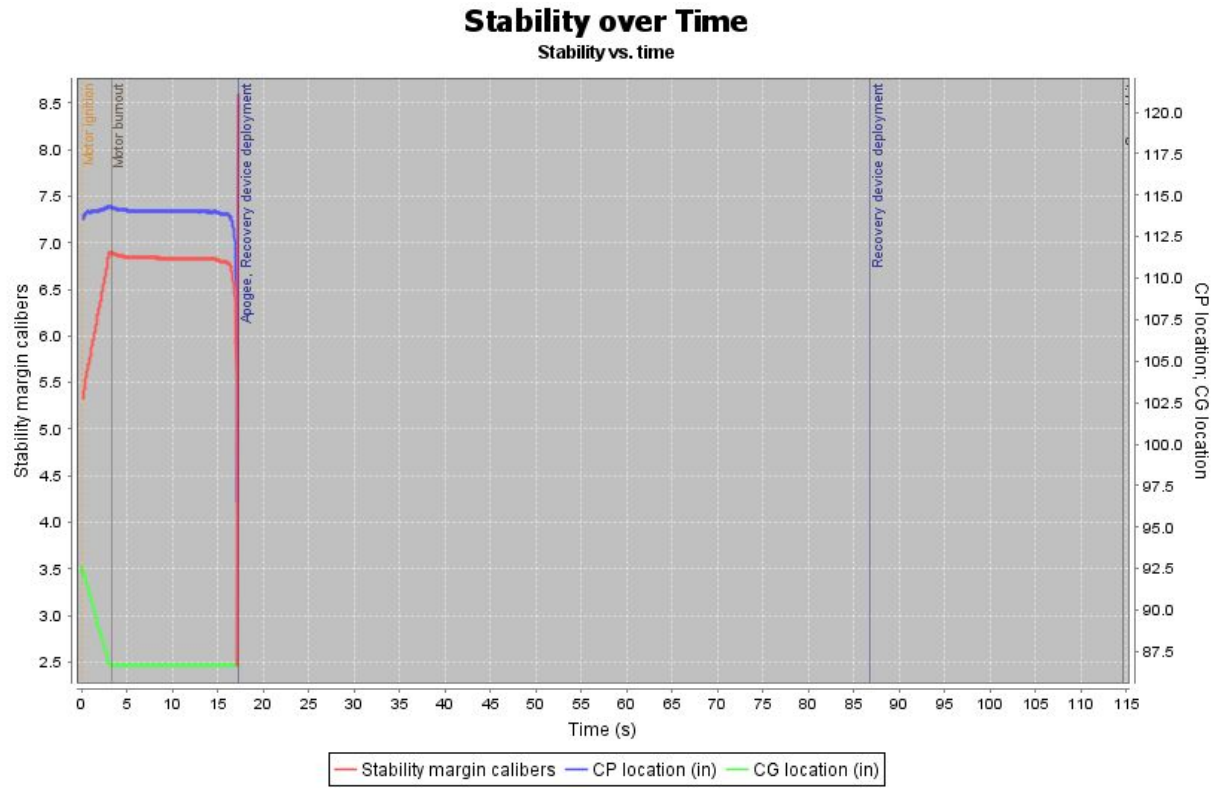


Figure 3.1.2.2: Stability, CG, and CP plotted over time

3.1.3 Fabrication

There are many parts involved when it comes to the fabrication of our rocket. One of the single most important aspects is what holds it together. We primarily make use of 30 minute Slow Cure, two part epoxy with a known shear strength of 3500 psi. While Epoxy may yield at a much higher shear strength, 3500 psi is well within the limit of proportionality. In addition, we used shredded carbon fiber to increase the strength of the fillets applied to the fins. All other fasteners are applied as necessary such as plastic rivets in the nose cone, shear pins between sections, and screws in the altimeter bay.

3.1.3a Motor Mount: Centering Rings

The first step in the fabrication of our rocket is to place and then epoxy on the centering rings that will:

- 1.) Separate the motor mount from the inner diameter of the aft tube.
- 2.) Secure the motor mount inside of the aft tube
- 3.) Secure the Fins

In order to properly apply the fillets to the centering rings, we sanded the excess epoxy, then reapplied and smoothed the epoxy with a wooden applicator. Below in Figure 3.1.3a.1 you can clearly see where the three centering rings go on the motor mount. The centering rings we used are made of baltic birch wood, found to have an average density of 0.234 pounds per cubic inch; and we chose to use phenolic tubing for our motor mounts. The bottom most centering ring and the middle centering ring will serve as the borders that will be flush with the fins. In other words, the fins sit comfortably within these two centering rings.



Figure 3.1.3a.1: Motor Mount with Centering Rings

3.1.3b Motor Mount: Fins

The fins are custom made from $\frac{1}{8}$ " thick G10 fiberglass by Public Missiles Ltd. We went with fiberglass to increase the overall weight of the rocket as well as increase the rigidity of the fins for the higher velocity the rocket will achieve. The fins are cut into a trapezoidal shape to allow the rocket to reach its optimum height as well as minimize the risk of catastrophic damage to the fins upon recovery. As mentioned above the bottom most centering ring and the middle centering ring border the fins as in Figure 3.1.3b.1. If you'll notice, drawn on the Motor mount is the exact placement the four fins will need to be epoxied in place to ensure a linear assent. These lines are drawn following the arc length formula:

$$s = r\theta$$

where,

s = arc length

r = radius of the outer diameter of the motor mount

θ = $\pi/2$ (must be in radians)

Thus the distance around the outside diameter of the motor mount that the lines are drawn is 6.236cm from one another.



Figure 3.1.3b.1: Motor Mount with One Fin

Once the first fin is placed on the motor mount and epoxied in place, we then proceeded to place the rest of the fins on the motor mount as shown in Figure 3.1.3b.2. After the epoxy dried, we sanded the epoxy where the fins were adhered to the motor mount and created fillets made from a carbon fiber and epoxy mixture.

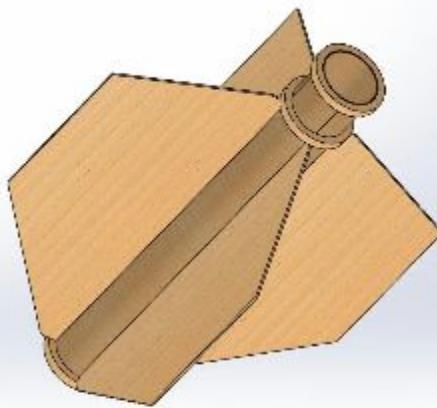


Figure 3.1.3b.2: Completed Motor Can

3.1.3c Motor Mount: Eye Bolts and Motor Retainer

The next step in the fabrication of our rocket is to attach eyebolts and the motor retainer. The eyebolts will be attached to the top most centering ring which are used to attach the drogue parachute. The motor retainer is attached to the bottom most centering ring which prevents the motor itself from falling out of the bottom of the rocket during ascent. Below in Figures 3.1.3c.1 and 3.1.3c.2 you can see the eyebolts and the motor retainer represented respectively.

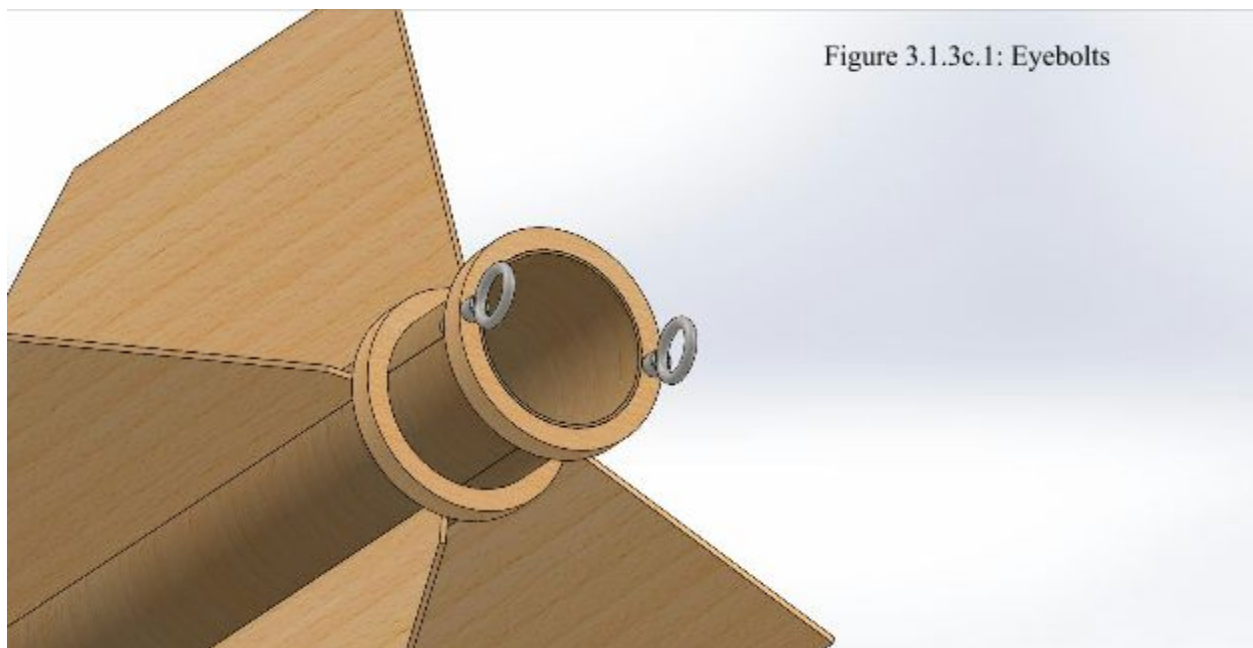


Figure 3.1.3c.1: Eyebolts

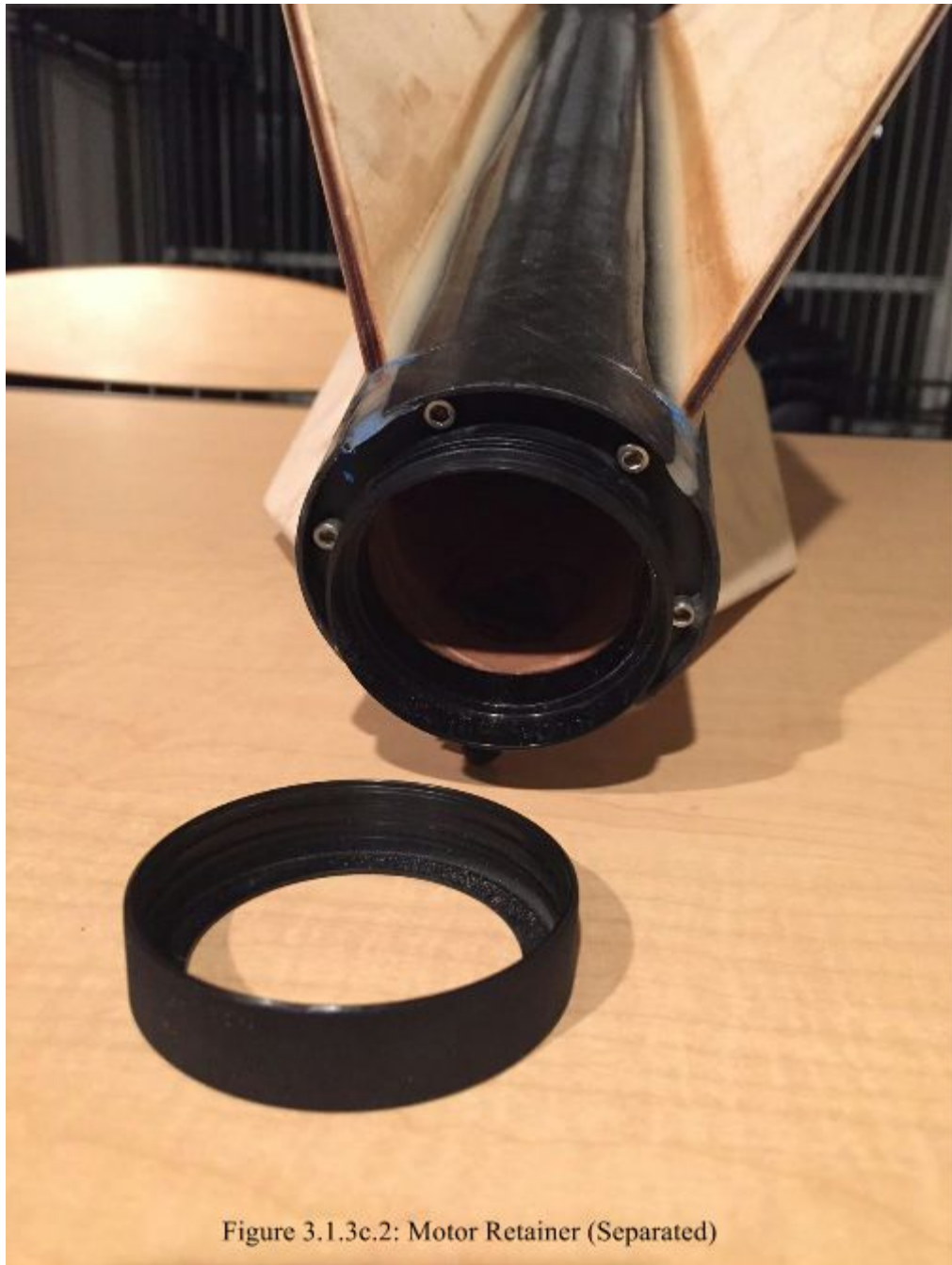


Figure 3.1.3e.2: Motor Retainer (Separated)

Below you can see the motor retainer screwed on to the end of the rocket. This, as stated above, is to prevent the motor from dislodging through the rear end of the rocket.



Figure 3.1.3c.3: Motor Retainer

3.1.3d Route the Aft Tube Fin Slots

After the motor mount is completed which includes the fins, eyebolts, and motor retainer the next step is to route the aft tubes fin slots. This is done so that we can slide the whole motor mount into the bottom of the aft tube and then secure it in place with epoxy. Though, before sliding the motor mount into the aft tube we must first attach paracord to the eyebolts, which will then be attached to our drogue parachute.

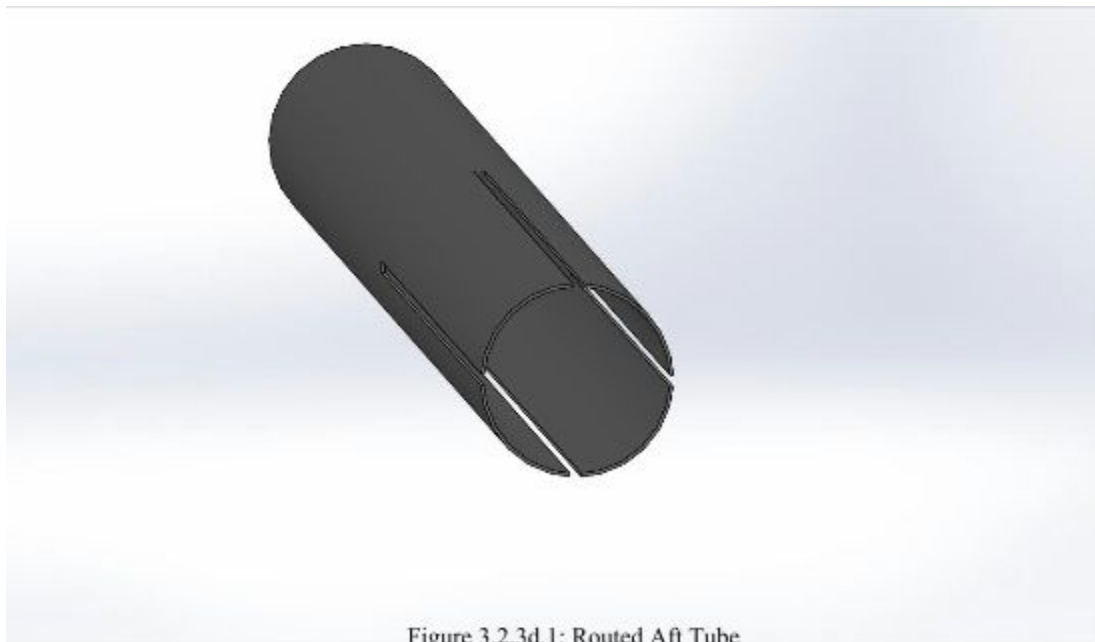


Figure 3.2.3d.1: Routed Aft Tube

Once this is complete we can then slide in the finished motor mount and apply heavy epoxy to hold it in place.



Figure 3.1.3d.2: Finished Aft Tube with Motor Mount and Fins



Figure 3.2.3d.3: Heavy epoxy coting below and around fins

It is pertinent that we assure our fins are secure after sliding the motor mount into the aft airframe. To do this we apply even more epoxy to the fins to create fillets for strength and aerodynamics.

Figure 3.2.3d.4: Fillets
Along Fins



3.1.3e Altimeter Bay

The Altimeter bay is where the primary sensor of the rocket is housed. In here there will be two altimeters and two batteries as a redundancy. The altimeters are used to sense when the rocket is at apogee, in which case the drogue parachute is deployed, and when the rocket is at approximately 500 feet from the ground, in which case the main parachute is deployed.



Figure 3.1.3e.1: Side View of Altimeter Bay Assembly



Figure 3.1.3e.2: Altimeter Bay Bulkhead

Here are the following steps in fabricating our altimeter bay:

1. Epoxy one inch fiberglass to center of the 16 inch coupler as shown in Figure 3.1.3e.
Drill vent hole into the fiberglass ring, sized in accordance with the final altimeter bay volume.
2. Create two bulkheads with eyebolts, blackpowder tubes, and slots for threaded leads as shown in Figure 3.1.3e.2.
3. Affix altimeters and batteries onto altimeter sled.
4. Affix turn switch (with the on direction being DOWN) to the outside of altimeter bay and then wire the switch to the altimeters and the batteries.
5. Feed eMatches through black powder tubes and wire each to the altimeters.
6. Complete the altimeter bay by attaching bulkheads and securing with wingnuts.

3.1.3f Altimeter Bay Integration

Once the altimeter is completed it can then be placed within the rocket. Though it mostly now becomes part of the rocket.

There are three steps to attaching the altimeter bay to the rocket:

1. Attach paracord to the upper half of the altimeter bay's eyebolt.
2. Screw upper half of the altimeter bay into the lower section of the fore airframe.
3. Attach paracord between the lower half of the altimeter bay and the paracord from the aft bay.

3.1.3g Payload Bay

The payload bay will be where our AGSE system will deposit our sample. We have decided to go with a containment system using a linear actuator so that it will secure around the payload as it is placed inside the launch vehicle. This containment system will prevent the sample from moving freely throughout the payload bay during flight. Once the sample is secured and the rover arm clear, linear actuators will close and lock the payload bay prior to being raised for launch.

The Payload Bay fabrication process is as follows:

1. A trapezoidal prism container will be 3-D printed from ABS plastic to hold the payload.
2. The container will be supported two cylindrical rods that will protrude through the lower bulkhead into the lower coupler assembly housing the linear actuator power source and linear actuator motor.
3. A coupler and a bulkhead will be attached below the payload bay and electronics systems.
4. Paracord will be attached from the bottom of the bulkhead to the fore airframe paracord.
5. The upper payload will contain an empty volume to store the payload and its container.

3.1.3h Nose cone

To secure the nose cone to the payload bay we drilled holes in the top most part of the payload bay, while also drilled holes in the nose cone. We then placed the nose cone on top of the payload bay and lined up the holes. Rivets were then placed in the holes to secure the nose cone to the payload bay as shown in Figure 3.1.3h.1.



3.1.3i Rail Buttons

In regards to rail button placement, we want the upper rail button to rest on our center of gravity and our lower rail button to be attached the lowermost centering ring. This positioning allows us to maintain stability for our rocket on the launch rail and gives us adequate time to have it reach its stable velocity.



Figure 3.2.3i.1: Bottom
Most Rail Button



Figure 3.2.3i.2: Top Most Rail Button

3.2 Subsystems

3.2.1 Nosecone

For our final design we have chosen to go with a plastic HDPE (High Density Polyethylene) o-give nosecone style from Public Missiles Ltd. as modeled below in figure X.

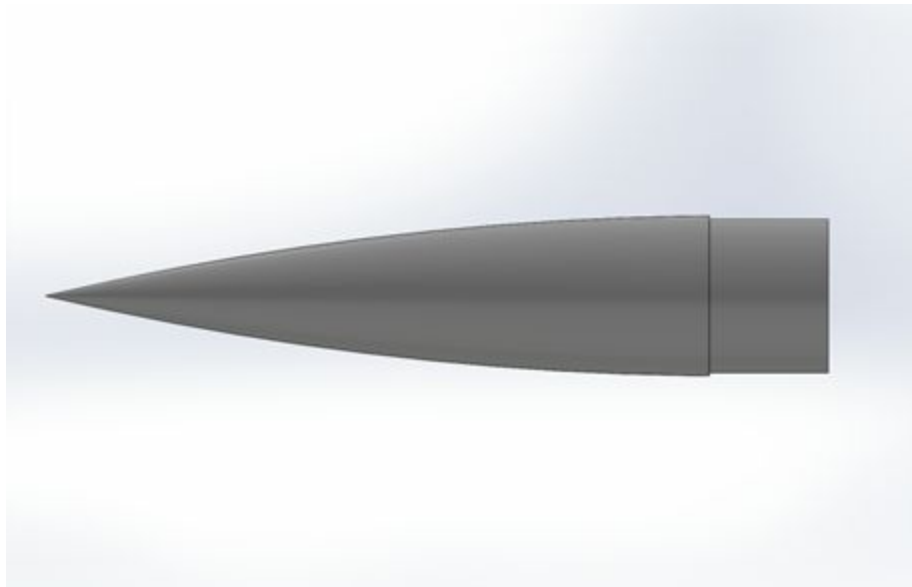


Figure X: O-GIVE Nosecone Modeled in Solidworks

This particular nosecone model was chosen for several reasons which fit into our greater design scheme. The sandable ridges along the shoulder gave us the flexibility to go with the fiberglass airframe from Wildman Rocketry while still allowing the team to be confident that we could ensure a snug fit between the nosecone and the payload bay. Furthermore the hollow interior of the nosecone is able to have additional mass added and have the interior be foamed for rigidity. This capability of the PML nosecone will also allow us to use the nosecone as a mass ballast in order to bring our center of gravity further towards the nosecone without the need to further complicate our design.

3.2.2 Payload Bay



Figure 3.2.2.1: Closed Payload Bay Modeled in Solidworks



Figure 3.2.2.2: Open Payload Bay Modeled in Solidworks



Figure 3.2.2.3: Open Payload Bay Detail Top View Modeled in Solidworks

The payload bay will be located below the nosecone and electronics bay. The bay will be composed of two sections, a lower section housing electronics necessary for the AGSE (see section 4.2), and an upper section housing a payload sled and space for the insertion of the electronics bay or nosecone.

The lower section of the payload bay will be composed of an 8.5 inch coupler tube, with the 5.5 inch fiberglass epoxied over it, leaving a 1 inch shoulder towards the top and a 2.5 inch shoulder towards the bottom. An O ring will be placed on the upper 1 inch coupler shoulder, on top of the fiberglass to allow for an airtight connection between the upper and lower payload sections. Both ends will be secured in place with birch bulkheads with an electronics sled situated on two threaded rods running through the length of the bay. The lower bulkhead will be epoxied in place and have an eye bolt secured into the bottom. This will be attached to fore airframe as part of the recovery system.

The upper section of the payload bay will be composed of a section of 9.5 inch fiberglass airframe, with a bulkplate situated at 5.7 inches inside the tubing. The payload sled will be 3-D printed ABS plastic and will be located within the hollow portion of the payload bay, below the bulk plate. There will be an additional 3 inches above the bulkplate allowing for the insertion of the electronics pay or nosecone.

3.2.3 Motor

The vehicle will use a commercially available solid motor propulsion system. Specifically, the L910s rocket motor from Cesaroni Technology will be used and is certified by the Canadian Association of Rocketry. The vehicle motor is a solid ammonium perchlorate composite propellant that is comprised up of a variety of reactive metals, HTPB binder and also burn rate catalysts. The MSDS forms for each of these chemicals from the motor section can be found in the safety section of the design report. The motor is 75 millimeters in diameter and 14 inches in length. This motor has a total impulse of 2856.1 Newton-seconds, a maximum thrust of 1086.1 Newtons, and a burn time of approximately 3.2 seconds. OpenRocket simulations have been run on this motor to achieve a simulated apogee of approximately 5280 feet and a maximum velocity of approximately 748 feet per second. Table 3.2.4.2 summarizes briefly several of characteristics of the launch vehicle's motor.

The thrust curve shown in figure 3.2.4.1 (thrustcurve.org) has a fairly steady and consistent thrust ending around 3.2 seconds. Around the 2.9 second mark, the thrust decreases exponentially until burnout.

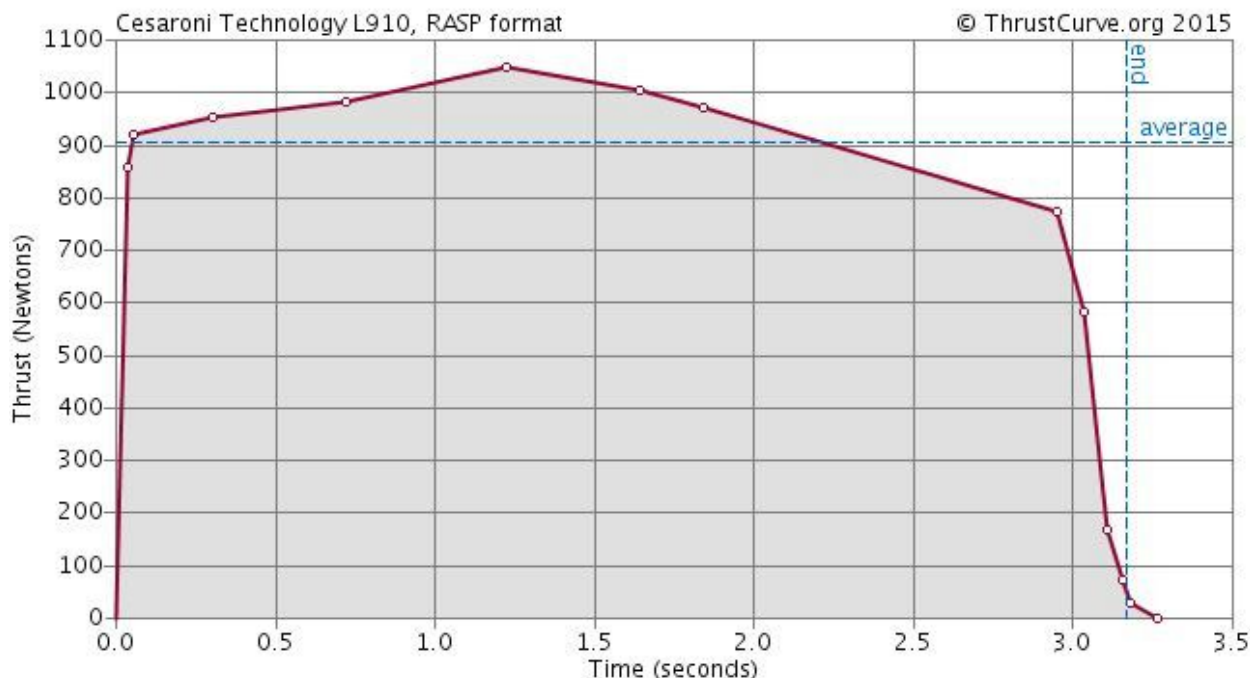


Figure 3.2.4.1. The thrust curve of an Cesaroni L910 motor

Table 3.2.3.2. List of the full-scale motor specifications

Motor Selected	CS L910s
Maximum Thrust	1086.1 N
Average Thrust	907.10 N
Thrust-to-weight ratio (Total)	8.93
Motor Diameter	75 mm

3.2.4 Fins



Figure 3.2.4.1: 1/8" G10 Fin

1/8" G10 fiberglass has been chosen for the fins for several qualities that it possess. Namely G10 fiberglass is waterproof and stronger than wood. In addition it is less likely to have material flaws that would weaken the overall fin. Due to the higher strength of the fiberglass than wood, the fins can be made thinner reducing overall and drag due to the leading edge thickness. In addition, G10 fiberglass can be readily attached with epoxy if the surface is appropriately roughed beforehand with sandpaper. From an economic standpoint, G10 was readily available for use and we are familiar with fiberglass builds. The relevant properties of the G10 fiberglass have been listed in the table below:

Table 3.2.4.1: G10 Fiberglass Specifications

Density (lb/in ³)	0.065
Length-wise tensile strength (ksi)	43
Cross-wise tensile strength (ksi)	38
Length-wise flexural strength (ksi)	66
Cross-wise flexural strength (ksi)	60
Length-wise flexural modulus (ksi)	2700
Cross-wise flexural modulus (ksi)	2400
Compressive strength (ksi)	44
Max coefficient of linear thermal expansion (in/in/ ⁰ F)	0.66x10 ⁻⁵
Max operating temperature (⁰ F)	284
UL94 Flammability Rating	H-B

The fins are to be attached to the motor can with epoxy resin and carbon fiber. To ensure precise fin attachment we used a fin jig and a laser cut sheet of fiberglass as a guide for a four fin placement. We chose a four fin design as this would allow us to bring the center of pressure further from the nose cone due to the fins have a sizeable surface area. Additionally the four fins will increase the total mass of the rocket, allowing us to achieve our target altitude with a slightly more powerful motor.

3.2.5 Propulsion Bay/ Fin Can

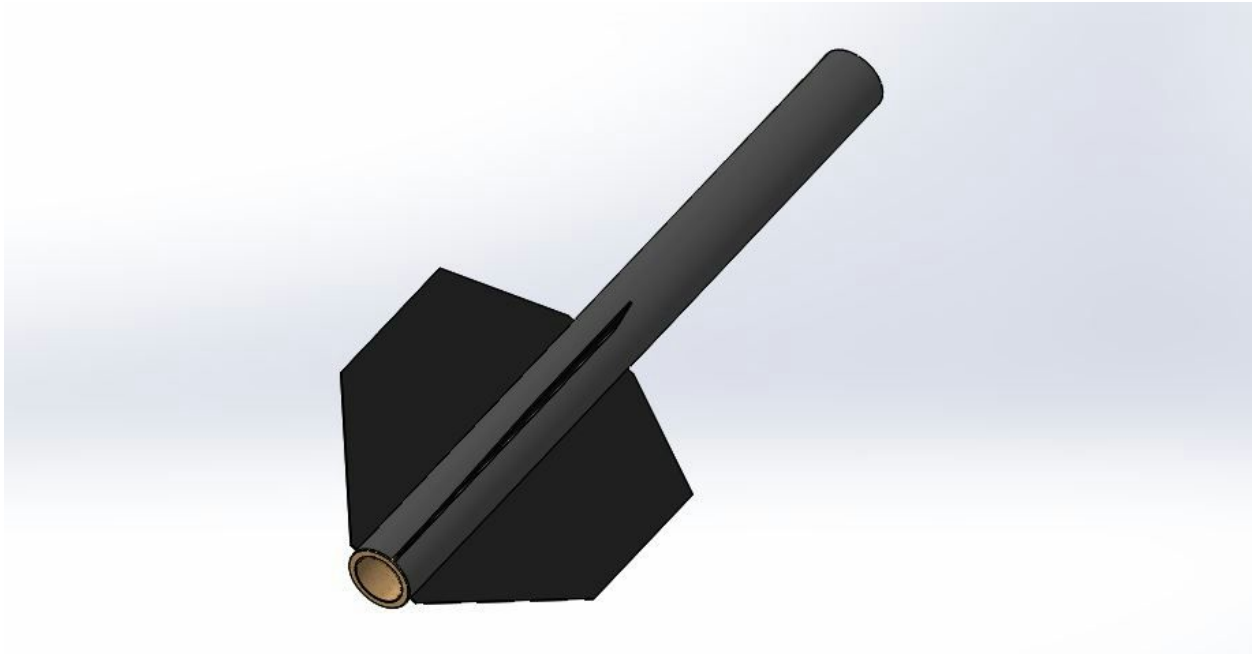


Figure 3.2.5.1 Full-scale propulsion bay/fin can

The launch vehicle propulsion bay will house the solid propulsion system motor mount as well as hold the launch vehicle stabilization fins. The propulsion bay will link with the forward bay through the 16 inch kraft phenolic tube altimeter bay. The propulsion bay will be 48 inches in length and will be fabricated using G-12 fiberglass tubing. The render of the full-scale propulsion bay can be seen in figure 3.2.5.1 above.

3.2.6 Motor Retention

The motor shall be secured in a 36 inch kraft phenolic motor mount. The motor casing will be prevented from moving upwards towards the nose cone via snap ring and it will be further held in retention by a 75 mm aeropack motor retainer to prevent the motor casing from sliding out of the motor mount tube. The motor retainer will be JB welded onto the lowest centering ring and allowed to protrude slightly from the bottom of the rocket. The simple threaded mechanism will allow the motor and casing to be inserted and removed with ease.



Figure 3.2.6.1 . The 75 mm Aeropack motor retainer

The motor mount will be held into place by three birch centering rings purchased from Public Missiles Ltd. They will be epoxied onto the motor mount using 30 minute epoxy, and will in turn be epoxied onto the airframe. Epoxy fillets will be formed along all connected edges in order to increase rigidity and shear strength by filling any remaining voids.

3.2.7 Altimeter and Electronics Bay

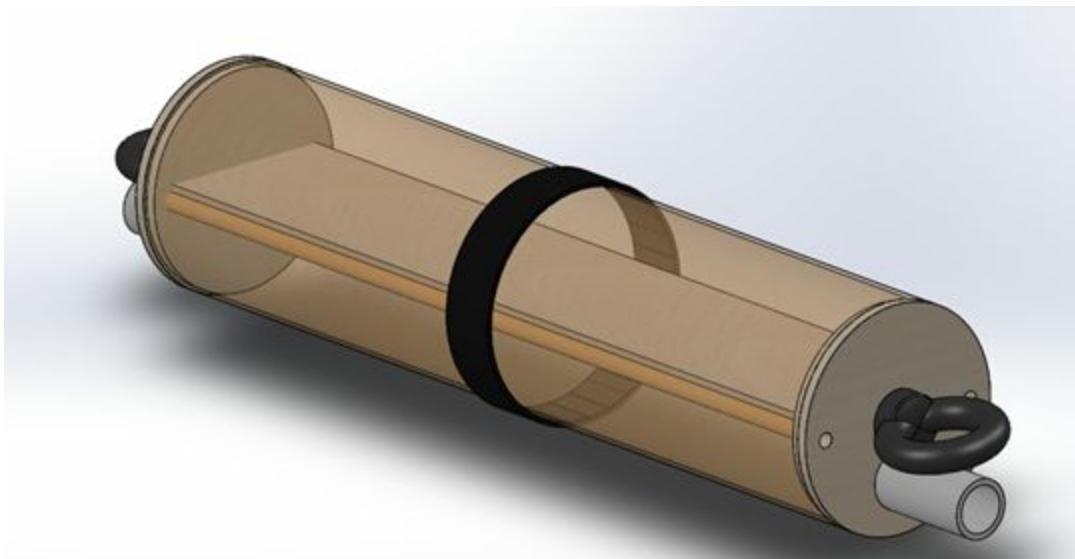


Figure 3.2.7.1 Solidworks Model of Altimeter Bay

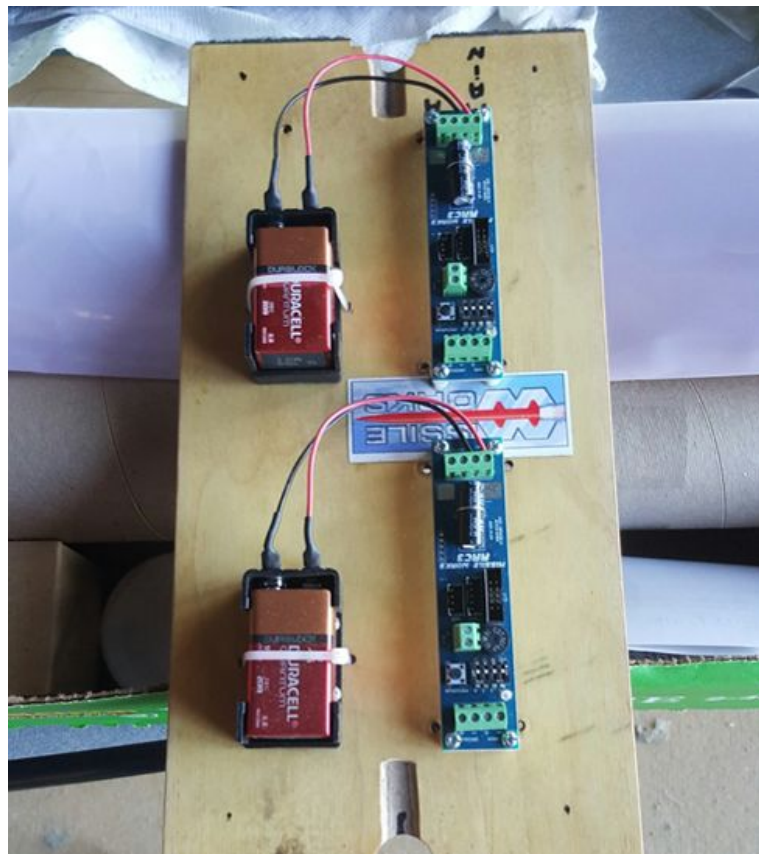


Figure 3.2.7.2 Altimeter Board Setup

Between the fore body tube and the aft body tube lies the altimeter bay. The bay is constructed from a coupler, a 1-inch ring of fiberglass, two wooden bulkheads, and two threaded rods that run the length of the bay. Four segments of 1-inch PVC pipe will protrude from either bulkhead

to hold black powder for section separation upon recovery. The pipes will be covered by plastic blast caps. The bay is attached to the fore tube with screws and to the aft tube by couplers. The fasteners present inside of the bay are wingnuts located on threaded bolts and four U-bolts to fasten the parachutes. Because the altimeters used are barometric, it was necessary to drill ports allowing air to flow through the bay. The diameter D to be drilled if using a single port depends only on the volume V of the bay (which depends on its radius R and length L).

$$V = \pi R^2 L$$

If the volume is less than 100 cubic inches, then

$$D = \frac{V}{400}$$

$$A = \frac{D^2}{4}\pi$$

are the recommended diameter (in inches) and area A (in inches squared) of a single port to be drilled in the bay. It is common to drill multiple holes, instead of a single port. To find the recommended diameter d to drill N number of ports...

$$d = 2\sqrt{\frac{A}{N\pi}}.$$

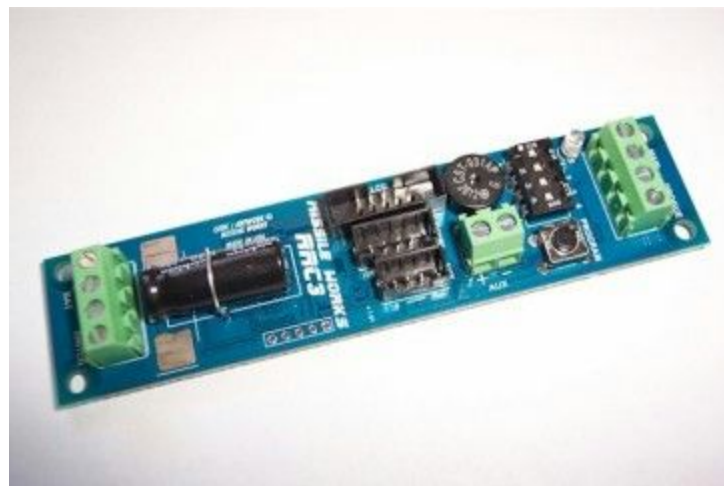


Figure 3.2.7.3 RRC3 Altimeter. Photo taken from Missile Works © website.

The bay is designed to hold two Rocket Recovery Controller 3 (RRC3) altimeters. The RRC3 uses high-resolution barometric pressure sensors to determine the precise altitude of the rocket so as to record the rocket's height at apogee for later reporting, and to deploy the drogue and main parachutes at apogee and at an altitude of 500 feet, respectively. This particular type of altimeter contains a solid dielectric capacitor which, unlike the standard electrolytic capacitor, can withstand virtual vacuum and near-space conditions.

3.3 Recovery

3.3.1 Design Overview

Recovery, although the last phase of the launch, is very important because it ensures the safety of the vehicle and observers. The recovery system will use dual-deployment in compliance with the Recovery Subsystem Requirements outlined in the NASA Student Launch handbook. The drogue parachute will be deployed at apogee to minimize drift. After the drogue parachute has been deployed and the rocket has descended to an altitude of 500ft the RRC3 altimeters will deploy the main parachute via an additional ejection charge. The ejection charges will be stored on the end of the altimeter bay, compacted by flame retardant material and covered with a blast cap.

The rocket airframes will be held together by shear pins as is customary to ensure there will be no separation prior to our selected event locations. Blast caps will be placed on both ends of the altimeter bay, they will have black powder charges, flame-retardant wadding, and e-matches which will be connected to the altimeter bay. For the purpose of redundancy we will use two RRC3 altimeters to ensure parachute deployment.

For the recovery system to be considered successful the following criteria must be met:

1. The drogue parachute must deploy at apogee.
2. The main parachute must deploy between 450-550 feet AGL.
3. All independent sections must have a maximum kinetic energy of 75 ft-lb upon impact.

Figure 3.3.1.1 is a graphic representation of our proposed dual-deployment recovery system, with all significant events.

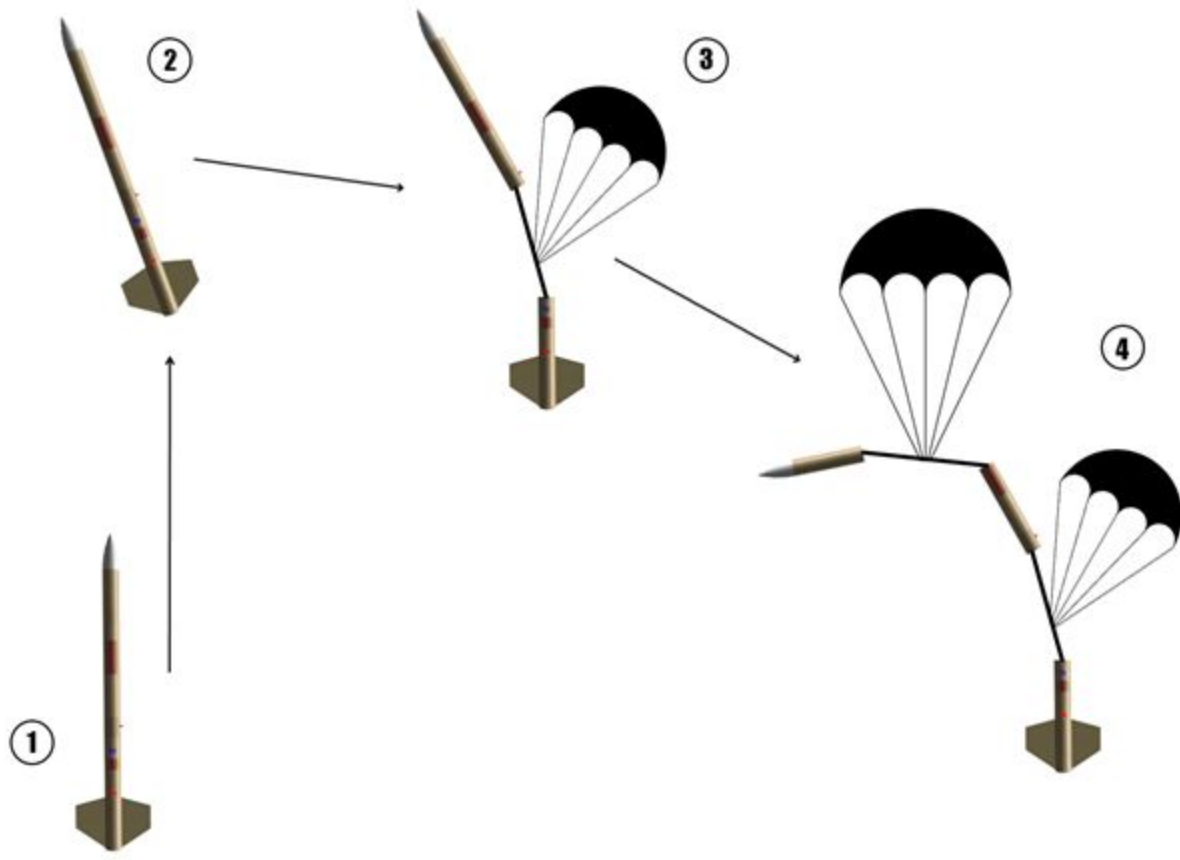


Figure 3.3.1.1: Recovery Sequence of Events

Table 3.3.1.1: Recovery Events and Descriptions

Event	Description
1	Launch (0 feet AGL)
2	Apogee (5280 feet AGL)
3	Drogue Deployment (Apogee)
4	Main Deployment (500 feet AGL)

3.3.2 Parachute Sizing and Selection

In regards to parachute selection we chose to look into companies we were familiar with which could provide consistent quality and compatibility with our design.

Parachutes are sized with the descent velocity of the rocket in mind. For a rocket of weight w (when all fuel has been ejected) and desired descent velocity v , the area A of the parachute can be found by the following equation

$$A = \frac{2w}{\rho C_D v^2},$$

where ρ is the density of air and CD is the drag coefficient calculated in section 3.1.1d. The air density in Huntsville, Alabama is recorded by the NOAA to be approximately 105% the standard pressure of air, which is 1.255 kg/m³, so ρ is approximately 1.31775 kg/m³. The empty weight of the rocket is 14.2 lbs. The max descent velocity of the rocket is 27.775 ft/s, a suitable velocity in order to maintain the heaviest separate section of the rocket, the fin can, stays within the required 75 ft-lb kinetic energy on impact. Using the Cert-3 Large parachute drag coefficient of 1.28 we found that the 57 sq. foot parachute would be more than adequate for our purposes.

Our final parachute choices are as follows in the table below.

Table 3.3.2.1: Drogue and Main Parachute Specifications

Parachute	Load Capacity	Surface Area	Drag Coefficient	Suspension Line	Net Weight	Packed Length
Cert-3 Large	16.2 – 35 lbs	57 ft ²	1.26	80 in	34.0 oz	17 in
Cert-3 Drogue	1.0 – 2.2 lbs	6.3 ft ²	1.16	24 in	6.0 oz	<7 in

The Cert-3 parachutes maintain a strong design with 5/8" mil-spec tubular nylon (2,250 lbs.) suspension lines sewn around outside canopy and being composed of zero-porosity 1.9 oz. silicone-coated balloon cloth.

3.3.3 Bulkheads and Connective Elements

With our parachute choices secured and confidence in their capacity to bear the load of our rocket we needed to ensure that all connections made within the recovery system are secure and safely designed.



Figure 3.3.3.1: Rocket Diagram with Parachute Cord Length and Parachute Locations

One potential problem to account for is the issue of discrete rocket parts, connected by parachute cord, colliding with each other upon descent. This is a problem as it can cause serious damage to the rocket structure, preventing reusability, or it can lead to entanglement with the parachutes which could lead to increased velocity descent and higher kinetic energy upon impact. One control for this situation is by including adequate parachute cord length between sections in order to ensure safe distance between separate sections. The rule we follow in design for determining parachute cord length is allowing for at least three times the rocket length in cord to connect each section, meaning for our 138 inch length rocket we allow 414 inches of cord between the payload bay and fore airframe, and an additional 414 inches of cord between the fore airframe and the fin can, leading to a total cord length of 828 inches.



Figure 3.3.3.2: Bulkhead with Eye Bolt



Figure 3.3.3.3: Centering Ring with Eye Bolts

The second vital structure aspect of the recovery system are the bulkhead connective elements which binds the parachute cord to the rocket components. Figure 3.3.3.2 above is a model of the style of bulkhead and eyebolt connection we use to ensure a rigid connection between the cord and rocket sections. This style of bulkhead is used on the rocket payload and both sides of the altimeter bay. The bulkheads are composed of Baltic birch and adhered with 30 minute slow cure epoxy. The eye bolts used are threaded into place with the nut and washer further secured with the slow cure epoxy as well for added strength.

The exception this bulkhead design is the connection to the fin can. Figure 3.3.3.3 shows the centering ring design used to secure parachute cord with a Y harness style. The eyebolts are threaded and epoxied onto the topmost centering ring of the motor mount before being epoxied to the motor mount with fillets on both sides of the ring to ensure strength and rigidity. The y harness allows the fin can to stay balanced when the drogue chute is released, preventing tilting and as a result unplanned tumbling.

An additional safety precaution used by our attachment scheme will be the use of Nomex parachute protectors being placed on the parachute cord, separating the parachutes from the black powder charges. Though the chutes we are using are durable, the chute protectors will ensure that no undue damage is done to the parachutes on separation.

3.3.4 Altimeter Wiring

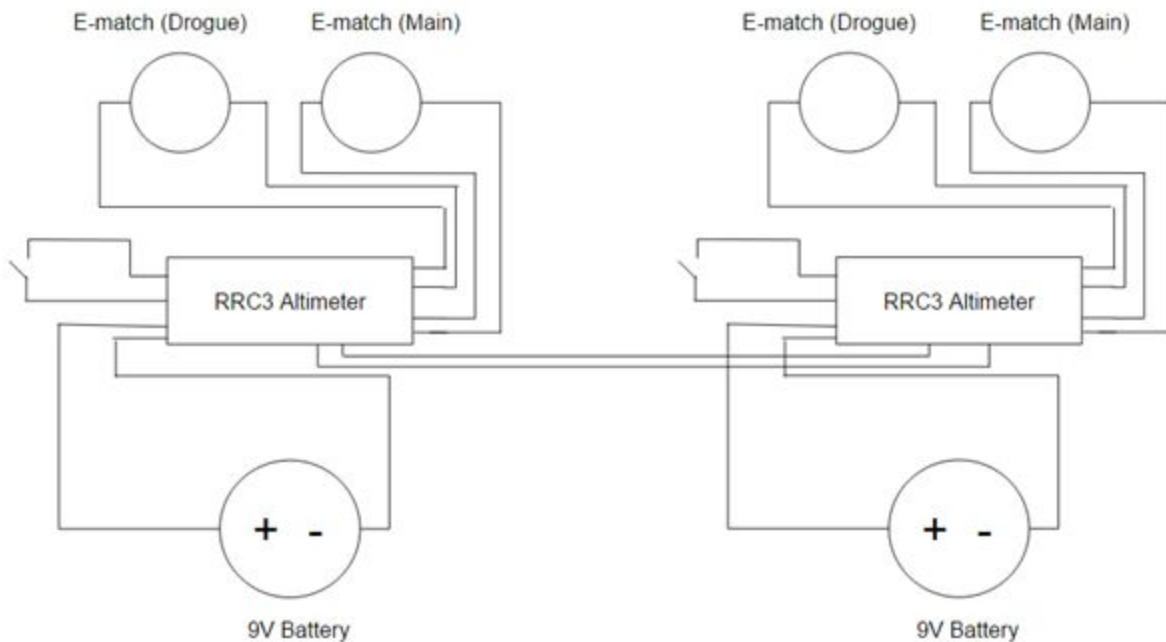


Figure 3.3.4.1: Altimeter Bay Wiring Diagram

3.3.5 Kinetic Energy and Descent Velocities

Table 3.3.5.1: Kinetic Energy and Descent Velocities

Section	Mass (lbf)	Drogue Descent (ft/s)	Main Descent (ft/s)	Kinetic Energy (lbfm-ft)
Nosecone/Payload	3.092	63.04	15.93	12.184
Fore Airframe	3.561	63.04	15.93	14.032
Aft Airframe	7.261	63.04	15.93	28.612

Table 3.3.5.1 above details the predicted descent velocities of the different rocket sections and their kinetic energies upon impact. The descent velocities were determined using OpenRocket and confirmed using the SkyAngle Descent Velocity calculator. Ultimately we found that the main descent velocity of 15.93 feet per second was well within the bounds to allow our heaviest section, the aft airframe, to land with a kinetic energy well below the boundary limit.

We have found the above information to be sufficient to call our design suitable for the purposes of providing a safe landing with minimal impact energy.

3.3.6 Drift Calculations

Modeling lateral drift of the rocket after chute deployment at apogee is a remarkably complex scenario. The constant variation of wind speed, the changing wind direction against the surface of the rocket, combined with the typical difficulties of rocketry, such as changing air density, changing rates of gravity, and the complications of fluid dynamics sum together to make an incredibly difficult challenge for someone who sets out to make a precise mathematical model of rocket drift caused by wind during recovery. For these reasons it is often acceptable to approximate the drift of the rocket using the simple equation,

$$Distance_{Drift} = Velocity_{wind} * Time_{Descent}$$

Table 3.3.6.1: Drift distances as generated from OpenRocket in variable wind conditions

Wind Speed (mph)	Lateral Drift (ft)
5	650
10	1300
15	2000
20	2525

Ultimately we decided to use OpenRocket to simulate the drift conditions for our launch vehicle. We found that though there was slight drift to apogee the majority of the lateral drift occurred during the recovery period. The values listed above in table 3.3.6.1 are representative of the drift distances in variable wind conditions.

3.4 Mission Performance Predictions

3.4.1 Performance Criteria

In order to classify the mission as a success the following criteria must be met:

1. The launch vehicle achieves apogee between 5,000 and 5,400 feet.
2. At apogee, the drogue parachute is successfully ejected.
3. Between 500 and 600 feet AGL, the nosecone and payload bay are separated from the rest of the vehicle, and the main parachute and payload parachutes are successfully ejected.
4. No portion of the vehicle or payload sustains any major damage during flight or landing.

3.4.2 Launch Vehicle Characteristics

The program OpenRocket was used to fully design and simulate the flight of our projected launch vehicle. Using this software the following launch vehicle characteristics were ultimately determined as can be seen in Figure X below.

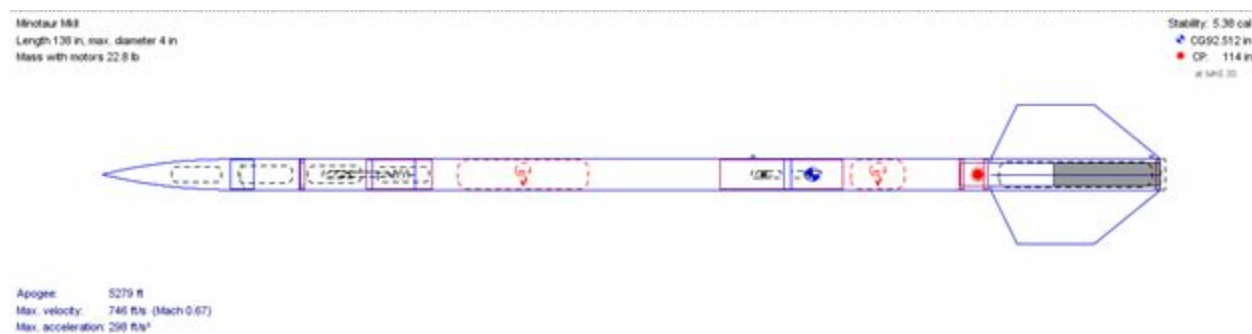


Figure 3.4.2.1: Minotaur Rocket Model from OpenRocket

- Length: 138 inches
- Diameter: 4 inches
- Max Diameter: 4 inches
- Empty Mass: 17.1 lbs
- Loaded Mass: 23.2 lbs
- Empty Stability Margin (CP/CG): 8.62cal (114in/79.544in)
- Loaded Stability Margin (CP/CG): 5.38cal (114in/96.891in)

3.4.3 Motor Selection

The full scale launch vehicle will use a Cesaroni Technology L910s solid propulsion unit. The team had used Cesaroni motors in previous competitions, all of which had proven to be reliable and efficient so the manufacturer choice was clear. When selecting the motor, the team had to account for multiple factors such as thrust to weight ratios, specific impulse, motor sizing and also chemical composition. The Cesaroni L910s is an APCP that will have a BATES grain geometry.

The team chose an APCP motor due to the fact that these types of motors tend to be very powerful and compact which results in moderately high specific impulses. A BATES grain configuration was desired by the team because the team preferred a steady thrust through the burn time of the motor. The team's motor has a total impulse of 2856.1 Newton-seconds and a burn time of approximately 3.2 seconds. The motor will have an average thrust of 907.1 Newtons throughout the 3.2 burn time. Conducted OpenRocket simulation data states that the launch vehicle with this L-motor is expected to achieve a apogee of approximately 5280 feet, exactly the desired altitude for the launch competition.

Factors including launch elevation and wind speed were accounted for in the team's OpenRocket launch simulations. These various simulation conditions yielded relatively consistent apogee data values. These simulations will be discussed more in detail in section 3.4.4. Several of the OpenRocket data plots can be seen in the figures illustrated below in section 3.4.4. as well. Table 3.4.3.1 depicts some of the motor characteristics that contributed to the overall selection of the propulsion unit.

Table:3.4.3.1 Table of Lanch Motor characteristics

Motor weight	5.760 lbs
Thrust-to-weight ratio	8.930
Average thrust	907.1 N
Specific Impulse	229.0 s
Motor Diameter	75.00 mm
Rail Exit Velocity	43.00 ft/s
Burn time	3.200 s
Maximum acceleration	300.0 ft/s ²

3.4.4 OpenRocket Simulations

In order to fabricate any sort of launch vehicle a plethora of dimension, motor and weather conditions testing and analysis must be conducted to ensure mission success as well as vehicle and pedestrian safety. Programs such as OpenRocket allow the user to conduct theoretical vehicle simulations that do not require the user to expend a pre-set mission budget. The team designed their initial and final launch vehicles using the OpenRocket program. Due to the conglomeration of ideas in the team the vehicle design was constantly being edited and tweaked in an attempt to ensure overall success and safety.

Once a final full-scale OpenRocket design was conceived, numerous flight simulations were implemented. A paramount component of the competition is reaching an apogee of exactly one mile. This factor was tested and simulated by the team through trial and motor research. Different sized and impulse rocket motors were tested on the program until a final CS L190s motor was selected. The graph of the altitude vs time using the CS L190s motor can be observed below in figure 3.4.4.1.

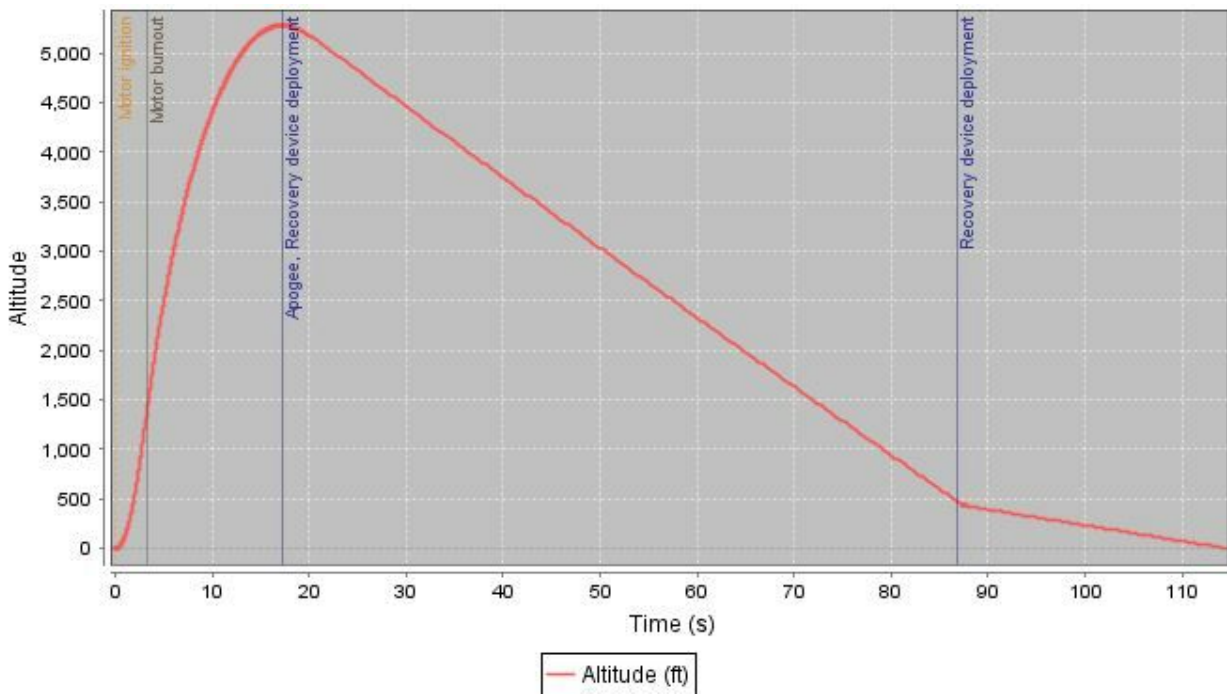


Figure 3.4.4.1 Graph of Altitude vs. Time

The graphs in figures 3.4.4.2 and 3.4.4.3 depict the vertical velocity vs. time and vertical acceleration vs. time for the team launch vehicle during its flight. Specific simulation data such as the graphs listed below were crucial to use as a reference when selecting vehicle materials and building the launch vehicle structure.

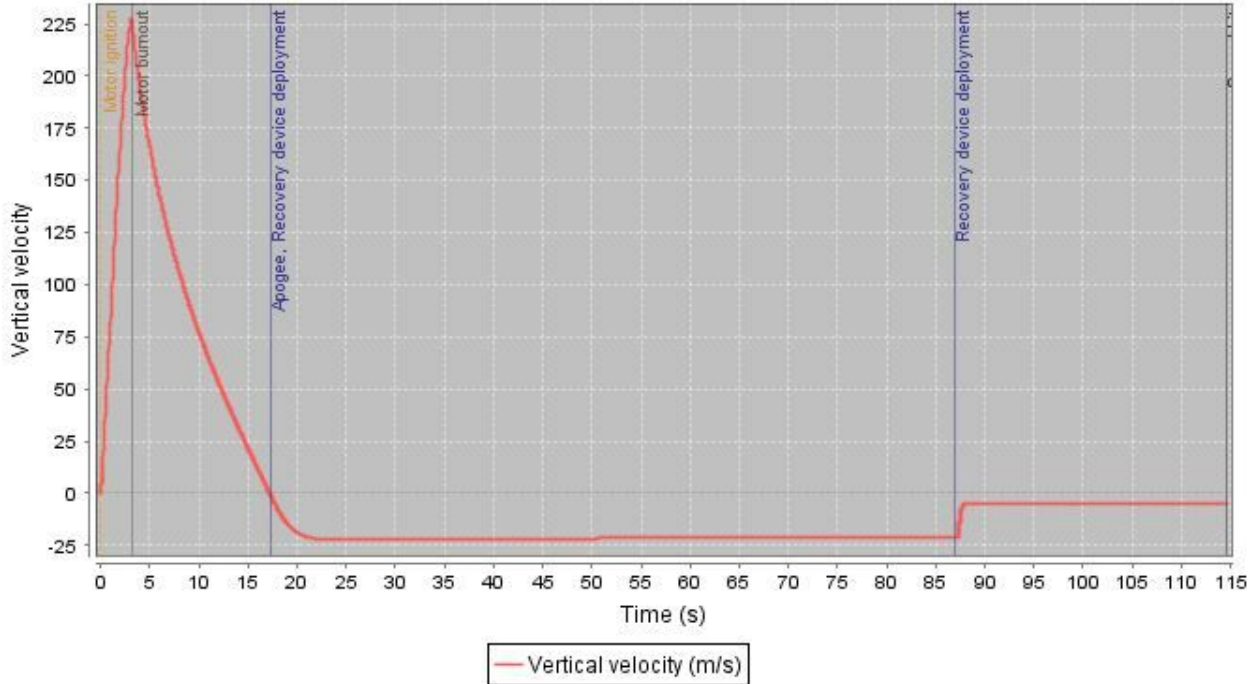


Figure 3.4.4.2 Graph of Vertical velocity vs. Time

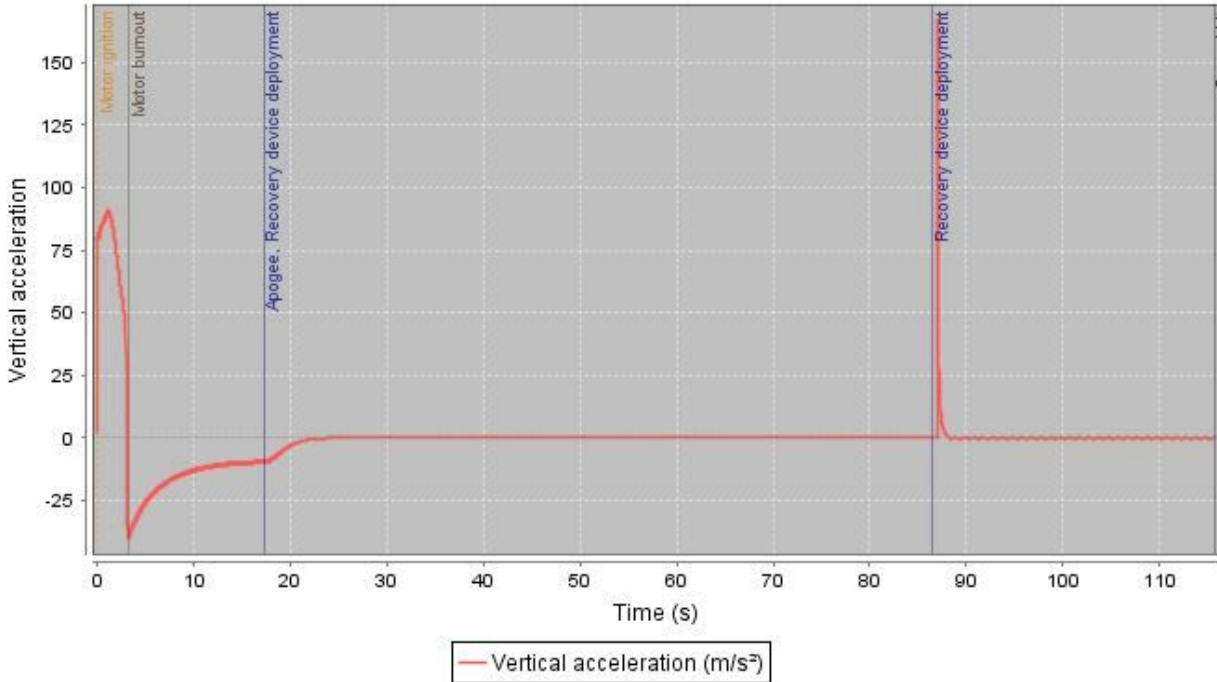


Figure 3.4.4.2 Graph of Vertical acceleration vs. Time

Various weather conditions were also tested on launch vehicle flight simulations in an attempt to prepare the vehicle for a number of conditions. Wind speed and launch elevation were the two main focuses of these weather condition simulations. The team found that launch elevation was directly proportional to flight apogee as previously expected. The launch elevation was set to approximately 620 feet to prepare for the elevation change in Huntsville, Alabama. It was also found that wind speed was inversely proportional to final flight apogee of the vehicle. As wind speed in the simulator increased, the apogee of the launch vehicle decreased.

The team analyzed the data and created vehicle modifications in specified areas in order to accommodate for the possible weather conditions.

3.4.5 Mass Statement

Table 3.4.5.1 Mass Statement of Rocket Sections

Section	Mass (lbs)
Nosecone	1.925
Payload/Electronics	2.59
Fore Airframe	4.445
Fin Can	8.145
Motor	6.1

Throughout the course of the build we anticipate a mass growth of about 10% to account for the use of epoxy, unaccounted for bulkheads and centering rings, and other miscellaneous components. However for all current components considered, they were either directly weighed, based off of dealer specifications, or calculated from preexisting knowledge. Moving forward we believe that we have a margin of error of about 3 additional pounds past the 10% mass increase before our rocket is in danger of not being able to fly with our current motor.

3.4.6 Launch Requirements and Solutions

Table 3.4.6.1 Launch Vehicle Requirements from Student Launch Handbook

Requirement Number	Description	Design	Verification
1.1	The vehicle shall deliver the payload to an apogee altitude of 5,280 feet above ground level (AGL).	The structural design and motor selection will be determined around the projected altitude.	The design shall be verified via simulation, calculations, and finally testing
1.2	The vehicle shall carry one commercially available, barometric altimeter	The launch vehicle will have two barometric RRC3 altimeters.	The design shall be inspected and tested.
1.3	The launch vehicle shall be designed to be recoverable and reusable.	The launch vehicle will engage a dual stage parachute recovery system that will limit the kinetic energy of all components upon impact.	The recovery system will be analyzed, inspected, simulated, and tested.
1.4	The launch vehicle shall have a maximum of four (4) independent sections.	The launch vehicle will have three independent sections upon recovery after aft bay separation and nosecone/payload separation.	The requirement will be reflected in design.
1.5	The launch vehicle shall be limited to a single stage.	The launch vehicle will have one stage.	The requirement will be reflected in design.
1.6	The launch vehicle shall be capable of being prepared for flight at the launch site within 2 hours.	The team will have launch day procedures that will be practiced to ensure launch on schedule.	The requirement will be reflected in design and practice.
1.7	The launch vehicle shall	All sensitive equipment	The requirement

	be capable of remaining in launch-ready configuration at the pad for a minimum of 1 hour without losing the functionality of any critical on-board component.	will be adequately protected.	shall be met in design and tested.
1.8	The launch vehicle shall be capable of being launched by a standard 12 volt direct current firing system.	The launch vehicle will be developed to work with standard 12 volt ematches.	The requirement shall be met in design and verified in testing.
1.9	The launch vehicle shall use a commercially available solid motor propulsion system using ammonium perchlorate composite propellant (APCP)	The team will purchase a commercially available APCP motor.	The requirement will be met in design.
1.10	The total impulse provided by a launch vehicle shall not exceed 5,120 Newton-seconds (L-class)	The team will purchase a commercially available L-class motor.	The requirement will be met in design.
1.11	Pressure vessels on the vehicle shall be approved by the RSO	No pressure vessels will be used in the launch vehicle.	The requirement will be met in design.
1.12	All teams shall successfully launch and recover a subscale model of their full-scale rocket prior to CDR.	The subscale rocket was launch 12/20/2015 successfully with a follow up launch planned for 1/15/16	The requirement shall be met in testing.
1.13	All teams shall successfully launch and recover their full-scale rocket prior to FRR in its	A full-scale launch in its final configuration is scheduled for 2/20/2015.	The requirement shall be met in testing.

	final flight configuration.		
1.14	Each team will have a maximum budget of \$7,500 they may spend on the rocket and its payload(s).	A detailed budget will be followed to ensure that the project remains under the maximum budget.	The requirement will be verified in inspection.
1.15	Vehicle Prohibitions.	No prohibited items will be used in the launch vehicle	The requirement will be verified in design.
2.1	The launch vehicle shall stage the deployment of its recovery devices, where a drogue parachute is deployed at apogee and a main parachute is deployed at a much lower altitude.	The recovery system will deploy a drogue at apogee and a main chute at 500 feet AGL.	The requirement will be verified in design and verified in testing.
2.2	Teams must perform a successful ground ejection test for both the drogue and main parachutes.	Ejection systems will be tested prior to launch.	The requirement will be met in testing.
2.3	At landing, each independent section of the launch vehicle shall have a maximum kinetic energy of 75 ft-lbf.	Simulations and hand calculations will be done to ensure a low maximum kinetic energy on impact.	The requirement will be met in calculation, simulation, and testing.
2.4	The recovery system electrical circuits shall be completely independent of any payload electrical circuits.	The recovery system will be managed by the RRC3 altimeters.	The requirement will be met in design.
2.5	The recovery system shall contain redundant, commercially available	The recovery system will use two RRC3 altimeters.	The requirement will be met in design.

	altimeters.		
2.6	Motor ejection is not a permissible form of primary or secondary deployment.	Motor ejection will not be utilized.	The requirement will be met in design.
2.7	A dedicated arming switch shall arm each altimeter, which is accessible from the exterior of the rocket airframe when the rocket is in the launch configuration on the launch pad.	Each altimeter will have a dedicated key switch available on the outside of the rocket.	The requirement will be met in design.
2.8	Each altimeter shall have a dedicated power supply.	Each altimeter will have one dedicated 9 volt battery.	The requirement will be met in design.
2.9	Each arming switch shall be capable of being locked in the ON position for launch.	The key switches used will be able to be locked in an on position.	The requirement will be met in design and verified in testing.
2.10	Removable shear pins shall be used for both the main parachute compartment and the drogue parachute compartment.	Shear pins will be used at separation points at the fore and aft bay.	The requirement will be met in design and verified in testing.
2.11	An electronic tracking device shall be installed in the launch vehicle and shall transmit the position of the tethered vehicle or any independent section to a ground receiver.	A TeleGPS will be implemented with the altimeter in electronics bay.	The requirement will be met in design and verified in testing.
2.12	The recovery system electronics shall not be	All electronic systems will be properly	The requirement will be met in design and

	adversely affected by any other on-board electronic devices during flight	integrated, shielded, and have appropriate cable management.	verified in testing.
--	---	--	----------------------

Table 3.4.6.2 Launch Vehicle Requirements as set forward by USF SOAR

Requirement Number	Description	Design	Verification
S1	The payload will be able to seal completely with no protrusions.	The design of the payload will focus on uniform closure with a linear actuator and paired sections.	The requirement shall be met in inspection, analysis, and testing.
S2	The parachutes will not be damaged by the ejection charge.	The chutes will both have Kevlar chute protectors separating them from the black powder charges.	The requirement shall be met in inspection, analysis, and testing.
S3	The parachutes shall not break off from the rocket after separation.	Appropriate weighted shock cord will be used in addition to checking all fastening systems and associated yield stresses.	The requirement shall be met in inspection, analysis, and testing.
S4	All epoxied sections, including centering rings and bulkheads will be able to withstand max thrust of the motor.	Calculations shall be done to determine the max shear strength of all epoxied sections.	The requirement shall be met in inspection, analysis, and testing.
S5	All components of the rocket will be held together until the time of separation.	Appropriate shear pins will be utilized.	The requirement shall be met in inspection, design, and testing.

3.5 Interfaces and Integration

3.5.1 Payload Bay System



Figure 3.5.1.1 Payload Containment System

The payload bay containment system was designed with integration in mind from the very start, using stock rocket components as a structure and choosing appropriate electronics and custom parts with these parameters. However for the payload bay system integration to be considered a success the following criteria must be met:

1. The system must be able to fit within the traditional volume of a payload bay, i.e 4 inch diameter and 24 inches in length.
2. All components must be capable of access from outside the rocket, or to be manipulated by the AGSE system.
3. The system must be able to function while the rocket is secured on a launch rail.
4. The system cannot adversely affect vital systems such as recovery or the altimeter bay.
5. The system must have it's own power source.
6. The system cannot interfere with vital rocket events such as launch, parachute deployment, or locating the launch vehicle.

With our design criteria in mind our team set out to build the system in a way that best reflected these constraints. The ultimate linear actuator system to detailed in section 4, can be inserted into the fore airframe as with any other payload bay. Furthermore radio control will allow the actuator to interact with the AGSE. Due to the simple design the payload containment system should not interfere with flight nor any other rocket systems.

3.6 Subscale Flight Verification and Results

3.6.1 Testing Plan

In order to test the stability and performance of our full scale design the team designed and fabricated a 3:4 scale rocket to be flown on a lower impulse motor. In lieu of the electronics and MAV payload that will be included in the full scale rocket, dead weight was placed in the payload bay of the subscale in order to simulate the mass. Laser cut Baltic birch plywood fins were used on the subscale as opposed to the G10 fins to be used on the full scale.

In order for the test to be considered a success the subscale rocket must be recoverable in a condition that would allow it to be relaunched, and all recovery separations must be completed successfully without jamming or tangling.

The subscale launch served a secondary purpose as an inaugural launch for new members to introduce them to safety procedures and launch protocol.

3.6.2 Launch Vehicle Characteristics

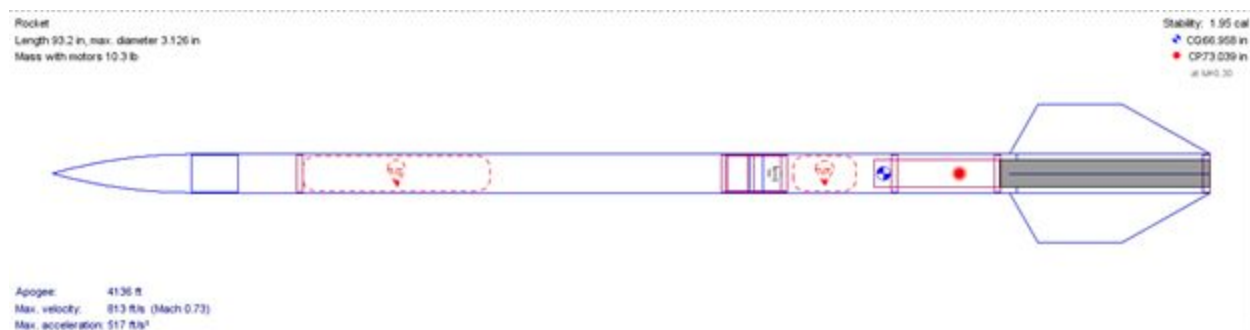


Figure 3.6.2.1: Subscale Launch Vehicle Configuration

The vehicle configuration was made similar enough to ensure that the test would yield adequate results for our team to consider for our full scale design, the subscale vehicle characteristics are listed in the table below.

Table 3.6.2.1: Subscale Vehicle Characteristics

Length (in)	93.2
Mass (Loaded/Empty) (lbs)	10.3/7.14
Projected Altitude (ft)	4136
Projected Max Velocity (ft/s)	813
Stability (cal)	1.95

3.6.3 Simulations

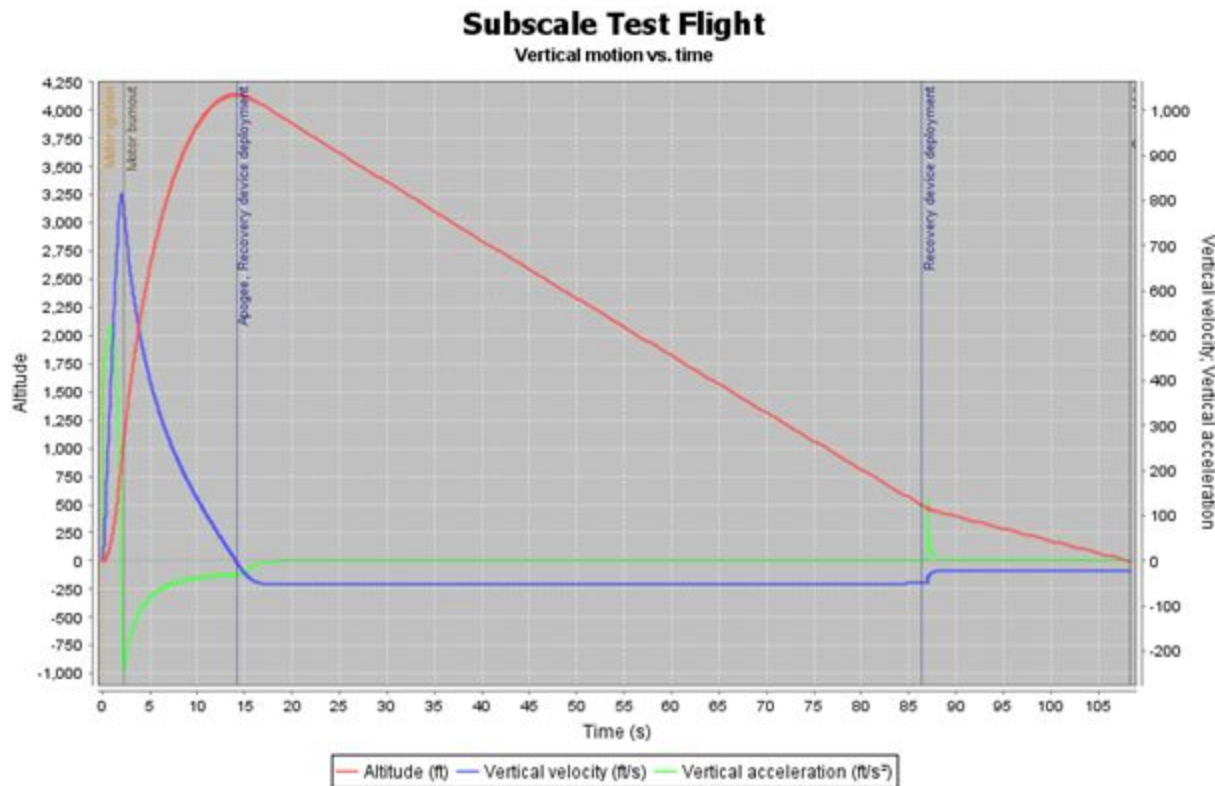


Figure 3.6.3.1: Subscale Flight Simulation

The above figure is the OpenRocket simulation that was run for the subscale design, showing a projected altitude of 4136 feet.

3.6.4 Testing Report and Post Flight Review

The rocket was launched to an altitude of 4092 feet with successful separation at apogee and the main parachute deploying at 500 feet. This tested altitude shows a 1.06% degree of error with the projected altitude of 4136 feet, validating OpenRocket's accuracy in ideal condition. Ultimately we believe that this was a successful test, validating our fabrication techniques and showing the overall stability and success of our design.

3.7 Safety

3.7.1 Safety Officer Responsibilities

Safety is critical at the Society of Aeronautics and Rocketry and the University of South Florida in its entirety. While our Safety Officer actively ensures the well-being of members and property, our entire team is expected to maintain constant awareness of all potential dangers. SOAR members are briefed of the potential hazards in our project and encourage them to voice any concerns.

The roles and responsibilities of the safety officer include, but are not limited to:

A. Monitor all team activities with an emphasis on safety, including:

- 1) Design of launch vehicle and Autonomous Ground Support Equipment (AGSE)
- 2) Creation of launch vehicle and AGSE
- 3) Set-up of launch vehicle and AGSE
- 4) Exhaustive ground testing of launch vehicle and AGSE
- 5) Sub-scale launch test(s)
- 6) Full-scale launch test(s)
- 7) Competition activities and launch
- 8) Recovery Activities
- 9) Educational Engagement Activities

B. Coordinate and implement the safety procedures outlined by the organization for the design, creation, set-up, launch, and recovery of the launch vehicle as well as the design, creation, set-up, and use of the AGSE.

C. Finding the relevant Material Safety Data Sheets (MSDS), sharing them with organization, and maintaining the appropriate folder in the organization's Google Drive, Material Safety Data Sheets. The Safety Officer will also ensure proper and safe conditions of materials during storage, transport, and implementation.

D. Analyze and record the team's hazard analysis tests, failure mode analysis, simulations, experimental data, and other relevant information sources for failures and potentially hazardous trends. As well as coordinating the compliance with safety procedures and improvements to reduce risk.

- E. Assist in the management and development of the team's hazard analysis, failure mode analysis, safety simulations, safety procedures, and guidelines.
- F. Maintaining responsible and appropriate organizational behavior at all stages of design, development, test, travel, and launch.
- G. Finally, the safety officer is expected to become familiar with all TRA, local, state, and federal laws, rules, customs, and regulations which apply to the use and transportation of motors, propellants, and other sources of risk. Based on this familiarity the safety officer is expected to ensure compliance with the aforementioned regulations.

3.7.2 Team Safety Procedures

Team Safety

A team safety meeting will be held before all tests and launches to ensure that all members are aware of all safety regulations. Each member is required to review all safety procedures and each member is responsible for remaining up to date on any updates to safety regulations.

Any member found to be in violation of any safety procedure at any time while working on the project will receive a verbal warning for the first violation. Should a member violate any safety procedures more than once, they will become ineligible to work on the project until their probation is appealed. Continued minor offenses or serious hazardous risks will make a given member ineligible to continue work on projects or participate directly in testing or launches until otherwise noted.

Hazard Recognition

The team Safety Officer will orchestrate all potentially hazardous activities, as well as brief the members who may participate in such activities on proper safety procedures, and ensuring that they are familiar with any personal protective equipment which must be worn during those activities. If a member fails to abide by the safety procedures, he will not be permitted to participate in the potentially hazardous activity. In addition to briefing the members on safety procedures, the team Safety Officer must remain in the immediate vicinity of the hazardous activity as it is occurring, so as to mitigate any potentially dangerous incidents and answer any safety questions which may arise

3.7.3 Launch Procedures

Pre-Launch Briefing

Prior to all launches, all attending members will be briefed on potential hazards and avoidance measures to be taken. The topics covered in each briefing will be as follows:

- Review of launch site regulations while emphasizing awareness of surroundings by all members
- Review of all relevant laws and/or regulations mandated by the Federal Aviation Administration, the National Fire Protection Association, Florida State Statutes, and Tripoli Rocket Association
- Draw attention to any hazards that may arise due to environmental conditions on the particular launch day
- Address any hazards that have not been mitigated and/or may be encountered during launch
- Delegate launch day checklists to appropriate individuals to ensure that all tasks are completed

Launch Day Operating Procedures

1. Prepare a table and safe area to begin prepping the rocket for launch.
2. All paracord should be pretied to eye bolts prior to arriving at the launch field. Attach the main and drogue chute to the center of their respective cords using a parachute knot, have advisor check before continuing.
3. Have mentor apply 3.5 g of black powder to the drogue blast tube, fill with flame retardant wadding and cover with a blast cap, do the same with the main blast tube with 4 g of black powder.
4. Ensure switch is in off position and attach batteries to the altimeters, the rocket should be handled with extreme care at this point.
5. Fully assemble rocket with shear pins.
6. Motor should be prepared before arrival at the field, have mentor visually inspect the motor.
7. Insert motor into motor mount, with safety goggles, carefully apply snap ring.
8. Screw cap on motor retainer.
9. With multiple people carefully slide rocket onto launch rail and raise to position.
10. Insert igniter into motor.
11. Turn on altimeters and wait for the three beeps confirming it is active.
12. Retreat to a safe distance and after RSO countdown ignite rocket.

13. If a problem occurs see NAR/TRA Personnel Duties below for appropriate response
14. After the field is opened by the RSO go to retrieve the rocket, careful to avoid the hot motor.
15. Inspect for damage or dislodged components, and listen for the altitude.

NAR/TRA Personnel Duties for Launch

The following launch procedure will be followed during each test launch. This procedure is designed to outline the responsibilities of the NAR/TRA Personnel and the members of the team.

1. A level 2+ certified member and an NAR/TRA Personnel will oversee any test launch of the vehicle and flight tests of the vehicle
2. The launch site Range Safety Officer will be responsible for ensuring proper safety measures are taken and for arming the launch system
3. If the vehicle does not launch when the ignition button is pressed then the RSO will remove the key and wait 90 seconds before approaching the rocket to investigate the issue. Only the project lead and safety officer will be allowed to accompany the RSO in investigating the issue
4. The RSO will ensure that no one is within 100 ft of the rocket and the team will be behind the RSO during launch. The RSO will use a 10 second countdown before launch.
5. A certified member will be responsible for ensuring that the rocket is directed no more than 20 degrees from vertical and ensuring that the wind speed is no more than 5 mph. This individual will also ensure proper stand and ground conditions for launch including but not limited to launch rail length, and cleared ground space. This member will ensure that the rocket is not launched at targets, into clouds, near other aircraft, nor taking paths above civilians. As well this individual will ensure that all FAA regulations are abided by.
6. Another certified member will ensure that flight tests are conducted at a certified NAR/TRA launch site.
7. The safety officer will ensure that the rocket is recovered properly according to Tripoli and NAR guidelines.

4) AGSE/Payload Criteria

4.1 Systems Overview

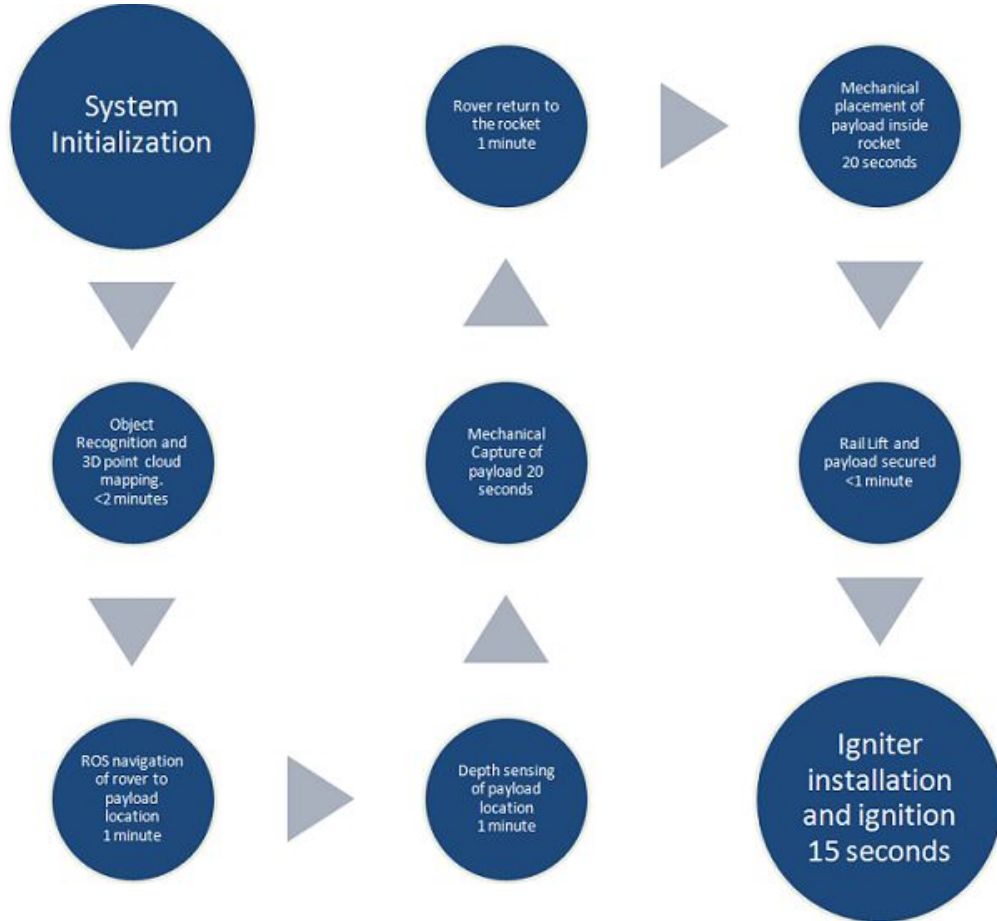
The AGSE must follow these requirements to ensure success

1. Team will place the launch vehicle in the horizontal position on the AGSE.
2. A master switch will be used to power on all autonomous procedures to be carried out.
3. A pause switch will be activated, temporarily halting all AGSE procedures and subroutines.
4. Once the launch vehicle has been inspected by the launch services official and grants permission to launch, a switch will then be activated to enable final launch procedures.
5. The Launch Control Officer will activate a hard switch, then provide a 5-second countdown.
6. At the end of the countdown, the LCO will activate the launch button to initiate the launch.
7. All AGSE systems shall be autonomous.
8. The system must suffer no delays once the launch switch is activated.
9. The system must complete all tasks within 10 minutes.
10. The capture/containment system must be able to retrieve the payload from 12 inches away from the vehicle MOLD line and from the ground.
11. No forbidden technologies will be used, such as
 - a. Components that rely on Earth's magnetic field
 - b. Sound-based sensors
 - c. Earth-based or Earth-orbit based radio aids
 - d. Open Circuit pneumatics
 - e. Air breathing systems

Along with the requirements above, the following requirements regarding the controls must be met for success.

1. A master switch to power all systems of the AGSE, where the switch must be easily accessible and hardwired into the AGSE.
2. A pause switch to temporarily shut down all actions carried out by the AGSE. The pause switch must be easily accessible and hardwired into the AGSE.
3. A safety light that indicates that the AGSE is powered on.

4.1.1 System Timeline



4.1.1.1 Figure describing the time allocated to each operation throughout the payload capture. The above times are estimations based on research and inspection.

4.2 Payload Capture and Containment

4.2.1 Overview

The objective of this system is to grasp the payload from the required position, raise it up to the launch vehicle's level, and then insert the payload into the specified payload bay of the rocket. For successful payload capture, a mechanical arm was designed to mount to the AGSE or to a possible rover that will retrieve the payload. The arm will start in a retracted position, and when activated, will extend 12 inches to the placed payload. The gripper assembly at the end of the arm will carefully grasp the payload. The arm will then rotate around its base, raise up to the payload bay of the rocket, and then be safely inserted into the payload bay. The payload bay will be directed by the system system to close when the payload is in place.

4.2.2 Design

The design of our payload capture and containment system is simple for the most part. It consists of 5 degrees of freedom and is constructed out of 304 stainless steel. Each component was carefully considered, being designed to ensure stability when arm is in motion. Placement of servo motors was considered, mirroring the mechanics of a human arm. Bottom plate of the base structure is designed to have the capability to be mounted to a rover or another structure.

Height (in)	Length (in)	Width (in)	Mass (lbm)
19.64	15.14	2.18	3.97

Figure 4.2.2.1: General dimensions of payload arm

4.2.2a Base Structure

The Base Structure of our robotic arm is 95mm in diameter with 4 appendages used to secure the structure to another object mobile or static. See figure 4.2.2a.1 below.

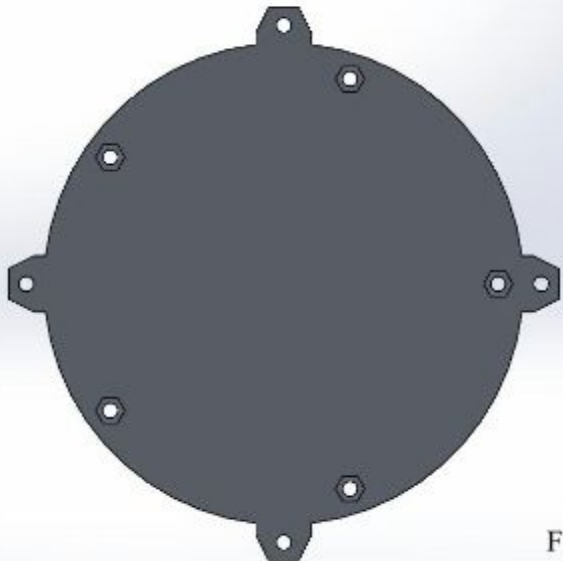


Figure 4.2.2a.1: Base Structure

The completed base structure can be seen below which includes 5 metal pillars which allow for a servo to be placed on the bottom of the top plate. The servo placed here will be used to rotate the entire structure 360 degrees thus giving us the first degree of freedom.

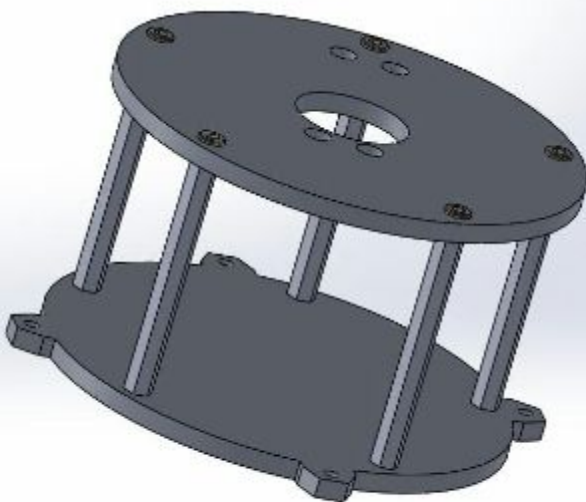


Figure 4.2.2a.2 Completed Base Structure

4.2.2b Shoulder Joint (2nd Degree of freedom)

The shoulder joint is designed on a base plate, which is mounted to the base structure. There are two long plates, each connected to a rotating servo, allowing the plates to swing up and down. This grants the second degree of freedom.

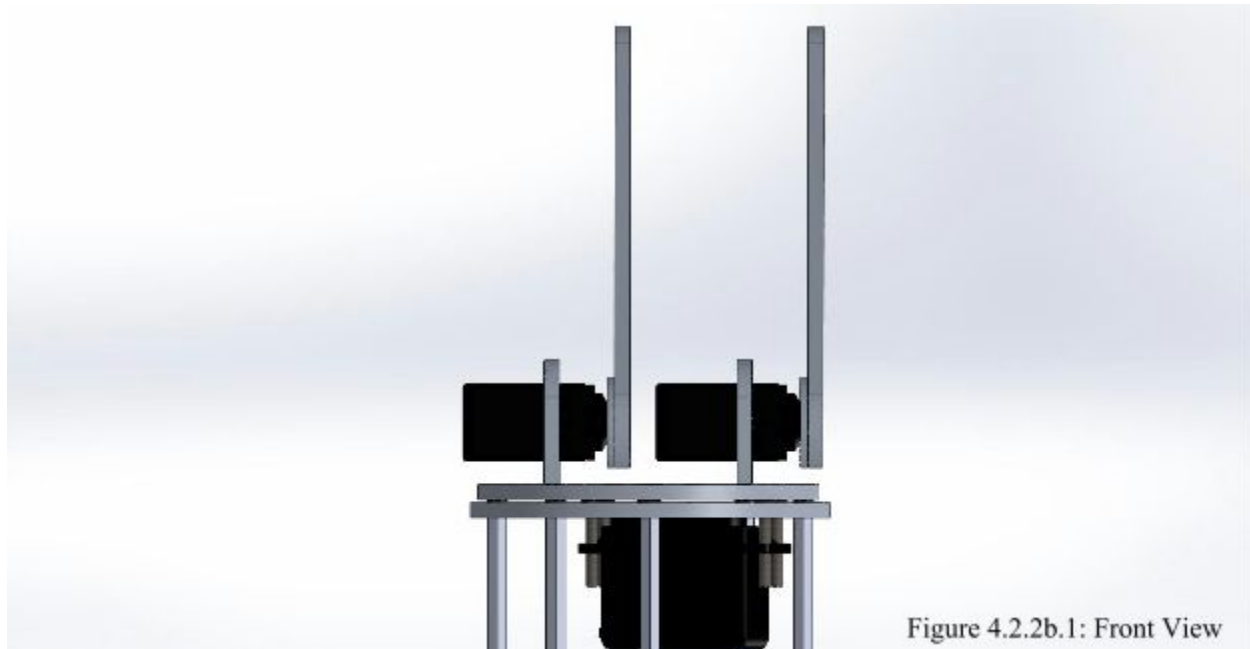


Figure 4.2.2b.1: Front View

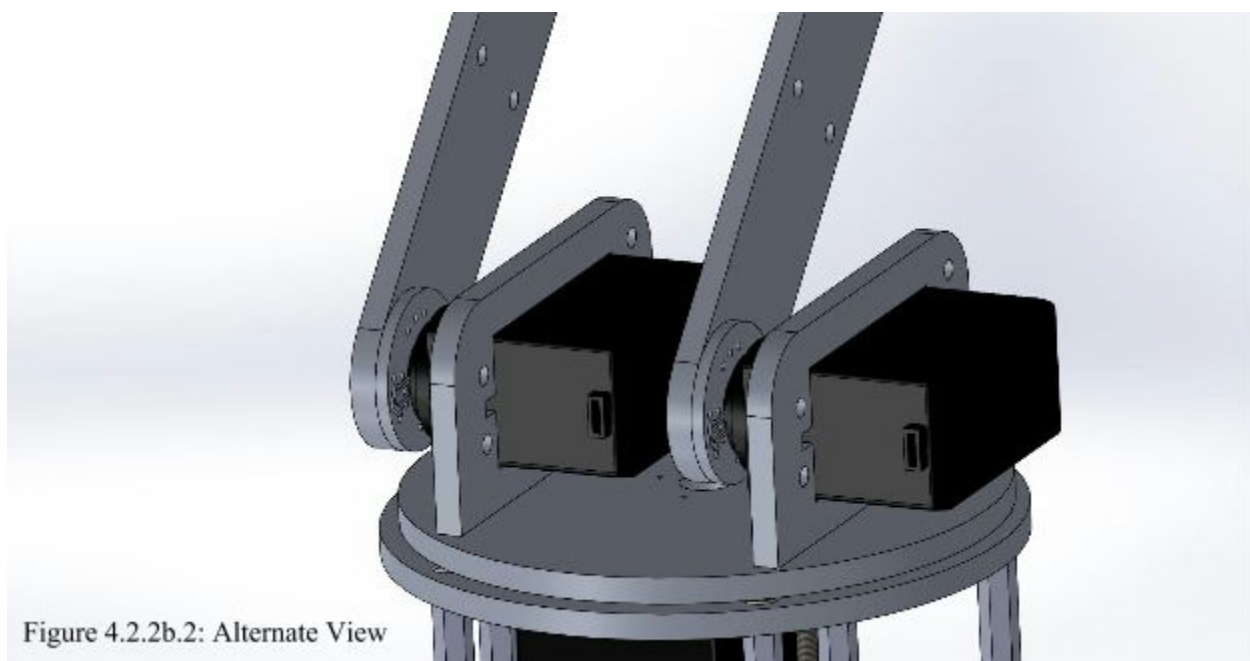


Figure 4.2.2b.2: Alternate View

4.2.2c Elbow Joint (3rd Degree of freedom)

The elbow joint provides the third degree of freedom. Mounted in between the two plates from the shoulder joint, the elbow joint contains one servo, allowing 180 degree rotation. The rotation allows the mechanical arm to extend and retract for proper payload retrieval.

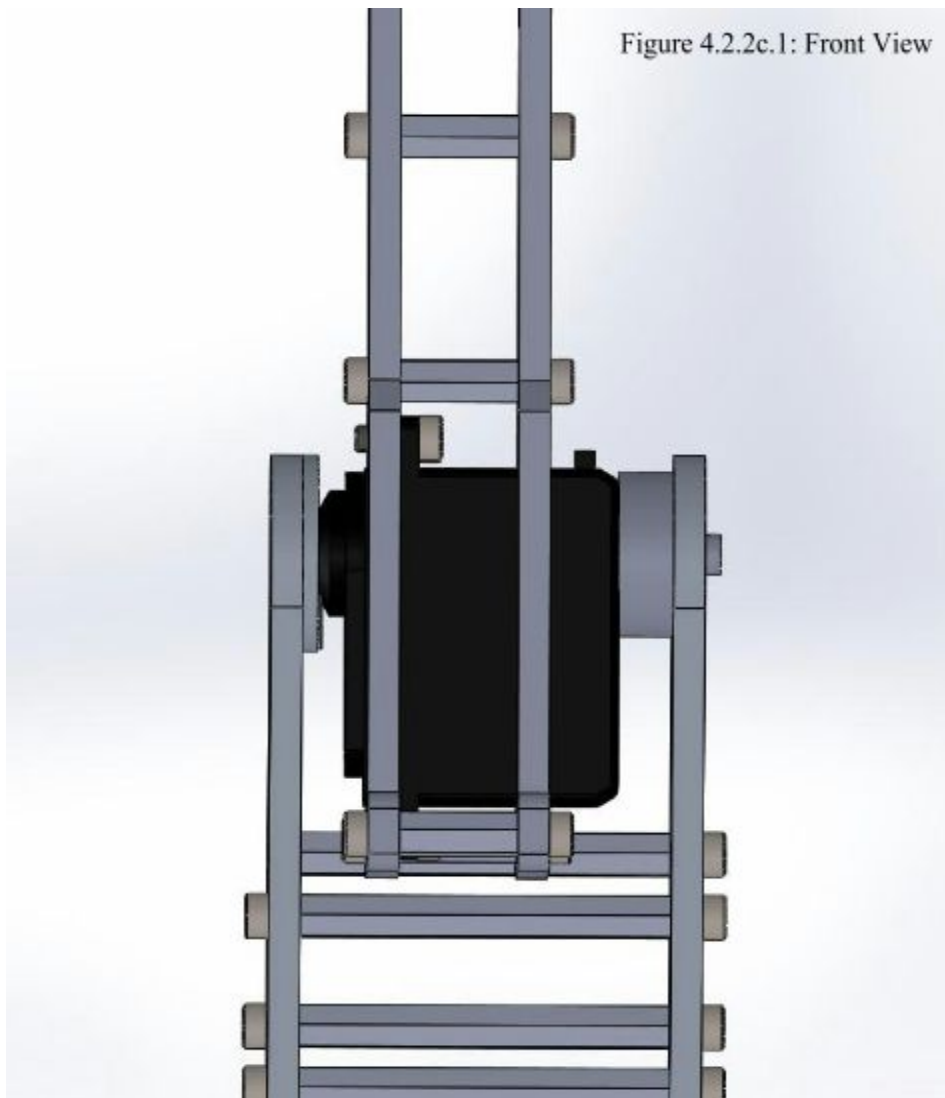




Figure 4.2.2c.2: Alternate View

4.2.2d Wrist Joint (4th & 5th Degree of freedom)

The wrist joint contains the last two degrees of freedom. One servo is mounted in between the plates from the elbow joint, allowing the end of the arm, or hand, to swing up and down. At the end of the wrist joint is a micro servo, which will allow the gripper to rotate 180 degrees. The micro servo grants the capability of twisting.

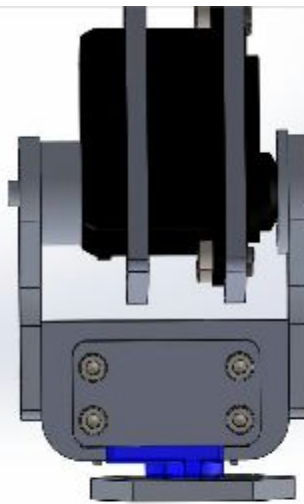


Figure 4.2.2d.1: Top View

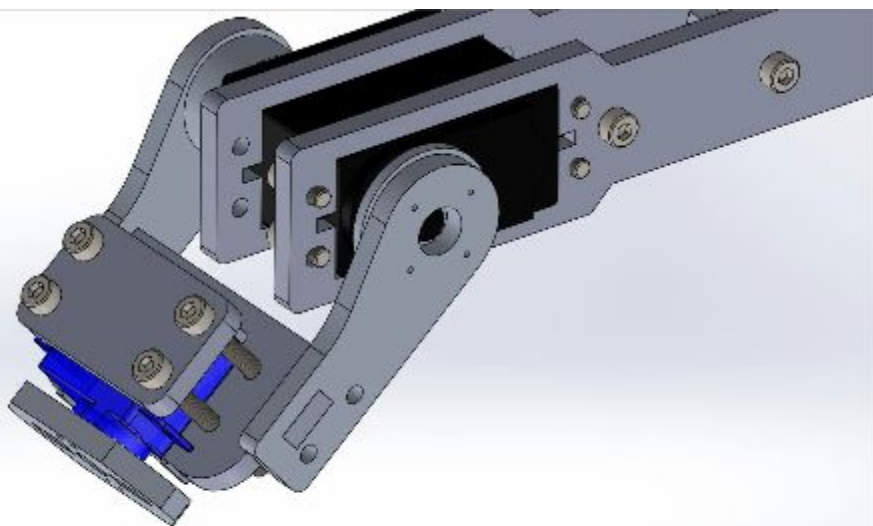


Figure 4.2.2d.2: Alternate View

4.2.2e Gripper Assembly

The gripper assembly consists of two four tooth gears which are turned by one micro servo on the bottom of the left gear. The design is meant to be a simple way to pick up the payload. In Figure 4.2.2e.1 You can see a top view of the gripper assembly which shows the gears and gripper appendages.

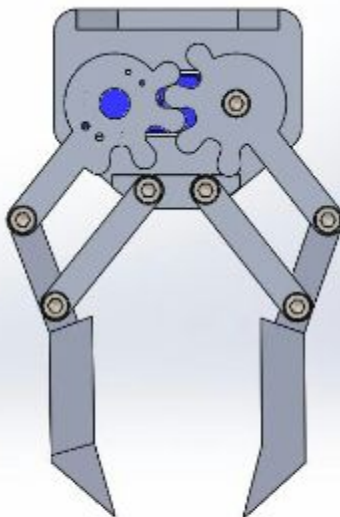


Figure 4.2.2e.1: Top View

Here in the alternate view we can see where the servo will turn the left gear which in turn opens and closes the gripper assembly.

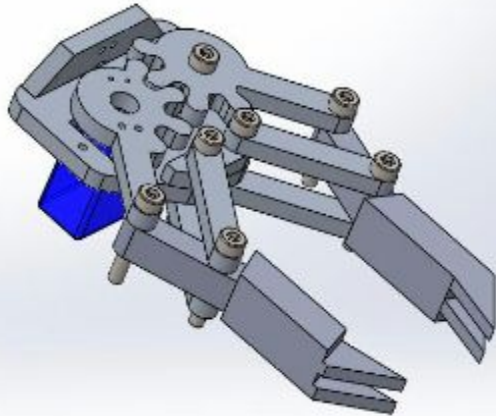
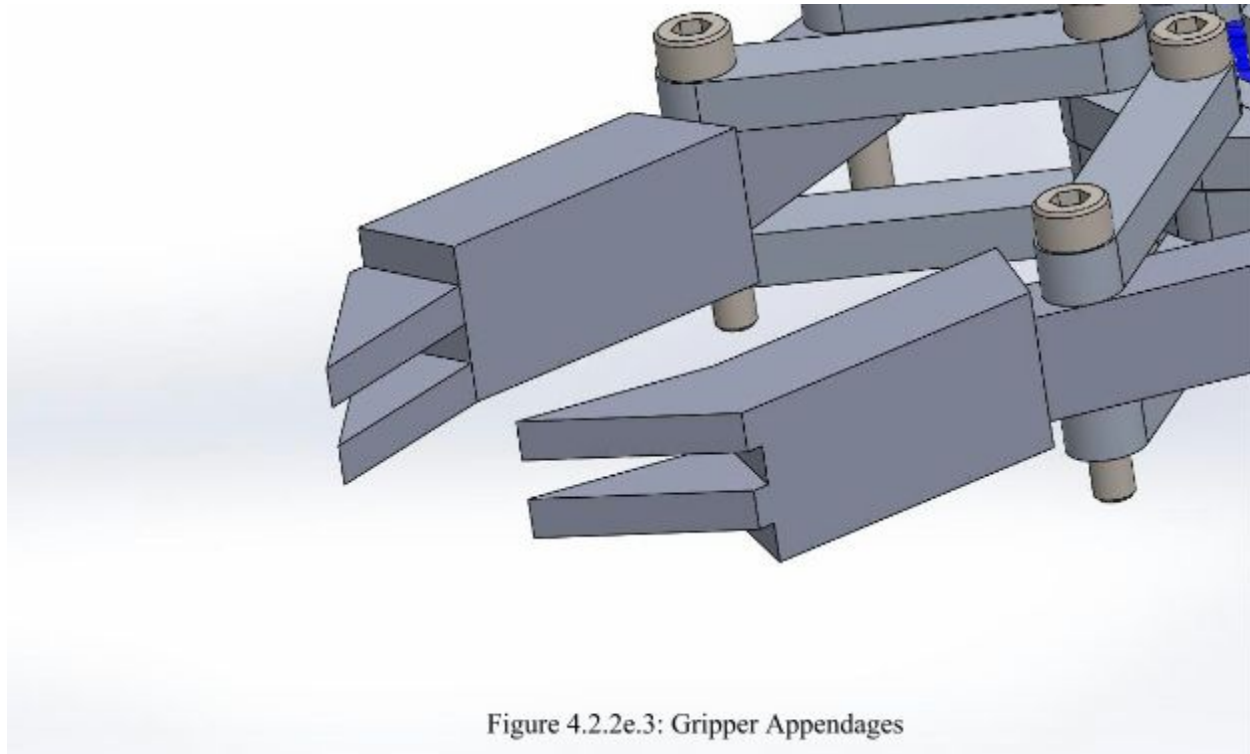


Figure 4.2.2e.2: Alternate View

Finally in Figure 4.2.2e.3 You'll notice the gripper appendages. The gripper appendages are designed to interlock with each other upon closing. They are angled in such a way to direct the cylindrical payload up and into their grasp. The angle and interlocking design allows for a more secure hold, decreasing chances of slip. The grippers were also designed so that they can not only pick up the cylindrical object we were tasked to pick up, but can easily pick up a plethora of different objects.



4.2.2f Complete Robotic Arm

The final design of our robotic arm can be seen below in Figure 4.2.2f.1. You'll notice that all of the preceding parts and assemblies have been assembled into one complete robotic arm.

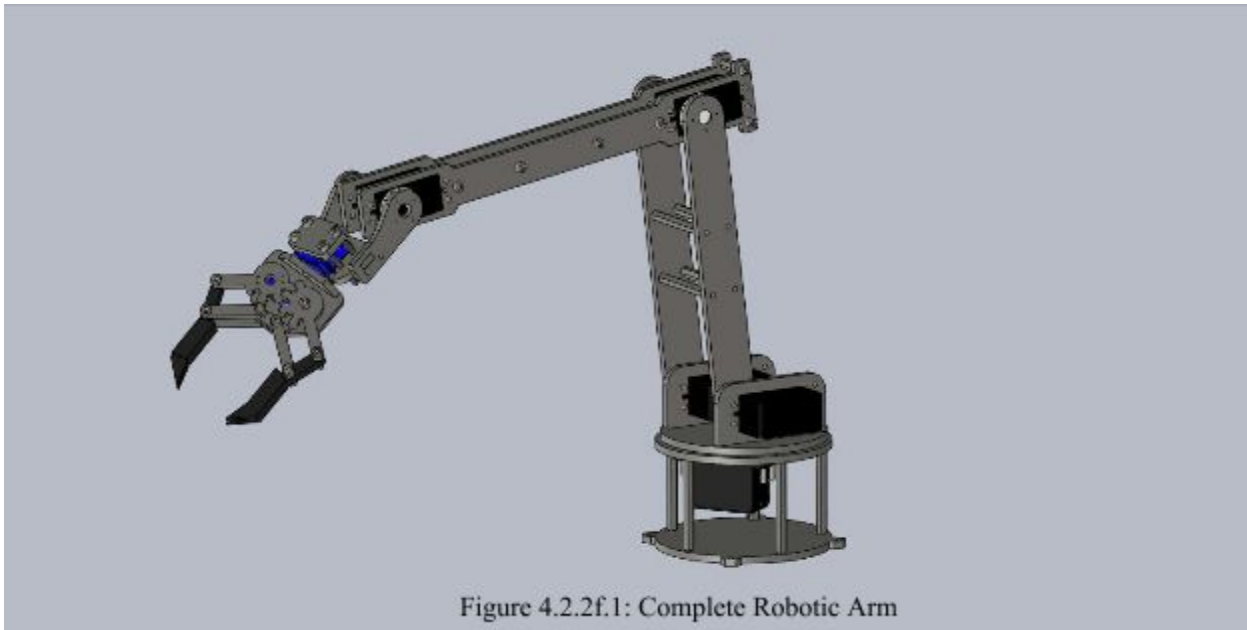


Figure 4.2.2f.1: Complete Robotic Arm

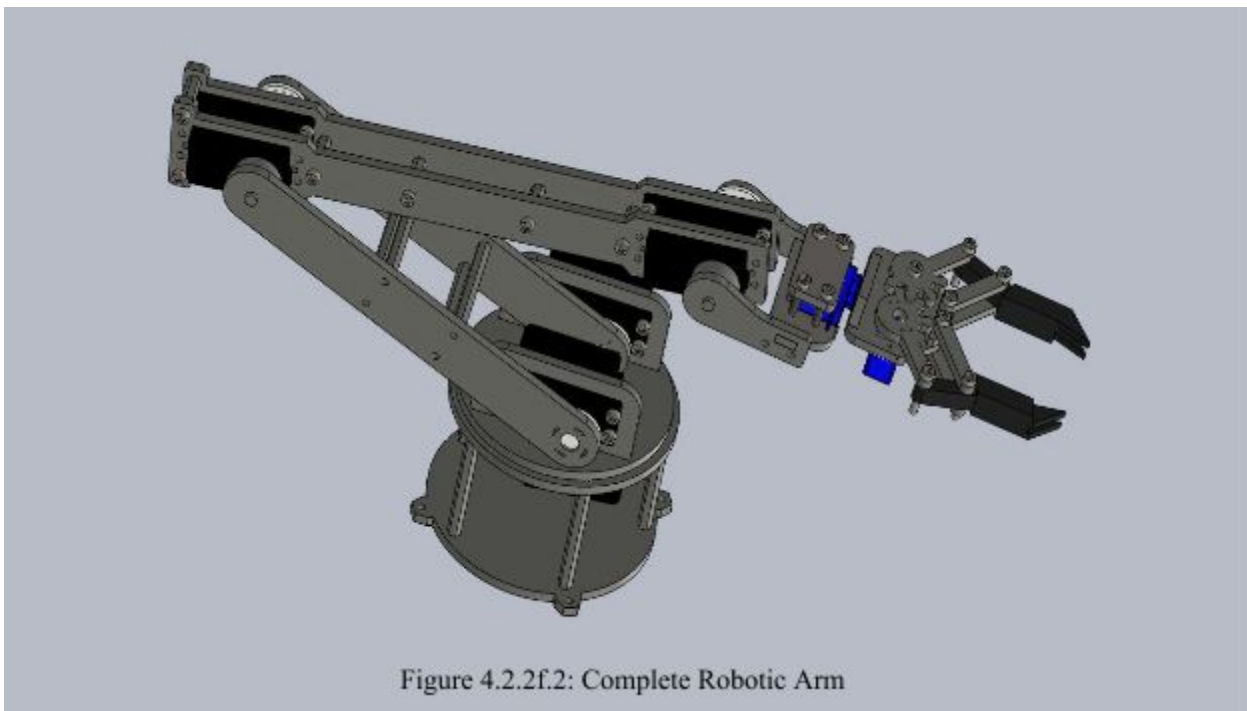


Figure 4.2.2f.2: Complete Robotic Arm

4.2.2g Wheel

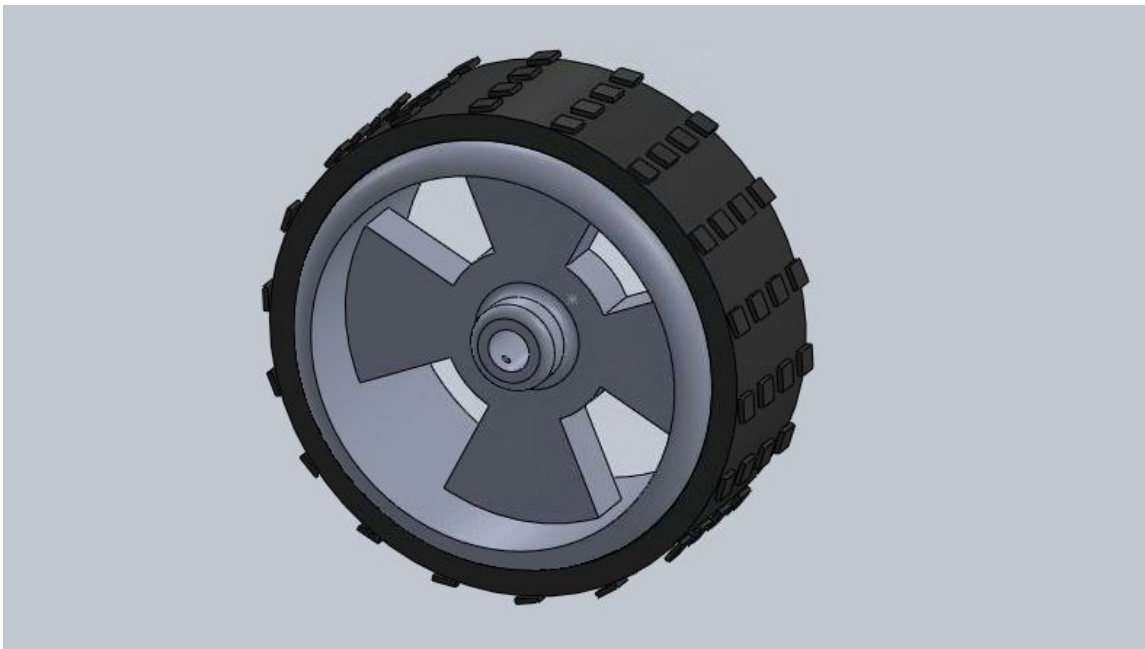


Figure 4.2.2g.1: Outer Wheel

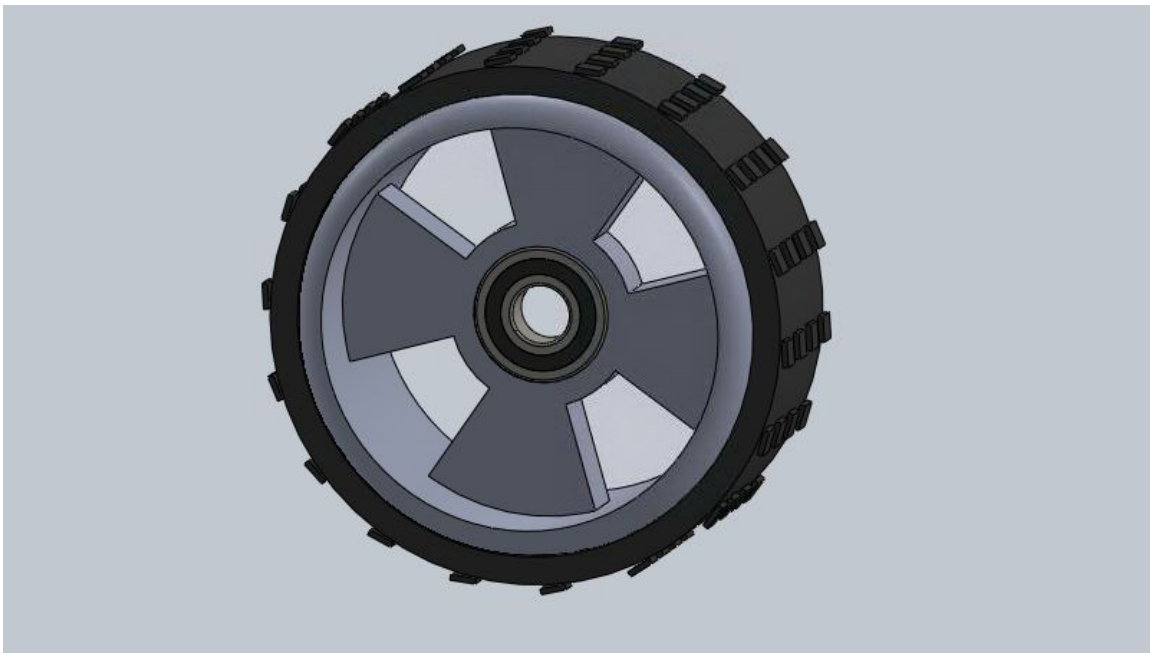


Figure 4.2.2g.2: Inner Wheel and Bearing

The wheels designed by the USF SOAR team feature rubber treading for safe navigation over uncertain terrain, a four inch outer diameter, a steel frame, and an attachment hole for affixing the motor securely to the wheel. We have designed two wheel designs, one for the outer motorized wheels and another for the inner caster wheels. They both feature unique attachments to the rover suspension system. The outer wheels will connect to the motor through a bolt firmly threaded against a flat end of the motor shaft, while the inner wheels will feature an axle running through the bearing, with washers on both sides, and a nut on the exterior end.

4.2.2h Suspension System

Our team decided to use NASA's tried and true model for our simulated planetary rover. Therefore we modeled our rover after the past Mars exploration rovers, a fitting tribute to the Mars Ascent Vehicle challenge. We experienced the struggles firsthand of designing a Rocker-Bogie suspension system. While a plethora of examples exist to study, the trials of designing a novel Rocker and Bogie system still provided a formidable challenge for our young team.

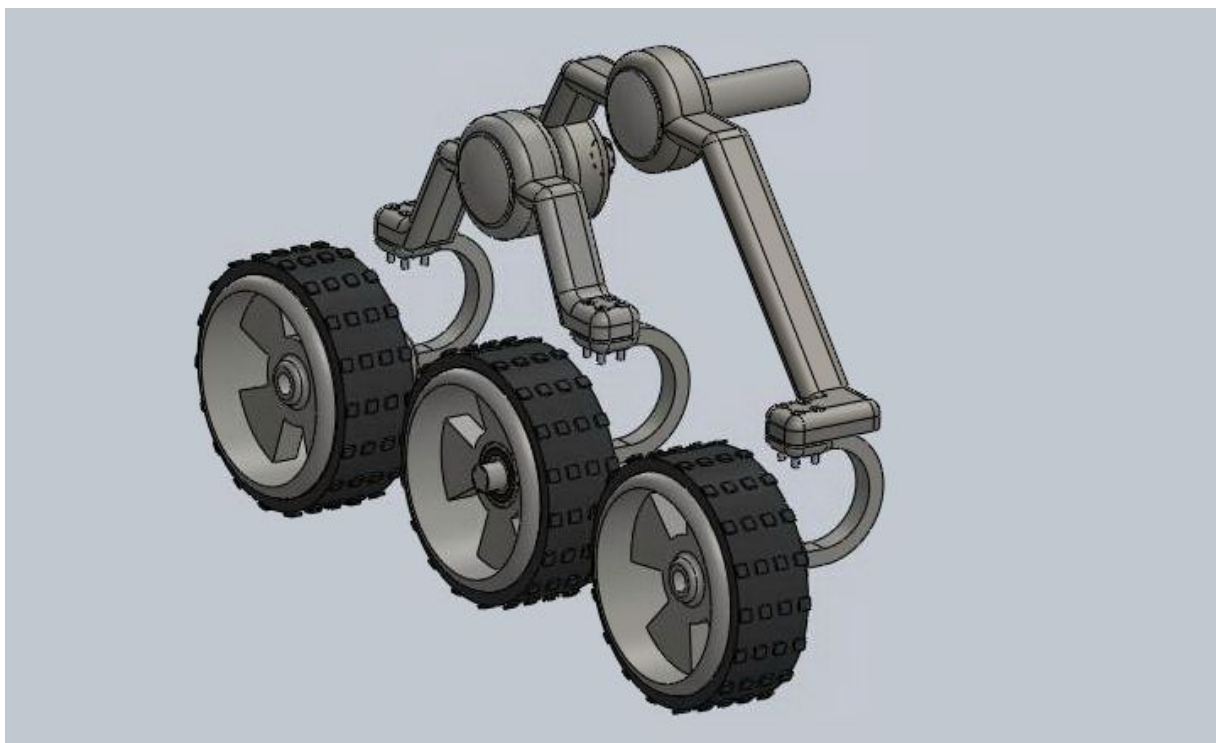


Figure 4.2.2h.1: Rocker-Bogie Suspension

One half of the Rocker-Bogie suspension design can be seen above, where many notable features can be analyzed. Most saliently, the large Rocker connecting to the Bogie beneath it will provide a wide angle of movement for the ability to overcome obstacles, a trademark feature of any successful robotic planetary exploration platform. A deviating feature from our rover to the

NASA rovers that can be seen in this picture is the free-spinning, nonmotorized middle wheel, while the NASA rovers feature six independently driven wheels. As documented previously this deviation was for compatibility with the Robot Operating System (ROS) differential drive local base controller. Additionally, this frees desperately needed GPIO pins on the Raspberry Pi, more motors and encoders would necessitate more processing and control.

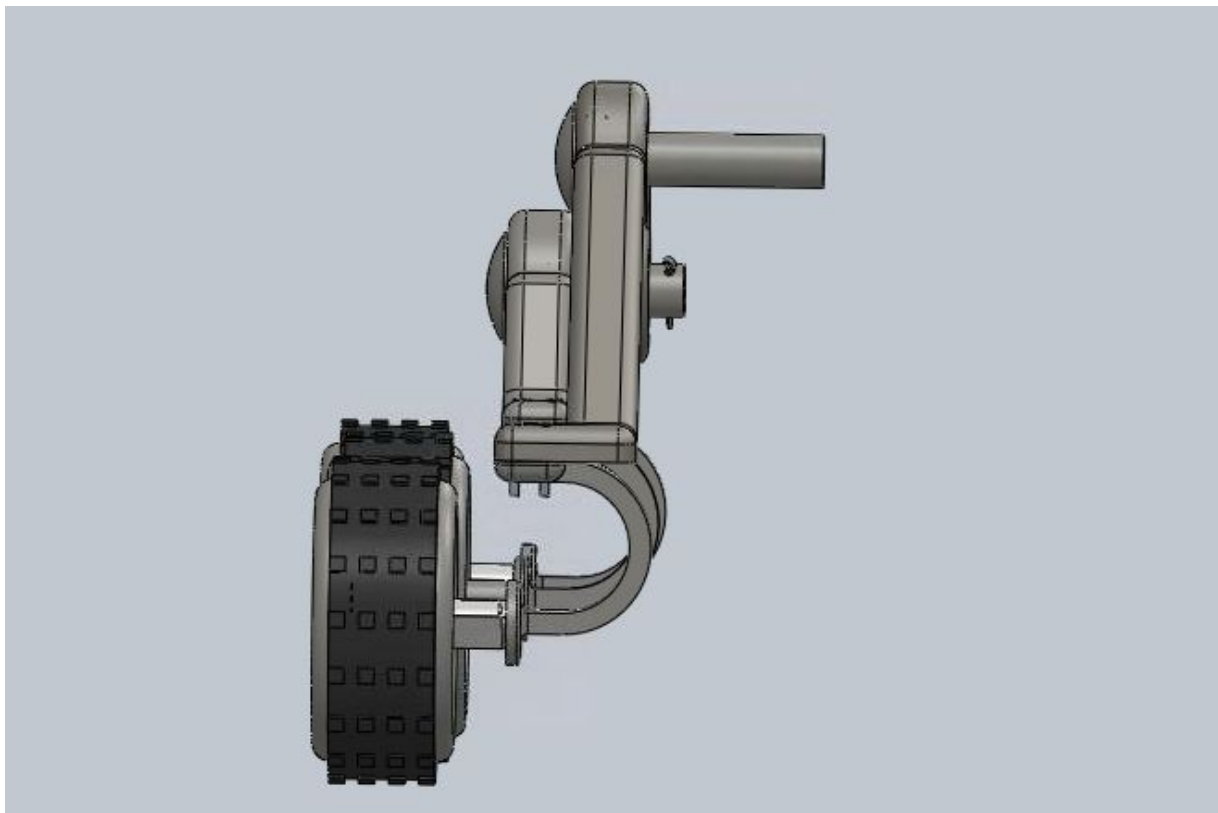


Figure 4.2.2h.2: Side View of Rocker-Bogie Suspension

Here we have a side view, or nearly head-on, of the Rocker-Bogie suspension. This angle allows us to inspect more features of the design. Namely, we can notice that the motor mounts hold one motor each on the outer four wheels. It is important to note that Solidworks has hidden the threading on many screws so that it can retain a low polygon count for faster processing.

4.2.2i Body

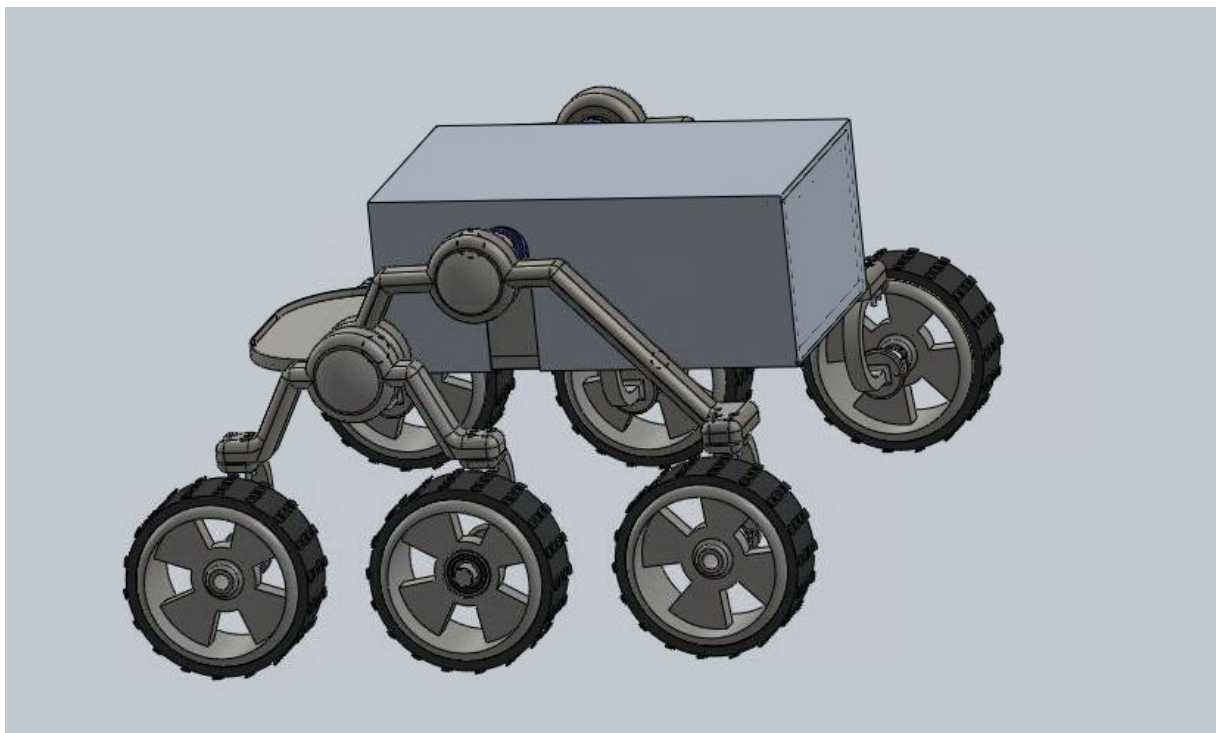


Figure 4.2.2i.1: Rover

A model of the rover can be seen above, this model shows the base where the arm will rest, however it does not currently have the arm bolted on to the front lip designed for it, additionally a Kinect will be mounted on a post above the arm angled slightly down so as to allow the image processing to have an unimpeded view of the local environment as well as for functional acquisition of the payload.

4.2.2j Environmental Concerns

It is a critical step to making a sustainable system that it must doubly minimizes its own impact on its environment and be resistant the constant eroding forces of nature. We take pride in knowing that our all electric automated ground support minimizes its impact on the environment through the use of reusable Lithium batteries and lack of byproducts or waste. Other than the batteries charging through the electrical grid, the only environmental impact of our AGSE system is the crushing by rolling of the wheels over the local environment.

However, our system may be vulnerable to harsh planetary environments such as Mars. While we will be well within safety margins for Huntsville, Alabama, our design would need to be environmentally encapsulated for the harsher environments. Dust, grit, sand, dirt, and various

other particles that may be introduced by the environment, as well as extreme temperatures, winds, water contact and other environmental features can degrade the structure of the platform over time. In extreme conditions, such as Mars, the length of time required to critical failure will be severely reduced. This is especially true if the delicate sensors and electronics become exposed to these forces of erosion. Proper shielding can safely protect the sensitive components and prolong their lifespan for exploration missions. However, given the mild Earth conditions at Huntsville, Alabama. A cost/benefit decision was made to forgo extensive shielding in favor of saving cost, reducing increased torque about the center axis by adding mass, and to not unnecessarily increase the power demand on the drive motors.

4.2.3 Fabrication

The fabrication of the Automated Ground Support Equipment includes the following:

1. 3 Hitec metal gear servos delivering anywhere from 107-133oz-in of torque.
2. 2 Hitec karbonite gear servos delivering anywhere from 72-89oz-in of torque.
3. 2 Hitec micro servos delivering anywhere from 15-18oz-in of torque.
4. 304 Stainless Steel
5. Socket Head Cap Screw (M3x0.5x8)
6. Socket Head Cap Screw (M3x0.5x12)
7. Socket Head Cap Screw (M3x0.5x20)
8. Socket Head Cap Screw (M3x0.5x30)
9. 4x Castellated Nuts
10. 4x Cotter Pins
11. Toggle Switch
12. Wireless Electrical Kill Switch Relay
13. Epoxy (J-B Weld)
14. 2x Raspberry Pi

15. 4x DC-DC Buck Voltage Regulators (03100233)

16. 16-Channel 12-Bit Servo Driver (PCA9685)

17. Lithium Polymer or Lithium Ion Battery

18. Kinect

19. 3x Xbee Series 1 RF Communication Module

20. DC Motor Controller (RS011MC)

21. 4x Motors with integrated quadrature encoders

22. SPI IC GPIO Expander (MCP23S17)

23. 8x Radial Ball Bearings

24. Rubber Tire Treading

Complementing the resources offered to our team by the University of South Florida, such as two on campus machining shops, access to an undergraduate engineering lab space fit with tools and components, as well as funding from student government, we also appreciate support offered by the local community. Our mission would be in jeopardy without the communities' support. Our team and NAR advisor, Rick Waters, allows us to use workspace for fabrication at his private workshop. Additionally, we have received a pledge from a local welding company to subsidize and aid the construction of the metal components of our AGSE.

At this stage in the development we have fabricated and successfully launched the subscale rocket design, we have sourced all of the components and submitted the parts list for the full scale launch vehicle. We have begun prototyping various features of the AGSE system, these include a miniature robotic arm for simulation and analysis, the Raspberry Pi for network derivation and testing of the ROS architecture, the servo driving board for integration and testing with the microcontroller, and the Xbee modules to test and verify the capabilities of the communication system. We have also utilized 3D printers for rapid prototyping of mechanical features of the AGSE, such as the differential gear system, and for the final design, such as the gripper appendages.

4.2.4 Mechanics of Solids

4.2.4a Material Properties

The Robotic Arm is made out of 304 stainless steel for its strength to cost ratio. Though it may not be the strongest of metals out there, it is very cost effective. Below in Table 4.2.4.1 you'll see some properties of 304 stainless steel.

Tensile Strength (MPa)	Yield Strength (MPa)	Modulus of Elasticity (GPa)	Poisson's Ratio	Density (g/cm ³)
585	240	193	0.29	7.75

Table 4.2.4.1: Important properties of 304 Stainless Steel

In Figure 4.2.4.2 you'll notice again that 304 stainless steel has a lower yeild point than for instance carbon steel. Carbon steel, though, is much more expensive than 304 stainless steel. Also, the objects that we will be picking up with the robotic arm aren't incredibly heavy and practically speaking, the 304 stainless steel on the robotic arm should never plastically deform.

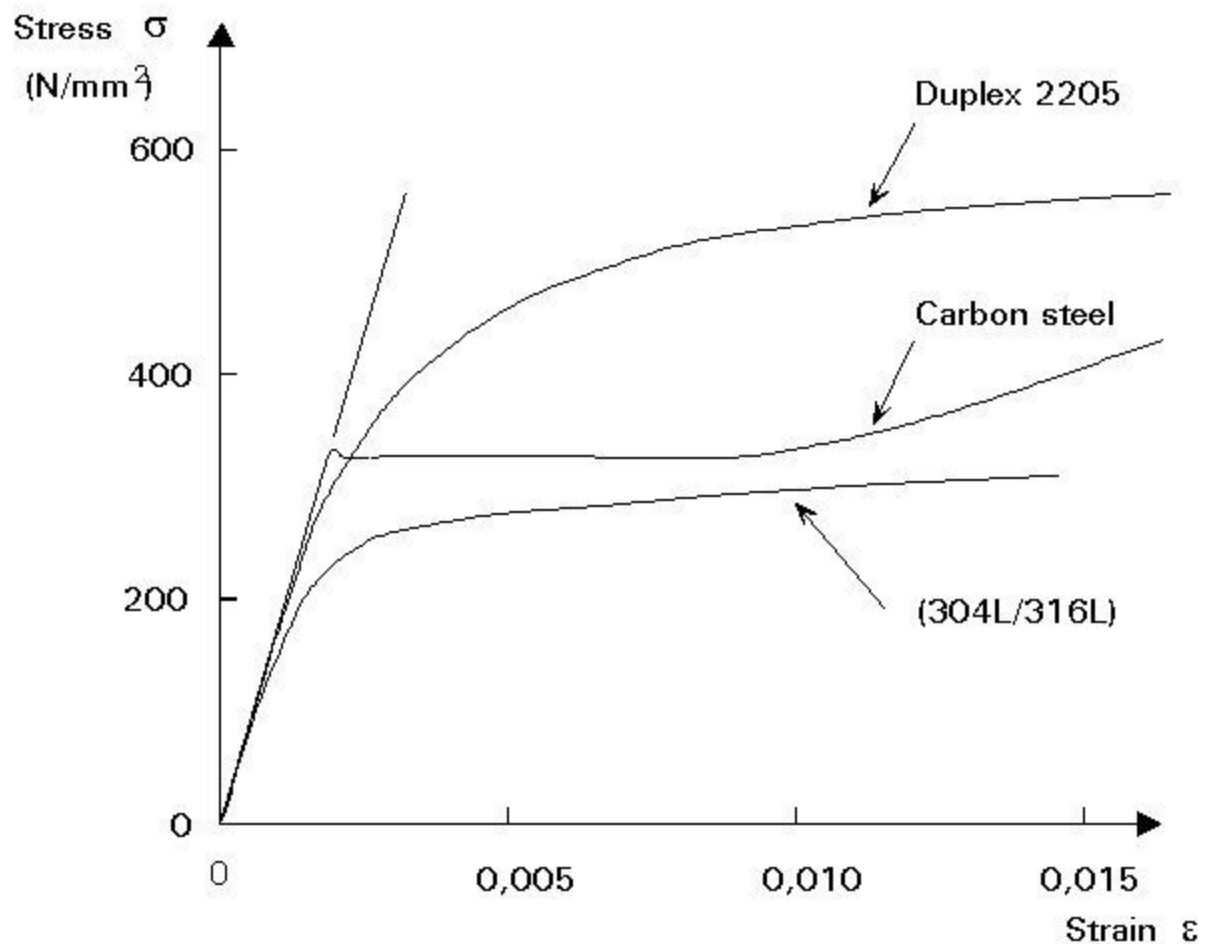


Figure 4.2.4.2: Stress-strain curve for 304 Stainless Steel

4.2.4b Mechanical Torque

A main concern of the design of the rover body is the torque applied on the rover by the weight of the arm, which could cause the rover to tip forward or flip if not balanced by the weight of components in the rear of the rover body. Keeping in mind that force applied further away from the axis of rotation results in a greater torque than a force applied near the axis, the rover has been designed such that its most probable axis of rotation is the axis connecting the two sides of the suspension to the differential gear through the main body. This axis has been placed very close to the arm as to reduce the potential maximum torque caused by the arm's increasing distance from the axis of rotation.

The torque τ caused by a force about a given axis can be calculated by taking the vector cross-product of the position vector \vec{r} pointing from the axis of rotation to the point where the force \vec{F} is acting (which, for a rigid body, can be approximated as the body's center of mass). The primary force applying torque to the rover will be the force of gravity acting on the components of the arm. The vectors \vec{L}_{gi} and \vec{L}_i represent the distance from the joint to the center of gravity for the i^{th} component and the total length of the i^{th} component, respectively. The angles φ_i and θ_i denote the angular degrees of freedom for each segment of the arm, excluding the spin of the wrist which will not significantly contribute to the total length of the arm.

The position vector of each component with respect to the center of mass can be calculated by vector addition, beginning with the vector, \vec{v} , spanning the horizontal distance from the center of mass of the entire system to the origin of motion for the shoulder of the arm. We then continue by summing the relevant vectors for each center of gravity, *exempli gratia*,

$$\begin{aligned}\vec{r}_1 &= \vec{v} + \vec{L}_{g1} \\ \vec{L}_{g1} &= q(L_1 \sin \varphi_1 \cos \theta_1, L_1 \sin \varphi_1 \sin \theta_1, L_1 \cos \varphi_1) \\ \vec{r}_1 &= (qL_1 \sin \varphi_1 \cos \theta_1, qL_1 \sin \varphi_1 \sin \theta_1 + v, qL_1 \cos \varphi_1)\end{aligned}$$

which yields the position vector for center of gravity of the first arm segment with respect to the system's center of gravity.

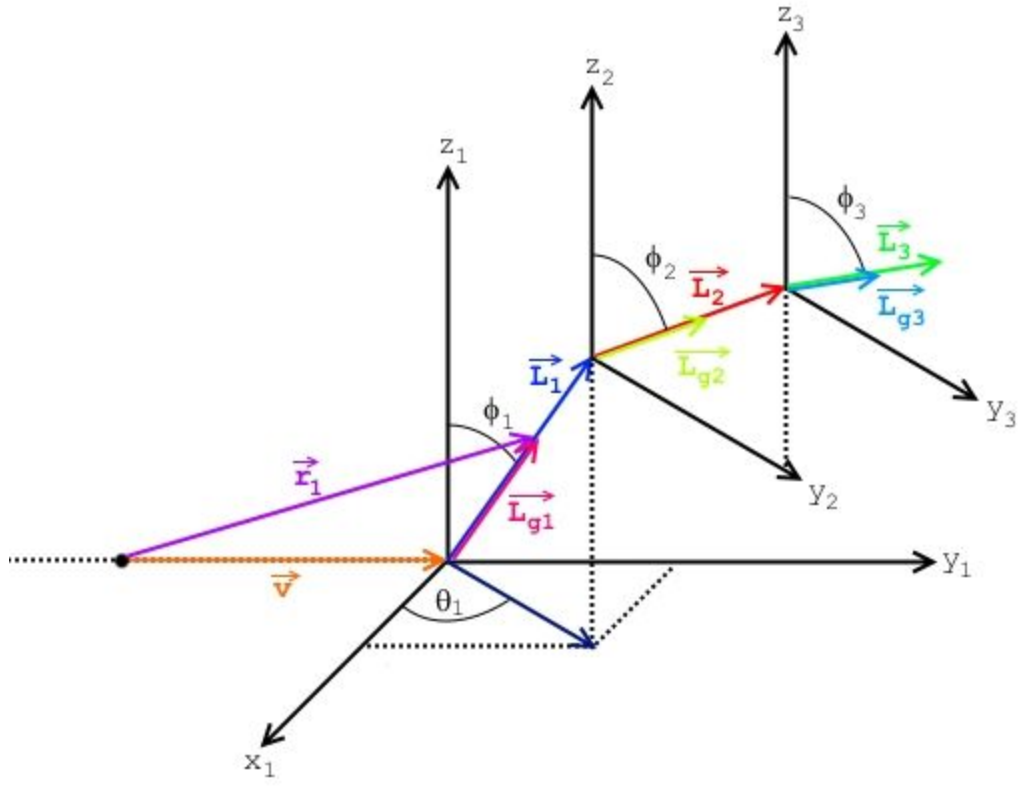


Figure 4.2.4.3: Vector addition diagram of possible arm positions.

After the acquisition of the position vectors, we move on to the evaluation of the cross-product for the torque, keeping in mind that \vec{L}_{gi} is some fraction, q_i , of \vec{L}_i . We have,

$$\vec{\tau} = \vec{r} \times \vec{F} = \vec{r} \times m\vec{g}$$

An analytic form of the torque due to the force of gravity on the i^{th} segment of the arm:

$$\vec{\tau}_i = \vec{r}_i \times \vec{F}_i = (r_{iy}F_{iz} - r_{iz}F_{iy}, r_{iz}F_{ix} - r_{ix}F_{iz}, r_{ix}F_{iy} - r_{iy}F_{ix}) = F_{iz}(r_{iy}, -r_{ix}, 0)$$

where only the z term of \vec{F} remains, because the force here is the force of gravity, which only acts in the negative z direction. For the 1^{st} segment, the torque looks like

$$\vec{\tau}_1 = m_1 g (-q_1 L_1 \sin \phi_1 \sin \theta_1 - v, q_1 L_1 \sin \phi_1 \cos \theta_1, 0),$$

where m_1 is the mass of the first arm segment, and each new segment acquires a few additional terms.

The total torque on the rover about the axle due to the arm can then be calculated by adding all of the torque vectors:

$$\vec{\tau}_{total} = \sum_i \vec{\tau}_i.$$

The torque due to the three main arm segments at a given moment, with respect to their angular positions φ_i and θ_i in their respective coordinate systems, and the fractions q_i of lengths L_i between their joints and centers is:

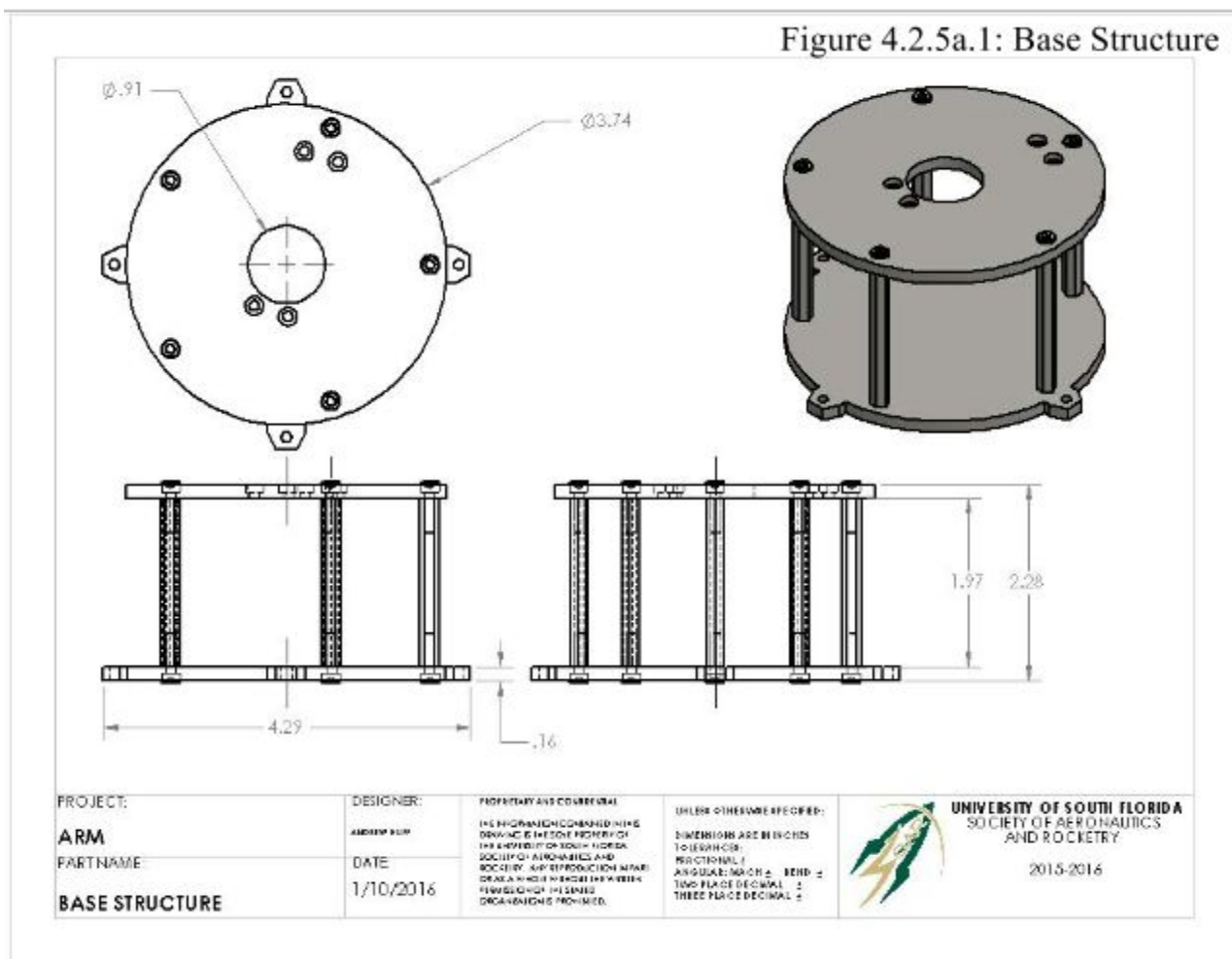
$$\vec{\tau}_{total} = -g [(L_1(q_1m_1 + m_2 + m_3) \sin \varphi_1 \sin \theta_1 + v(m_1 + m_2 + m_3) + L_2(q_2m_2 + m_3) \sin \varphi_2 + L_3q_3m_3 \sin \varphi_3, \\ -L_1 \sin \varphi_1 \cos \theta_1 (q_1m_1 + m_2 + m_3), 0)]$$

4.2.5 Arm Modeling and Schematics

4.2.5a Base Structure

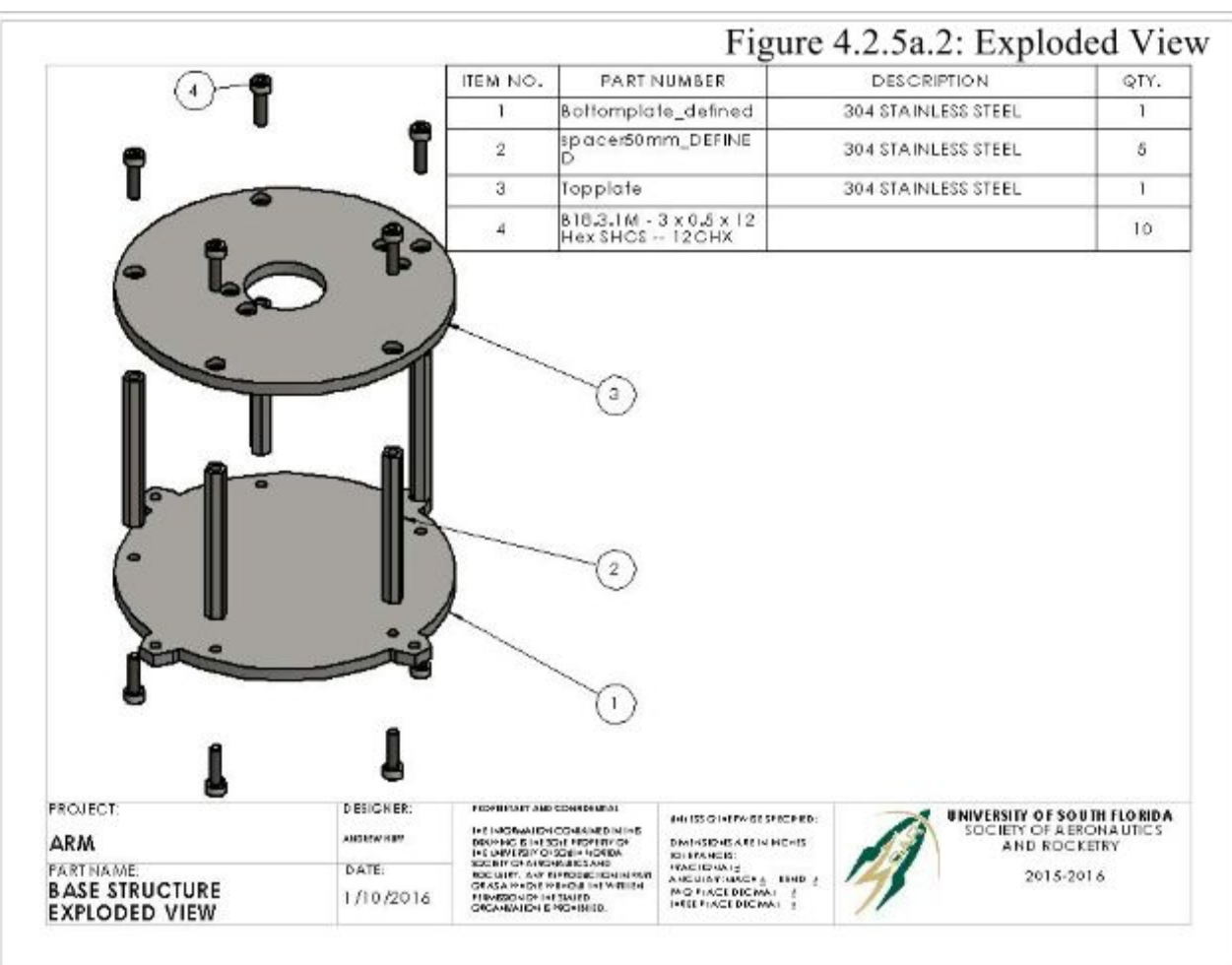
In Figure 4.2.5a.1 below, the Base Structure is shown to have a diameter of 3.74 inches with a inner hole of diameter 0.91 inches. Standing up, it has a total height of 2.28 inches. The bottom plate of this assembly has four small spaces for possibly mounting to a rover or other structure.

Figure 4.2.5a.1: Base Structure



In Figure 4.2.5a.2 below, the Base Structure and all of its components are displayed.

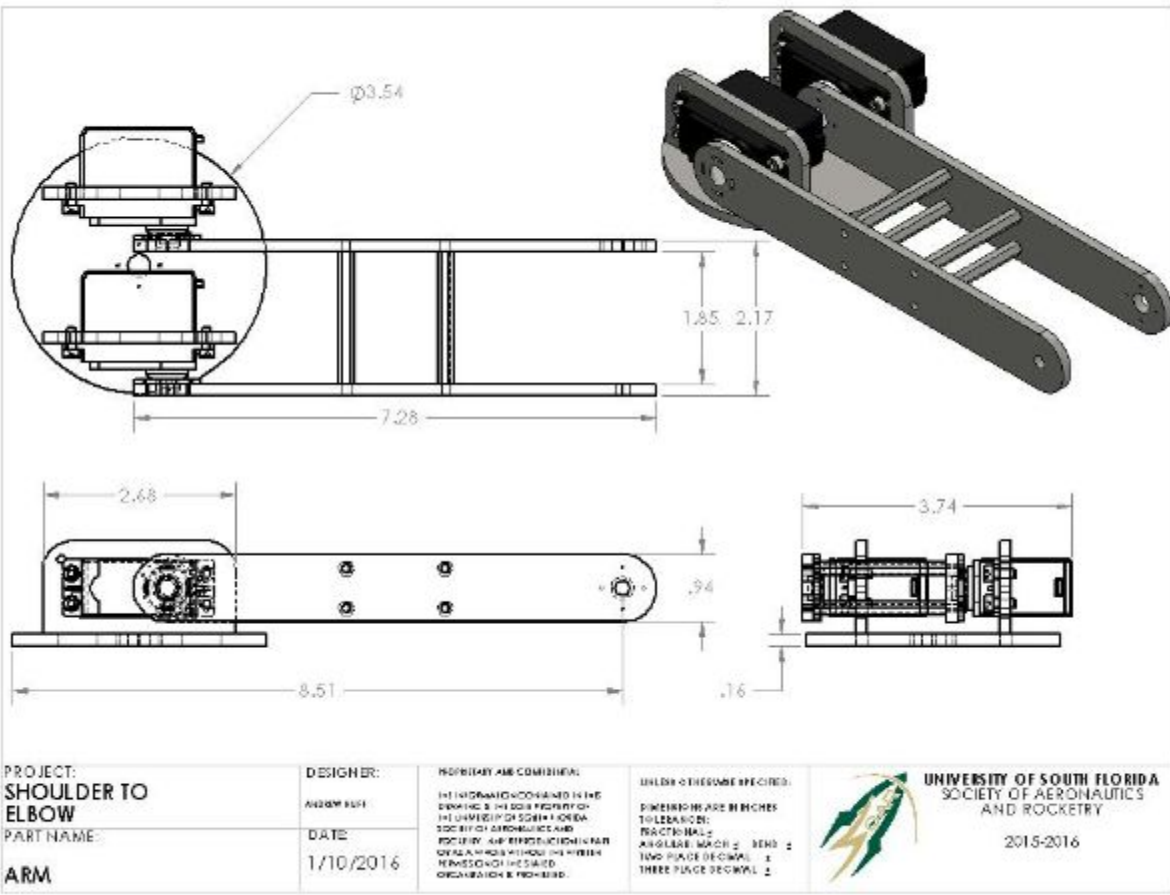
Figure 4.2.5a.2: Exploded View



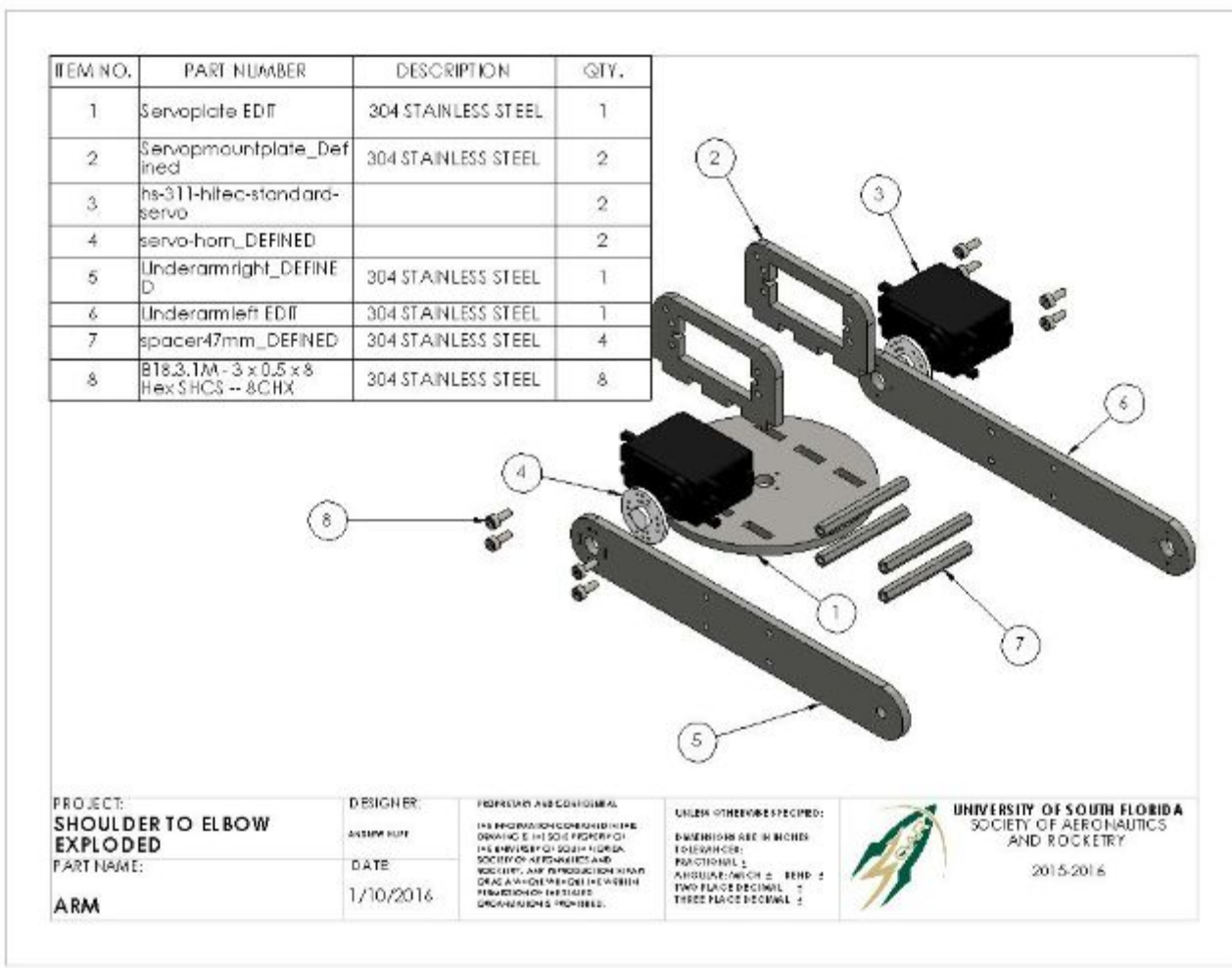
4.2.5b Shoulder to Elbow

Figure 4.2.5b.1 below displays the Shoulder to Elbow assembly. It is constructed of a mounting plate of diameter 3.54 inches and two plates that are 7.28 inches from end to end. The plates are separated a distance of 1.85 inches and have a total width of 2.17 inches.

Figure 4.2.5b.1: Shoulder to Elbow



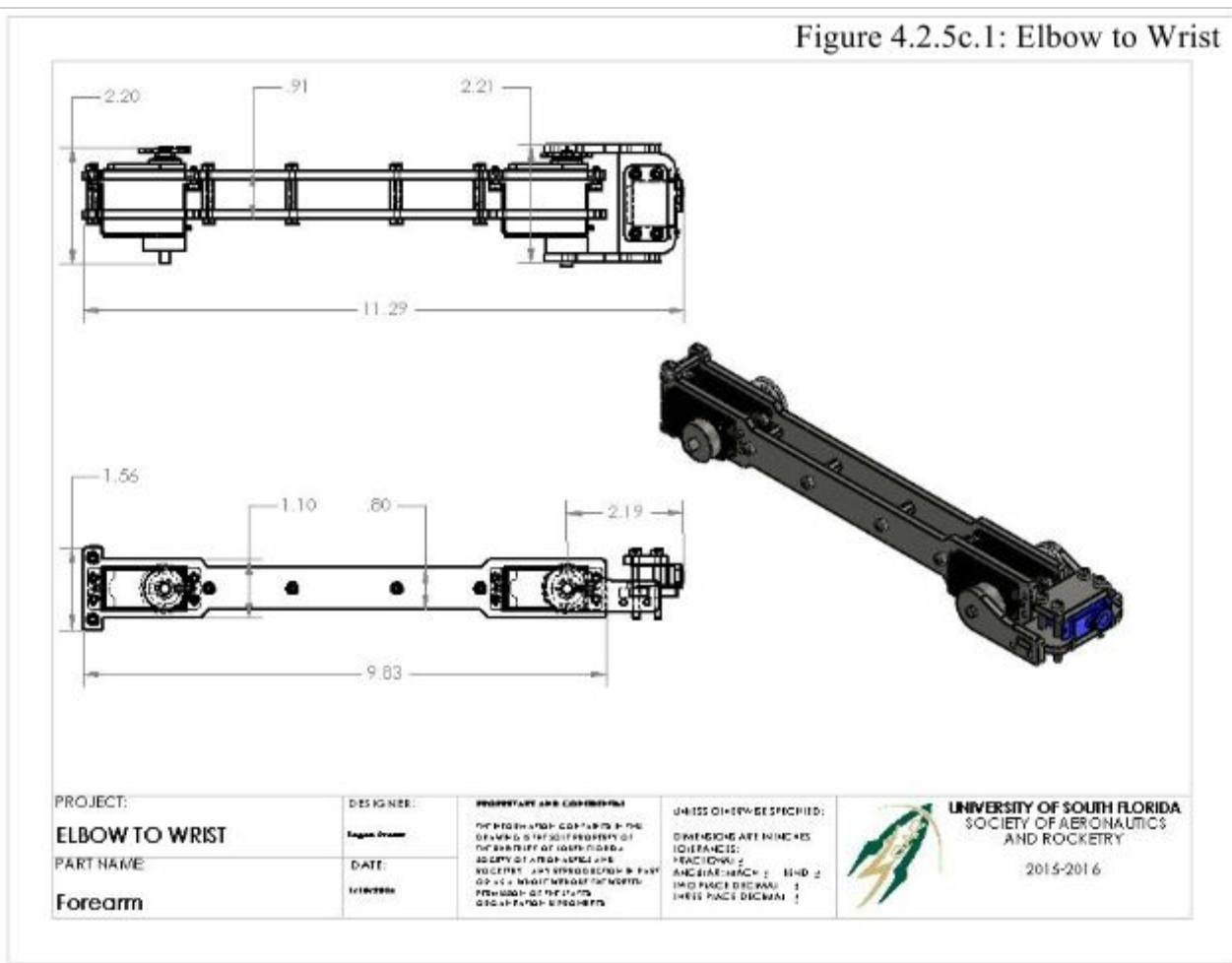
In Figure 4.2.5b.2 below, the exploded view of the Shoulder to Elbow is displayed with all of its components.



4.2.5c Elbow to Wrist

Below in Figure 4.2.5c.1 is a Schematic from the elbow to the wrist (including the wrist) of the robotic arm. From the elbow to the end of the wrist is 11.29 inches. Without the wrist attachment the length of this segment is 11.29 inches. The wrist itself has a reach of 2.19 inches and a width of 2.21 inches.

Figure 4.2.5c.1: Elbow to Wrist



Below in Figure 4.2.5c.2 you'll see an exploded view of Figure 4.2.5c.1 and every part involved in its creation.

Figure 4.2.5c.2: Exploded View

ITEM NO.	PART NUMBER	DESCRIPTION	QTY.
1	hs-311-hitec-standard-servo		2
2	servo-horn_DEFINED		2
3	Upperarm EDIT	304 STAINLESS STEEL	2
4	spacer15mm_DEFINED	304 STAINLESS STEEL	6
5	B18.3.1M -3x0.5x8 Hex SHCS-BCHX		20
6	bearingelbow EDIT	304 STAINLESS STEEL	1
7	bearingwrist EDIT	304 STAINLESS STEEL	1
8	Wristrightside EDIT	304 STAINLESS STEEL	1
9	Wristleftside EDIT	304 STAINLESS STEEL	1
10	Wristservoplate EDIT	304 STAINLESS STEEL	1
11	Servo		1
12	Wristclamp plate EDIT	304 STAINLESS STEEL	1
13	B18.3.1M -3x0.5x30 Hex SHCS-30CHX		4

PROJECT: **ELBOW TO WRIST EXP VIEW**

PARTNAME: **Forearm**

DESIGNER: **Eugenio Sauer**

DATE: **1/10/2016**

PROPRIETARY AND CONFIDENTIAL
COPYRIGHT © 2016 UNIVERSITY OF SOUTH FLORIDA SOCIETY OF AERONAUTICS AND ROCKETRY. ALL RIGHTS RESERVED.
NOTICE: THE INFORMATION CONTAINED IN THIS DRAWING IS THE PROPERTY OF UNIVERSITY OF SOUTH FLORIDA SOCIETY OF AERONAUTICS AND ROCKETRY. IT IS NOT TO BE COPIED OR DISSEMINATED IN WHOLE OR IN PART WITHOUT THE WRITTEN APPROVAL OF THE DESIGNER OR MANUFACTURER.

DIMENSIONS ARE IN INCHES
TOLERANCES:
+0.000/-0.000
AND 0.000/+0.000
TWO PLACE DECIMAL
THREE PLACE DECIMAL

**UNIVERSITY OF SOUTH FLORIDA
SOCIETY OF AERONAUTICS
AND ROCKETRY**

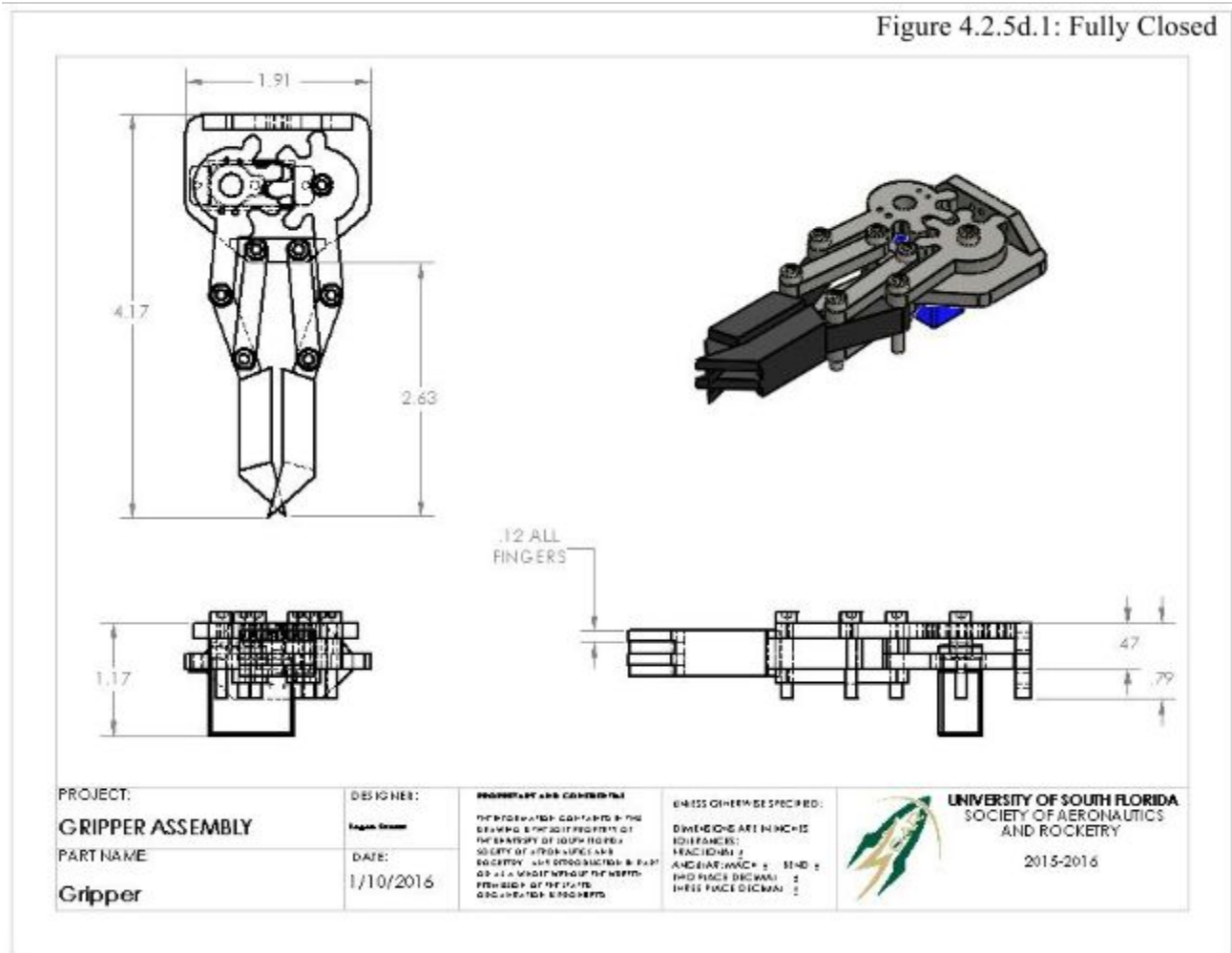


2016/2016

4.2.5d Gripper Assembly

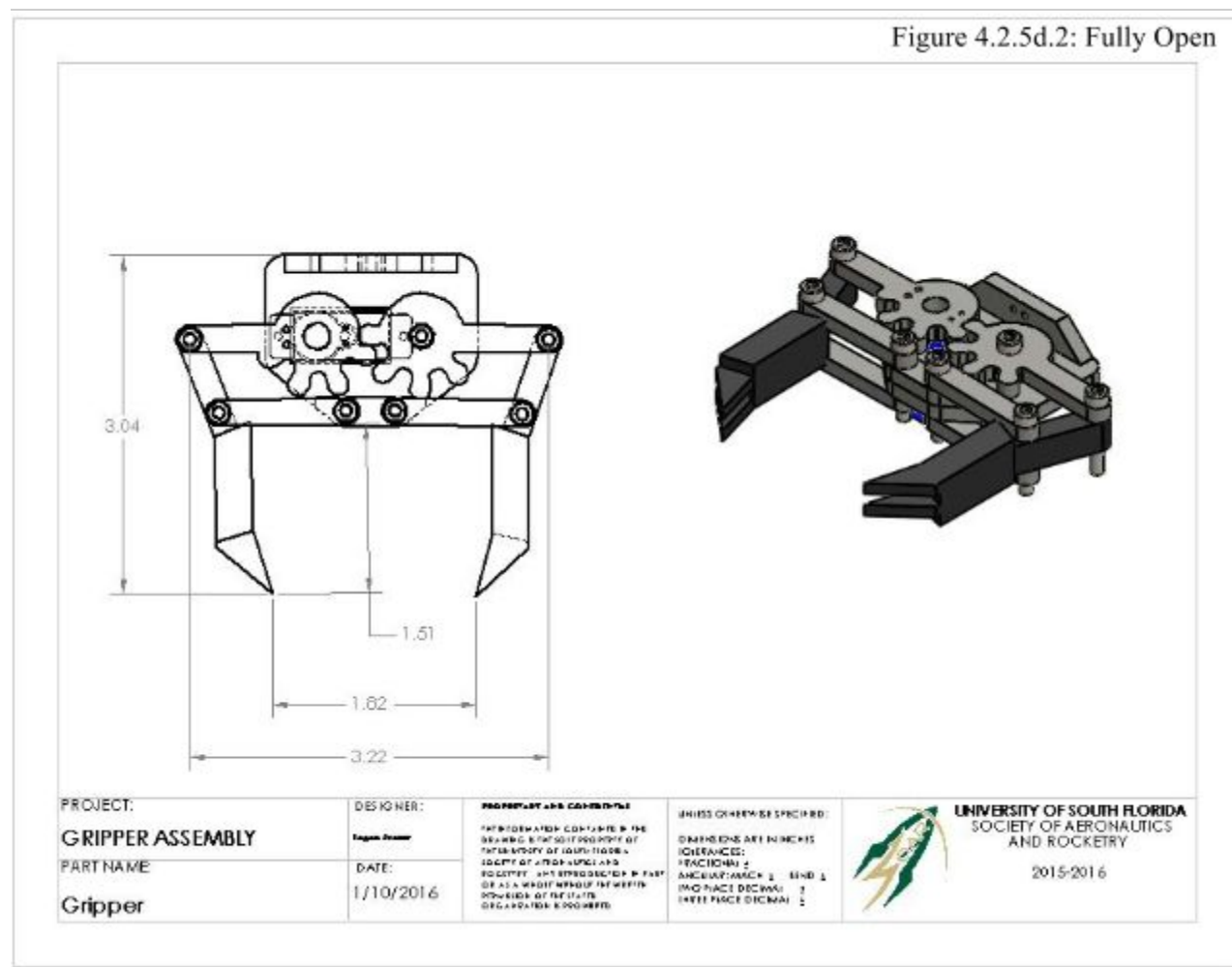
Below in Figure 4.2.5d.1 the gripper assembly is shown fully closed. When fully closed the gripper can reach approximately 4.17 inches from the wrist joint and the fingers themselves have 2.63 inches of reach themselves. The gripper assembly is only a mere 1.17 inches in height including the micro servo.

Figure 4.2.5d.1: Fully Closed



In Figure 4.2.5d.2 we can see the gripper fully open. When fully open the gripper has approximately 1.62 inches of clearance between the left and right grippers. In this position the gripper becomes 3.04 inches long and is now 3.22 inches in width. This is the widest our gripper assembly will ever become.

Figure 4.2.5d.2: Fully Open



In the following figure, figure 4.2.5d.3, you will be able to see the exploded view of the gripper assembly and every part that is involved with its creation.

Figure 4.2.5d.3: Exploded View

ITEM NO.	PART NUMBER	DESCRIPTION	QTY.
1	Servoconnector_DEF1_NED	304 STAINLESS STEEL	1
2	Gripperservoplate_EDIT	304 STAINLESS STEEL	1
3	Servo		1
4	Liftgears Defined	304 STAINLESS STEEL	1
5	Gearleft	304 STAINLESS STEEL	1
6	Gearright	304 STAINLESS STEEL	1
7	Parallelbar_DEFINED	304 STAINLESS STEEL	4
8	Liftparallelbar Defined	304 STAINLESS STEEL	1
9	Gripper appendage Left	ABS PLASTIC	1
10	Gripper appendage Right	ABS PLASTIC	1
11	B18.3.1M - 3x0.5x20 Hex SHCS -- 20CHK		7

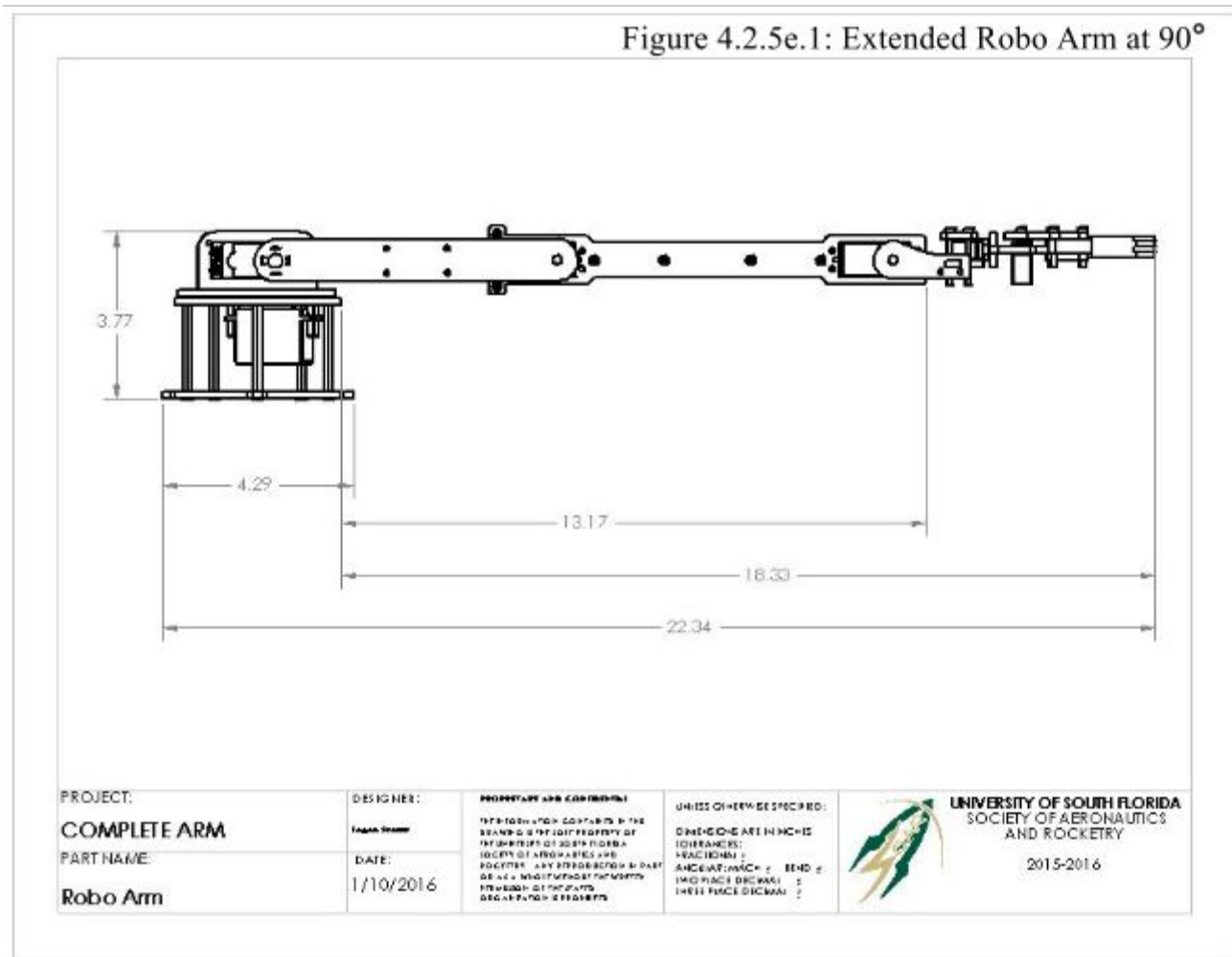
PROJECT: **GRIPPER ASSEMBLY EXPLDED VIEW** DESIGNER: **Elijah Jester** INCHES ARE SPECIFIED.
DIMENSIONS ARE IN INCHES
TOLERANCES:
INCHES/MILLIMETERS
AND MIL INCHES/MILLIMETERS
ONE PLACE DECIMAL ±
TWO PLACE DECIMAL ±
THREE PLACE DECIMAL ±

PARTNAME: **Gripper** DATE: **10/20/15** UNIVERSITY OF SOUTH FLORIDA
SOCIETY OF AERONAUTICS
AND ROCKETRY
2015-2016

4.2.5e Completed Robotic Arm

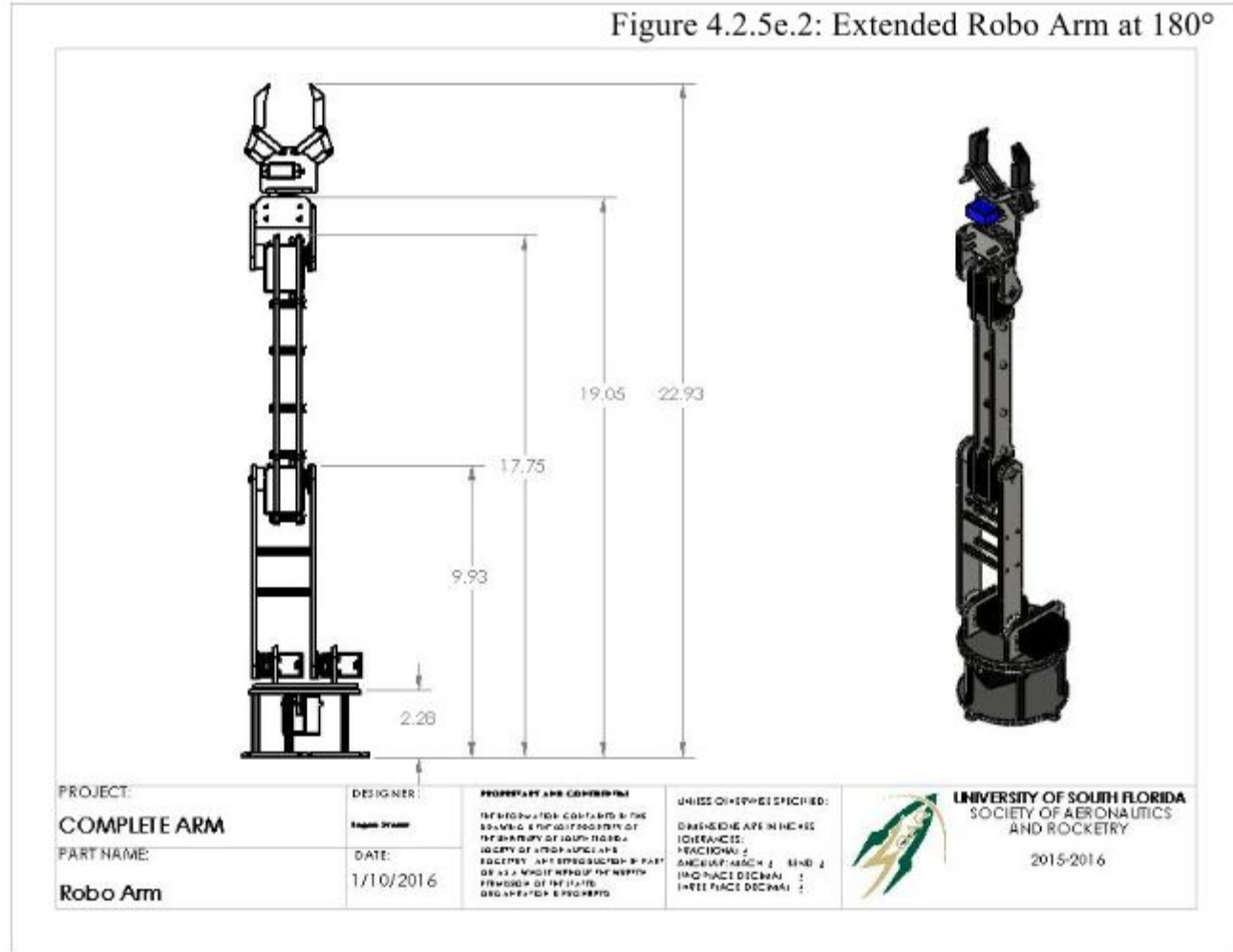
Figure 4.2.5e.1 shows the extended robotic arm. Here we can clearly see that from base to wrist the robotic arm had approximately 13.17 inches of reach. From the base to the very tips of the gripper there is 18.33 inches of reach. The total length of the robotic arm is 22.34 inches. When the arm is extended linearly from the base at 90 degrees the height of the arm assembly is 3.77 inches.

Figure 4.2.5e.1: Extended Robo Arm at 90°



The Robotic arm while extended straight up in the air reaches an approximate height of 22.93 inches from the very bottom of the base structure. The distance from the bottom of the structure to the wrist of the robotic arm is 17.75 inches. This is the distance the robotic arm can comfortably reach objects above. See Figure 4.2.5e.2 below for more information on height.

Figure 4.2.5e.2: Extended Robo Arm at 180°



4.2.7 Challenges and Verification Plan

4.2.7a Challenges

Design Impediment	Solution
Discern when the payload has been captured by the Robotic Arm.	The Raspberry Pi will be able to read the degree orientation of the robotic gripper. If the servo controlling the gripper reads a degree measurement less than the pre-set limit, than the system knows that the payload has not been obtained.
Lift the payload off of the ground a certain distance X.	A robotic arm with 5 degrees of freedom and gripper assembly with approximately 14 inches of reach.
Rotate the robotic arm to prepare for payload insertion.	Robust servo to rotate the robot arm assembly from capture to containment
Place payload into the containment bay.	Hardcode motions for the robotic arm to successfully place the payload into the payload bay from a specified position.

4.2.7b Verification Plan

Requirement	Method of Completion	Method of Verification
Arm and gripper assembly must capture and hold payload.	AGSE team will design and fabricate a mechanical arm that will pick up the payload from the ground to then be placed in the rocket.	Each subsystem of the mechanical arm will be tested individually.
If at anytime during the autonomous process the pause button is pressed the system must stop immediately.	The Raspberry Pi on board will continuously be running in a conditional statement looking for any signal triggered by the pause button.	The pause button will be tested thoroughly throughout every process during the capture and containment process to ensure complete halt of all actions.

We will be allotted 10 minutes to capture the payload, contain the payload, lift the rocket, and launch the rocket.	The servos on the robotic arm and gear ratio on the launch rail were chosen for their robustness and speed.	Test and time the entire process to make sure the allotted time limit is not only met but that we fall well below the 10 minute time limit.
The entire AGSE system will be completely autonomous.	The robotic arm and all other subsystems will be controlled by a Raspberry Pi.	Test the Raspberry Pi with all the subsystems to make sure each can perform its task with no human interaction.

4.2.8 Payload Containment

The payload containment system consists of three unique features that help it achieve its purpose; an L16 linear actuator, a custom 3-D printed payload sled, and a sealing coupler setup. The linear actuator is radio controller, allowing the AGSE to communicate with it within the rocket, sending it commands to open or close the payload sled. The payload sled will be 3-D printed out of ABS plastic, it is being shaped for both the constraints of the coupler tubing as well as for the shape of the MAV payload itself. Ultimately the payload containment design is made to nest two sections of fiberglass together, with o-ring closure to seal and reveal the payload inside. See section 3 for structure description of the containment system.

4.2.9 Payload Modeling

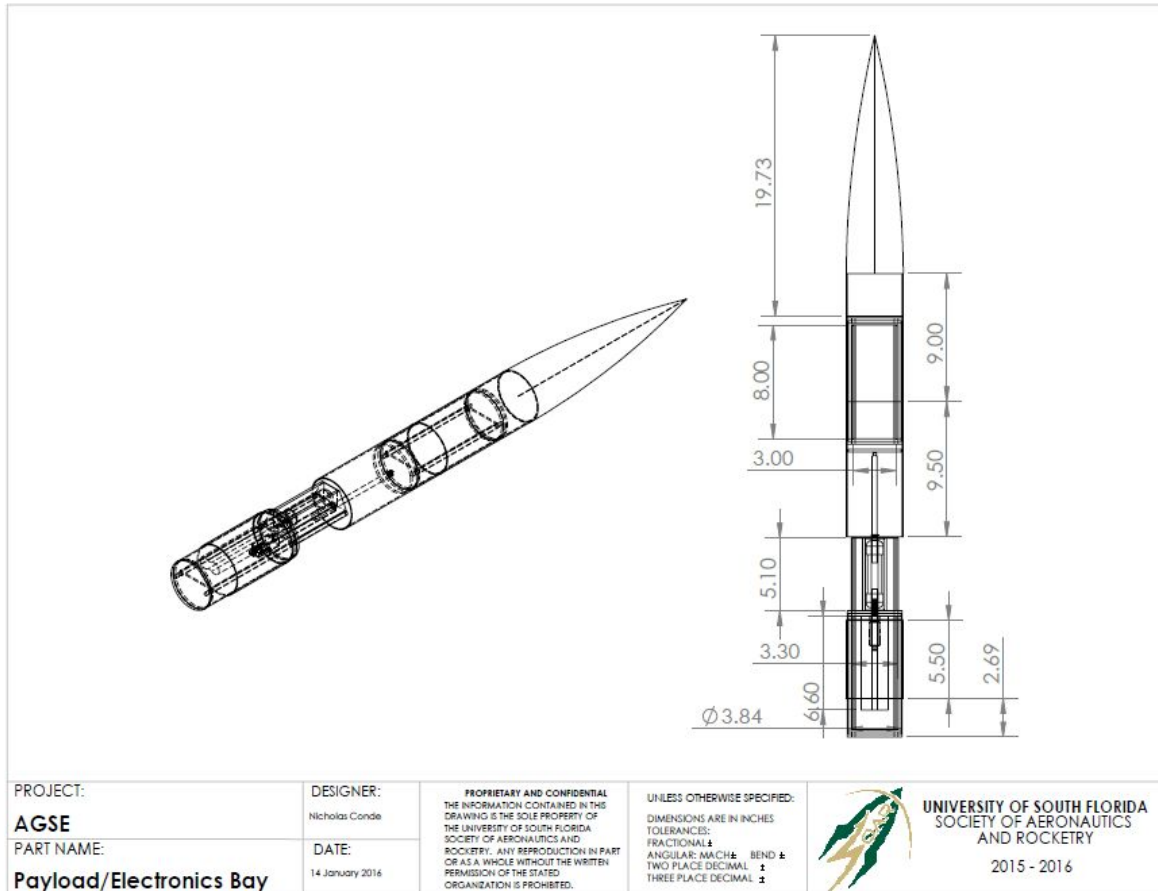


Figure 4.2.9.1 Dimensional Drawing of the Payload System

4.3 Launch Platform

4.3.1 Vehicle Erection System Overview

The vehicle erection system must raise the rocket from a horizontal position to 85 degrees from horizontal. This will be accomplished by coupling the launch rail to a shaft which is driven by an electric motor through a worm gear set. The drive system is mounted on a rectangular base. The figure below shows the design of our vehicle erection system.

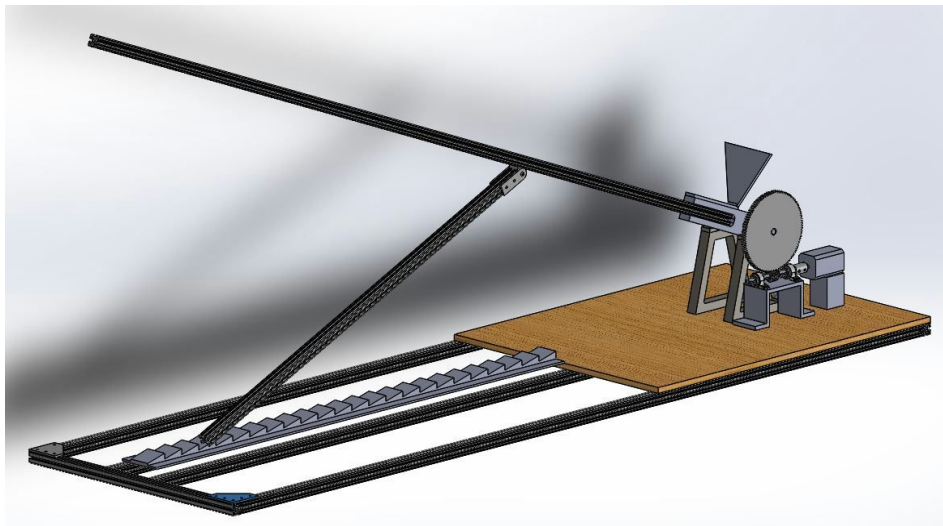


Figure 4.3.1. 1: Launch vehicle erection system

4.3.2 Design of Vehicle Erection System Components

4.3.2.a Worm Gear Set and Motor Selection

The mass properties of the rocket and launch rail were used to compute the maximum torque required to lift the rocket from the horizontal position using the formula below.

$$T_{max} = X_{gv} * W_v + X_{gr} * W_r$$

The variable are defined and their values are given in the table below.

Table 4.3.2.a. 1: Explanation of variables in above equation.

Variable	Value
X_{gv} , Launch vehicle C _g measured from axis of rotation	138 in
X_{gr} , Launch rail C _g measured from axis of rotation	60.0 in
W _v , Weight of the launch vehicle	22.82 lb
W _r , Weight of the launch rail	10.5 lb

The resulting maximum torque is 2087 in-lb. This will be the required output torque of our drive system. The next step in the design process was to select a trial worm gear set. In the end a worm gear set was chosen with a gear ratio of 100. The specifications of the worm gear set are given in the table below.

Table 4.3.2.a. 1: Worm gear set specifications.

Parameter	Value
ϕ , normal pressure angle	14.5°
λ , lead angle	4° 34'
μ , coefficient of friction(estimated by AGMA formula)	0.15
D, pitch diameter of gear	10 in
d, pitch diameter of worm	1.25 in

The tangential force on the gear(W_{gt}) was needed to compute the input torque requirement and can be calculated by the following formula.

$$W_{gt} = 2 * \frac{T_{max}}{D}$$

In order to select the motor, the input torque required was computed using the following formula from Shingley's Handbook of Machine Design.

$$W_{wt} = W_{gt} * \frac{\cos(\phi)*\sin(\lambda) + \mu*\cos(\lambda)}{\mu*\sin(\lambda) - \cos(\phi)*\cos(\lambda)}$$

Where W_{wt} is the worm tangential force. The results are W_{gt} = 417 lb and W_{wt} = -99.21 lb. The input torque can be calculated from:

$$T_{in} = d * W_{wt}/2$$

The resulting T_{in} is 62.02 in-lb of torque. We will therefore need a motor and power supply to output that much torque. The worm gear set will also need to be properly lubricated. The low lead angle of the worm should render the set non-backdrivable. A redundant ratchet mechanism will still be used. Finally a mechanical stop rigged with a motor cutoff switch will be activated when the launch vehicle is erected to the specified 85 degrees from horizontal.

4.3.2.b Shafts, Couplings, and Bearing Selection

There are three shafts in our design the worm shaft, gear shaft, and motor shaft. The worm shaft will be subject to the axial, tangential, and separation forces of the worm gear set and the torque output of the motor. The gear shaft will be subject to the same forces generated at by the worm gear set as well as the weight and torque applied by the launch vehicle and launch rail. The motor shaft will be subjected only to a torque load. These forces generate bending, torsional, and axial stresses within the shafts. It is important that the shaft has an infinite fatigue life and does not deflect too much. Once the worm gear set was selected the shaft diameters were fixed and it was necessary to check the stress and deflection levels.

The shaft coupling chosen must be able to transmit the required torque. Shaft couplings will be used to couple the motor shaft to the worm shaft, the worm to the worm shaft, the gear to the gear shaft, and the launch rail to the gear shaft.

Bearing must be able to provide the reaction forces for the shafts. In order to deal with the large separation, axial, and tangential forces generated by the worm gear set, the worm shaft and gear shaft were supported at each end by a bearing. The axial load on the worm shaft is equal and opposite of the tangential force on the gear and the axial force on the gear is equal and opposite of the tangential force on the worm. These forces were given above as $W_{gt} = W_{wa} = 417 \text{ lb}$ and $W_{wt} = W_{ga} = -99.2 \text{ l lb}$, where W_{wa} and W_{ga} are the axial forces on the worm and gear respectively. It is clear the bearings must be able to support a thrust and radial loading.

4.3.2.c Launch Rail

The launch rail chosen must be able to support the launch vehicle during erection and hypothetically guide it during takeoff. Therefore the stiffness and mass of the launch rail is a concern. The launch rail must also accommodate the launch lugs in order to guide the rocket during takeoff. A logical choice for the launch rail is T-slotted extruded aluminum. Adequate stiffness is ensured by selecting a large enough cross-section.

4.3.2.d Platform and Mounting of Drive System

The platform will be constructed of T-slotted extruded aluminum and plywood. A metal frame will be constructed to fix the bearings in place. The motor will be mounted to a block of material to position it correctly for coupling with the worm shaft.

4.3.3 Ignition Station

The igniter will be fed into the rocket motor via two opposing rollers. The rollers will be driven by a small electric motor and the igniter wires will be driven by friction into the rocket motor. Experimentation will be done to find the most reliable place to mount this mechanism. An elastomer covering will ensure a large coefficient of friction between the rollers and igniter.

4.3.4 Fabrication

The platform will be constructed first. The extruded aluminum frame of the platform will be assembled and the plywood will be fastened on to the extruded aluminum frame. The frame to mount a single gear shaft bearing will then be assembled into place. A bearing will then be assembled onto that mount. The second gear shaft bearing and mount will be assembled to each other. To ensure alignment of the two gear shaft bearings the shaft will be placed in the bearing previously mounted to the platform to determine the precise location at which the second bearing must be mounted. A similar procedure will be carried out to mount the worm shaft bearings. The gear, worm, and rail mount will be placed on their respective shafts along with the keys. The motor will be positioned carefully so the motor shaft is aligned with the worm shaft in order for them to be coupled. Finally the rail will be fastened to its mount and the ratcheting mechanism will be assembled in place.

4.7 Electronics Systems

4.7.1 Overview

The electronic systems for the AGSE will be centered around two separate processing units: Raspberry Pi system housed on the rover, and an external processing platform that will perform a majority of the image processing computations to reduce the computational requirements of the Raspberry Pi. The Raspberry Pi will be interfaced with a Kinect sensor, an Xbee transmitter and receiver, all servo motors for the robotic arm, and the motors that correspond to each wheel of the rover. Upon initialization of the system, the central PC will retrieve the necessary information from the Kinect sensor to generate a 3D point cloud of the scene and recognize the payload. With the 3D point cloud data and payload location within the point cloud as a goal, the navigation system within ROS will guide the rover to the payload. Once the rover has reached the payload, the PC will retrieve the necessary information from the Kinect to determine the location of the payload in world units via stereo parameters. Given a distance in world units from the rover, the robotic arm will reach the specified distance in front of the rover and retrieve the payload. Upon recognition that the payload has been secured within the claw of the robotic arm, ROS will update the new goal of the rover to be the rocket. Once the rover has reached the rocket, the arm will place the payload inside the rocket.

4.7.2 Components

4.7.2.a Raspberry Pi and Accompanying Software

The Raspberry Pi will be interfaced with the following hardware:

- Kinect Sensor via USB
- Servo Motors for the Robotic Arm controlled via PWM
- Motors for the rover wheels controlled via GPIO

The Kinect sensor will serve the primary role in acquiring the necessary images for generating the 3D point cloud to be used for the rover navigation in ROS. The Kinect will also be responsible for acquiring the necessary images for stereo vision so that the location of the payload can be described in world units. The Kinect will be connected to the Raspberry Pi via USB, and all necessary images for object recognition, 3D point cloud generation, and depth estimation will be streamed wirelessly to the PC for processing. The Kinect will also be used locally on the Raspberry Pi to interface with ROS and perform the rover navigation.

Servo Motors were chosen for the robotic arm due to the motors ability to rotate to a certain angle. The chosen Servo Motors respond to a PWM signal generated on the Raspberry Pi. Due to the limited availability of PWM pins on the Raspberry Pi, a PWM controller from Adafruit was selected that uses the I2C pins on the Raspberry pi to generate several PWM outputs. Two functions will be designed, one function that will generate the appropriate PWM commands to move the claw robotic arm to the ground a certain distance from the rover defined by the input, and one function that will raise the arm to place the payload into the rocket.

Finally, the motors for controlling the rover wheels will be interfaced to the Raspberry Pi via a controller that uses the SPI pins of the Raspberry Pi to control multiple GPIO pins. The appropriate GPIO outputs will be generated through the navigation system in ROS which will be discussed in more detail in later sections.

4.7.2.b Master PC and Computer Vision

The main purpose of the external PC is to handle the computations of the image processing functions. Image processing functions will be performed via MATLAB and the image processing and image acquisition toolbox. The image acquisition toolbox includes a function for importing a 3D point cloud from the Kinect sensor. Additionally, MATLAB includes several functions and methods for object recognition and stereo vision and calibration.

4.7.2.c Subsystem Communication

The wireless communication module in this design uses the Xbee Radio frequency transmitter and receiver. This 2.4 GHz device operates on what is colloquially referred to as the ISM band, for its extensive use by Industrial, Scientific, and Medical communities. As such, the device is in accordance with IEEE 802.15.4 specifications. The theoretical range of the Xbee series one module in use is one mile, far exceeding the demands for the NASA Student Launch Initiative.

The Robot Operating System employs the universal asynchronous receiver/transmitter (UART) devices to establish a network of point-to-point communication between the offboard processing and the embedded robotic frame. The offboard processor initializes a “Master Node” through Matlab and as Master stores all network messages published by the nodes. Messages are the prototypical communication method for the ROS network, publishers subscribe to topics in which they stream information, while subscribers “listen” to the information published on those topics.

For inter-subsystem communication between electrical components we will use two separate and familiar methods. Those being the Serial Peripheral Interface (SPI) bus and the Inter-Integrated Circuit (I2C) bus. These communication protocols both use the hierarchical master-slave relationship between the communicating systems, with the Raspberry Pi being the master to the

MCP23S17 GPIO extender for seamless functional control of the motor controller and of the PCA9685 servo driving board for the robotic arm's servos. Utilizing these components will take processing and hardware strain off of the Raspberry Pi, expanding the capability that this embedded system has for control.

4.7.2.d Rover Controls and Navigation

The rover will be controlled via an automatic navigation system included in ROS.

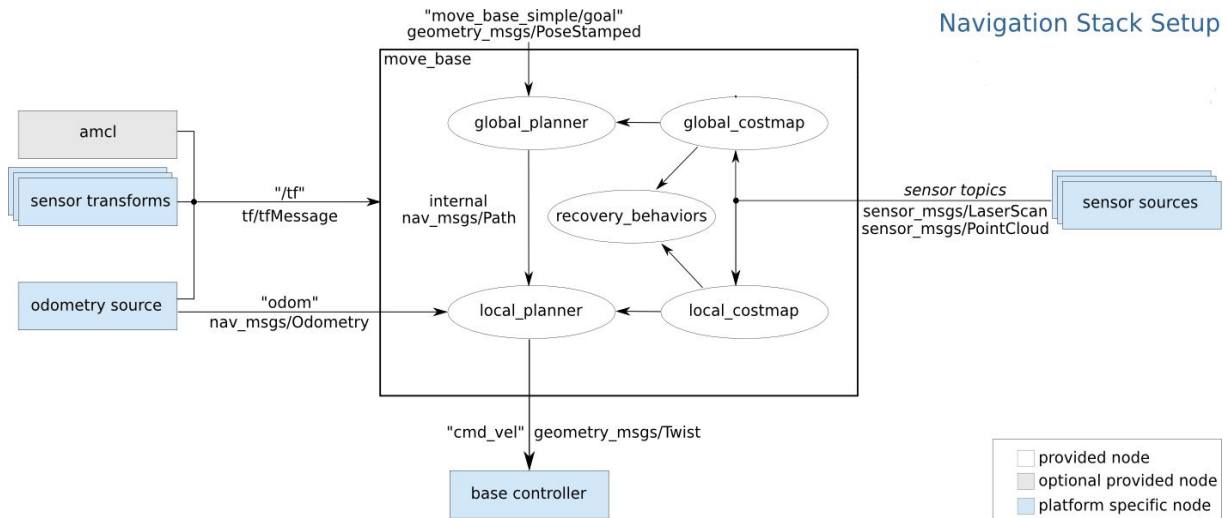


Figure 4.7.2.d.1 - ROS Navigation Overview

This flow chart is a modified form of one found at wiki.ros.org and shows the flow of the rover navigation software architecture. As can be seen on the right hand side, sensor topics, the ROS navigation requires a 3D point cloud, or laser scan, of the desired area, the local and global maps therefore subscribe to the topics in which the sensor streams are publishing to generate a global and local mapping and overlay these maps with a cost map around obstacles. A destination, which in this case is the payload, is set by color and shape object recognition through MATLAB and published to a topic subscribed to by the global planner. The local planner will jointly use information from the cost mappings, the global planner, and with the optical incremental encoders, a form of odometry sensors, on the motor to implement a trajectory planner to plot a course to the destination. The ROS navigation uses the laser scanner within the Kinect as well as odometry sensors on the rover wheels to localize the robot in the map and to keep track of the rover's progress to the destination. We will also attempt to implement the amcl probabilistic localization system, which uses only the visual data to track the pose of the robot in the generated map. Finally, the base controller will publish a command velocity geometry message. This will take the form of a linear and angular velocity vectors to be interpreted by the differential drive controllers. In turn, the differential drive controllers will send a PWM signal to

the motor controllers to directly control the speed of the wheels on each side of the rover. Finally, the recovery behaviors serve to shut down the robotic platform in the event of sensor or motor failure, or in the event of encountering an obstacle. This will protect the safety of the AGSE system as well as the safety of operators and spectators.

4.7.3 Challenges and Verification Plan

In order to verify the correct operation of the AGSE as a whole, preliminary tests on individual components and subsystems will be performed as follows. First a test will be conducted with the Kinect camera and accompanying object recognition and 3D point cloud software operating in isolation i.e. the mechanical arm and accompanying software for controlling the arm, as well as the communication system will not be connected. For this test the image processing software will be configured for recognition of the payload given video input from the Kinect, and the generation of a 3D point cloud of the surrounding area, as well as the determination of the payload location within the generated 3D point cloud. The purpose of this test is to verify that the image processing software is working correctly with the Kinect camera and that the payload can be correctly recognized and located within the generated 3D point cloud. Additionally, this test will determine the limitations of the payload recognition and location such as the maximum distance where the payload can be accurately recognized and located. Next the arm will be tested in isolation. The mechanical arm will be connected to the Raspberry Pi and a program will be run that controls the operation of the arm. During this test the mechanical arm's ability to respond to location information and directions from the Raspberry Pi software will be evaluated.

Additionally, during this test the mechanical arms physical ability to successfully retrieve and secure the payload will be evaluated. For example, is the mechanical arm physically able to grab the payload? What is the maximum range for which the arm can still accurately retrieve and secure the payload? After testing the the abilities of the image processing software and the mechanical arm individually, the abilities of the image processing software working in collaboration with the mechanical arm will be evaluated. For this test the main concern is with the high level operation i.e. can the image processing software communicated accurate stereo parameter information to the mechanical arm and can the mechanical arm properly use the real world location of the payload to accurately secure the payload.

The communication capabilities of the Xbee systems will be evaluated in isolation. First the communication link itself will be verified by sending and receiving simple messages. Once the communication link is verified the integrity of the data to be sent will be evaluated. For example, 3D point cloud data will need to be sent from the main image processing platform to the Raspberry Pi. In order to test the capability of sending 3D point cloud data, a previously generated and examined 3D point cloud will be sent via the Xbee system and observed on the

receiving end. Rover navigation will also be tested using a known 3D point cloud and goal. During this test the features, capabilities and limitations of the ROS navigation will be tested.

Once the performance of the operations involving the retrieval of the payload is understood, the transportation of the payload to the rocket, and the payload's security within the rocket will be evaluated. The first test in this section will evaluate the capability of the software to locate and realise the destination within the rocket. Next an evaluation of the physical interaction between the mechanical arm and the compartment within the rocket for securing the payload will take place. For example, are the mechanical arm and payload compartment within the rocket physically compatible in that the mechanical arm can successfully reach and interact with the payload compartment to the extent that the payload can be properly released and secured? Finally, the systems ability to recognize and communicate the payload being successfully transported and secured within the rocket will be evaluated along with the systems ability to successfully prepare the rocket for launch given that the payload has been properly secured.

4.7.4 Schematics

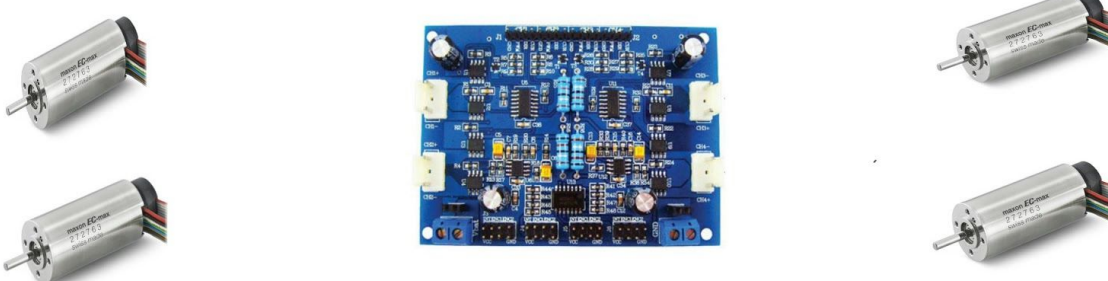
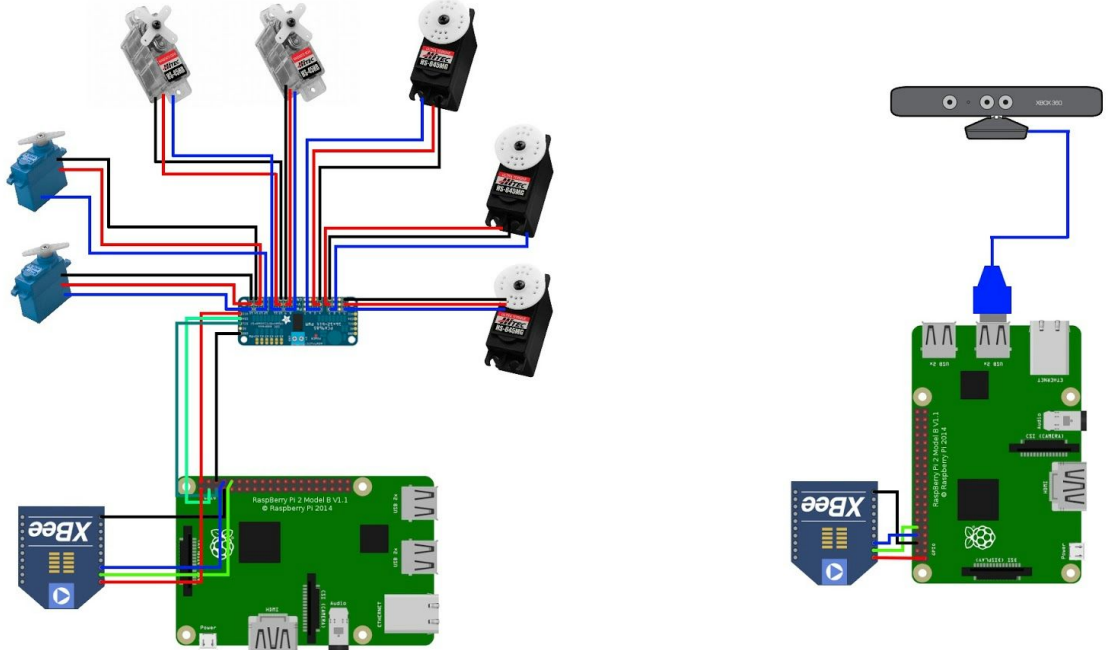


Diagram 4.7.4.1: Electrical Systems Overview

5) Project Plan

5.1 Budget Plan

Figure 5.1.1 Total Projected Budget

BUDGET	Amount
Structure	\$766.64
Recovery	\$697.28
Propulsion	\$710.85
AGSE	\$2,761.80
Subscale	\$1,175.58
Travel	\$4,200.00
TOTAL	\$10,312.15

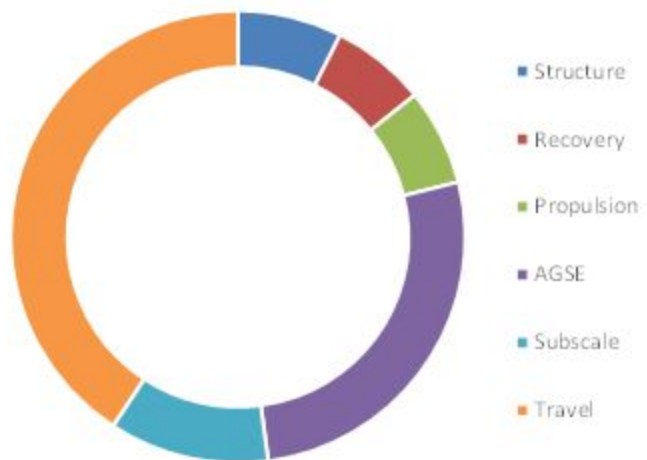


Figure 5.1.2 Structure Budget

STRUCTURE PROJECTED BUDGET			
ITEM NAME	PRICE	QUANTITY	SUBSYSTEM
Kevlar Tape 1" - 10 yard roll	\$27.45	1	STRUCTURE
1/2 INCH G10 FIBERGLASS SHEET 2 SQUARE FOOT	\$72.00	2	STRUCTURE
Retainer Assembly, 75 mm	\$50.00	1	STRUCTURE
Centering Rings	\$4.64	4	STRUCTURE
Fiberglass Wrapped Payload Section	\$45.29	1	STRUCTURE
Couple/Bulkhead Assembly	\$10.34	1	STRUCTURE
Phenolic Airframe Tubing	\$22.49	1	STRUCTURE
Bulkplate 3.0"	\$1.99	3	STRUCTURE
Phenolic Coupler Tube	\$3.69	1	STRUCTURE
3.9" Plastic Nosecone	\$21.95	1	STRUCTURE
3.9" Coupler/Bulkhead Assembly	\$6.89	4	STRUCTURE
98mm G12 Fiberglass Tube 3 ft.	\$92.30	1	STRUCTURE
98mm G12 Fiberglass Tube 4 ft.	\$93.38	2	STRUCTURE
30 Minute Epoxy	\$17.98	4	STRUCTURE
Hardware	\$38.40	1	STRUCTURE

Figure 5.1.3 Propulsion Budget

PROPELLION PROJECTED BUDGET			
ITEM NAME	PRICE	QUANTITY	SUBSYSTEM
L910 Motor	\$132.95	3	PROPELLION
75mm 1400Ns - complete motor	\$312.00	1	PROPELLION

Figure 5.1.4 Recovery Budget

RECOVERY PROJECTED BUDGET			
ITEM NAME	PRICE	QUANTITY	SUBSYSTEM
Strap Nylon Shock Cords 2"	\$2.49	26	RECOVERY
Tubular Nylon Shock Cords 1" x 7 yards	\$2.49	26	RECOVERY
RRC3 Altimeters	\$69.95	2	RECOVERY
Nomex Chute Protector 9x9 for 3" Tube	\$6.95	2	RECOVERY
Cert 3 Drogue	\$27.50	2	RECOVERY
Cert 3 Large Parachute	\$145.00	1	RECOVERY
TeleGPS	\$214.00	1	RECOVERY

Figure 5.1.5 Travel Budget

TRAVEL PROJECTED BUDGET			
ITEM NAME	PRICE	QUANTITY	SUBSYSTEM
Accomadations	\$90.00	30	TRAVEL
Bus	\$1,500.00	1	TRAVEL

Figure 5.1.6 Subscale Budget

SUBSCALE PROJECTED BUDGET			
ITEM NAME	PRICE	QUANTITY	SUBSYSTEM
75mm G12 Fiberglass Tube 5 ft.	\$102.55	1	SUBSCALE
75mm G12 Fiberglass Tube 3 ft.	\$61.53	1	SUBSCALE
75mm G12 Fiberglass Tube 4 ft.	\$93.38	1	SUBSCALE
Plastic Nosecone	\$21.23	1	SUBSCALE
Phenolic Coupler Tube	\$3.69	3	SUBSCALE
2.0" Bulkhead	\$1.90	4	SUBSCALE
K630BT Motor	\$195.00	2	SUBSCALE
54mm 1400Ns - complete motor	\$145.00	1	SUBSCALE
54 mm Retainer Assembly	\$38.00	1	SUBSCALE
Baltic Birch 3 SQ FT	\$8.17	1	SUBSCALE
Phenolic Airframe Tubing	\$14.99	1	SUBSCALE
Strap Nylon Shock Cords 2"	\$2.49	7	SUBSCALE
Tubular Nylon Shock Cords 1" x 7 yards	\$2.49	7	SUBSCALE
RRC3 Altimeters	\$69.95	2	SUBSCALE
Nomex Chute Protector 9x9 for 3" Tube	\$6.95	2	SUBSCALE
Cert 3 Drogue	\$27.50	2	SUBSCALE
Hardware	\$38.40	1	SUBSCALE

Figure 5.1.7 AGSE Budget

AGSE PROJECTED BUDGET			
ITEM NAME	PRICE	QUANTITY	SUBSYSTEM
Tetrix Max	\$595.00	1	AGSE
Tetrix Prime	\$329.00	1	AGSE
Tetrix Gripper	\$9.95	1	AGSE
Servos	\$22.95	5	AGSE
Lynx Motion Arm	\$300.00	1	AGSE
Microcontrollers	\$15.00	3	AGSE
worm shaft	\$21.10	1	AGSE
gear shaft	\$18.27	1	AGSE
worm shaft key	\$15.00	1	AGSE
gear shaft key	\$15.00	2	AGSE
worm	\$43.13	1	AGSE
worm gear	\$196.10	1	AGSE
bearings 1	\$65.70	2	AGSE
bearings 2	\$11.78	2	AGSE
3ft extruded aluminum	\$21.78	2	AGSE
10ft extruded aluminum	\$61.94	5	AGSE
6ft extruded aluminum	\$39.31	1	AGSE
brackets and joints	\$50.00	1	AGSE
plywood	\$24.92	1	AGSE
Nuts/bolts/screws	\$30.00	1	AGSE
L16-R Miniature Linear Servo for RC	\$70.00	1	AGSE
12V Tenergy 2000mAh NiMH Battery Pack with Bare Leads for RC Airplanes	\$23.92	2	AGSE
Microsoft Kinect Xbox One	\$149.99	1	AGSE
Raspberry Pi Kit	\$86.27	1	AGSE
Xbee Pro	\$37.95	1	AGSE

5.2 Funding Plan

To complete this project our organization has largely been relying on the student organization funding our team receives through our university. Moving into a new semester we intend to achieve sponsorships from local businesses, develop several crowdfunding projects, and to accept donations for SOAR merchandise and apparel. In addition to these sources of revenue, in regards to our significant travel needs we are applying for a travel grant from our university to cover the entirety of that budget item.

5.3 Timeline

Table 5.3.1 Key Dates Taken from SOAR NSL Gaant Chart

Proposal Due	8/7	9/11
Design		
Website Established	10/23	10/23
Rocket Design	10/2	10/14
Rocket Models Developed	10/15	10/21
AGSE Design	10/2	10/14
AGSE Models Developed	10/15	10/21
Budget Established	10/21	10/28
Subteams Establish	10/14	10/21
Subteam Budgets Established	10/21	10/28
Subscale Materials Ordering	10/21	10/28
Subscale Materials Shipping	10/28	11/6
PDR		
First Draft	10/21	10/28
Editing	10/29	11/4
Completion	11/5	11/5
Powerpoint	10/29	11/4
Presentation	11/23	11/23
Subscale Rocket		
Vehicle Design	10/21	10/28
OpenRocket Simulation	10/28	11/6
Motor Can Fabrication	11/8	11/13
Altimeter Bay Fabrication	11/14	11/16
Recovery Systems Fabrication	11/16	11/18
Payload/Nosecone Fabrication	11/14	11/16
Vehicle Assembly	11/16	11/20
Subscale Launch	11/21	11/21
CDR		
First Draft	12/14	12/27
Editing	12/28	1/14
Completion	1/15	1/15
Powerpoint	12/14	12/27
Presentation	TBA	TBA

Full Scale Rocket		
Vehicle Design	12/14	12/27
OpenRocket Simulation	12/28	1/8
Motor Can Fabrication	1/22	2/4
Altimeter Bay Fabrication	2/5	2/11
Recovery Systems Fabrication	2/5	2/11
Payload/Nosecone Fabrication	2/5	2/11
Vehicle Assembly	2/12	2/19
Test Launch	2/20	2/20
AGSE		
Overall System Design	10/28	11/6
Vision System Development	11/8	11/29
Arm Design	11/8	11/29
Launch Rail Design	11/8	11/29
Rover Design	11/8	11/29
Containment Design	11/8	11/29
Systems Fabrication	1/8	1/29
Prototyping	1/30	2/12
Testing	2/13	3/5
Educational Outreach		
Great American Teach In	11/19	11/19
USF Engineering Expo	2/19	2/20
Local High School Outreach	1/21	1/21
FRR		
First Draft	2/15	2/1
Editing	3/1	3/13
Completion	3/14	3/14
Powerpoint	2/15	2/19
Presentation	TBA	TBA
Competition	4/12	4/17
PLAR		
First Draft	4/18	4/25
Editing	4/25	4/28
Completion	4/29	4/29

In terms of the critical path, the next pivotal step is waiting for parts and materials to arrive for fabrication. Once parts are in for the rocket we can engage in the most difficult step of fabrication, the fin can, and move onto the electronic systems from there. In terms of the AGSE now that key modeling aspects are done we can engage in fabrication and parts ordering.

5.4 Educational Engagement

We maintain that one of the simplest and most effective methods of engaging students is to visit the schools and personally speak to students about STEM. These meetings will be established by contacting local schools and requesting permission to speak in the classroom as well as give demonstrations. This will be organized by the Education Engagement Officer.

Engagement at Local Schools

We will be visiting Young Middle Magnet school in the Spring to share with them our work on the AGSE. This will serve to further inspire the students at this school, which is geared toward STEM education and specifically robotics. In addition we will be reaching out to other schools and after-school programs for opportunities to showcase STEM.

Engagement at USF

Our team will be participating in the Engineering Expo hosted by the University of South Florida. This event is designed for campus organizations to showcase a STEM related project to both the USF community and local schools. This will serve as a platform for us to share STEM and rocketry with other students in an education and engaging way. The Engineering Expo is set to occur in February of 2016. We plan to demonstrate our developments with the AGSE to students in addition to demonstrating our current rocket repertoire.

We are also currently involved in aiding the USF Student Veterans Association in the basics of rocketry. We will be continuing to support them in the completion of their first rocketry competition, specifically hybrid rocketry.

Online Engagement

In addition to sharing our events online we will host videos and presentations online that look at the different STEM fields. These will allow our team to engage a wider audience outside of the immediate Hillsborough County area. These will be hosted on our organization's website, along with interactive forums and chat boxes where individuals may ask questions of our group or start discussions.

6) Conclusion

The Society of Aeronautics and Rocketry at USF is a group of aspiring scientists, engineers, and more, seeking to further mankind's pursuit of space exploration, and inspire an appreciation for STEM in the local community. The NASA Student Launch and the Centennial Challenge have been a significant guiding force for our organizations goals for this academic year, introducing many new members to our growing team and passing knowledge to many other students. As we move forward towards final fabrication we are determined to put our best foot forward, make our organization a longstanding cornerstone of our university, and establish the NASA Student Launch Initiative as a yearly endeavor to improve upon every year.

7) Appendix I – Risk Assessment

Severity		
Description	Value	Criteria
Catastrophic	1	Could result in death, significant irreversible environmental effects, complete mission failure, and/or monetary loss greater than \$5000
Critical	2	Could result in severe injuries, significant reversible environmental effects, partial mission failure, and/or monetary loss between \$500 and \$5000
Marginal	3	Could result in minor injuries, moderate reversible environmental effects, and/or monetary loss between \$100 and \$500
Negligible	4	Could result in insignificant injuries, minor reversible environmental effects, and/or monetary loss of less than \$10

Probability		
Description	Value	Criteria
Almost Certain	1	Greater than 90% chance of occurrence
Likely	2	Between 50% and 90% chance of occurrence
Moderate	3	Between 25% and 50% chance of occurrence
Unlikely	4	Between 1% and 25% chance of occurrence
Improbable	5	Less than 1% chance of occurrence

Risk Assessment Matrix				
Probability Value	Severity Value			
	Catastrophic (1)	Critical (2)	Marginal (3)	Negligible (4)
Almost Certain (1)	2- High	3- High	4- Moderate	5- Moderate
Likely (2)	3- High	4- Moderate	5- Moderate	6- Low
Moderate (3)	4- Moderate	5- Moderate	6- Low	7- Low

Unlikely (4)	5- Moderate	6- Low	7- Low	8- Low
Improbable (5)	6- Low	7- Low	8- Low	9- Low

Lab and Workshop Risk Assessment						
Hazard	Cause/Mechanism	Outcome	Severity of Risk	Probability of Risk	Risk Level	Mitigation
Using power tools	1. Improper training with power tools, hand tools, and/or other lab equipment 2. Improper use of PPE	1a. Mild to severe cuts and/or burns to personnel 1b. Damage to rocket and/or rocket components 1c. Damage to equipment/tools	3	3	Low	1. All individuals to use tools with be trained on each tool. No individual will attempt to learn how to use the tool on their own and no individual will use the tool who is not trained on that tool. Safety glasses will be worn at all times within the lab and workshop. Lab and workshop will be kept clean and cleaned after each use to ensure no debris is left that may cause injury 2. Any additional PPE will be worn as instructed by the tool manufacturer or as required. All individuals will be instructed on proper use of PPE
Working with chemical components	1. Chemical splash 2. Chemical fumes	1. Mild to severe burns 2. Skin and/or lung aggravation and/or damage due to inhalation of fumes	3	4	Low	1. MSDS documents will be readily available at all times for all chemicals. MSDS documents will be reviewed before each use of chemicals. Gloves and safety goggles designed for chemical splash will be worn at all times by all personnel when working with and/or near hazardous chemicals 2. When working with chemicals that will generate fumes all work is to be done in a well-ventilated area. All personnel will minimize inhalation by wearing appropriate PPE which may include vapor masks when there is a risk of serious fume inhalation

Metal and/or carbon fiber shards	1. Sanding and/or grinding rocket components	1a. Splinters and/or shard in personnel skin and/or eyes 1b. damage to rocket and/or rocket components	3	3	Low	1. All members will be trained in proper methods in sanding and grinding. No member who is untrained will attempt to sand and/or grind any materials. All personnel will wear proper safety glasses and gloves while in the vicinity of any sanding/grinding
----------------------------------	--	---	---	---	-----	--

AGSE-Launch Pad Functionality Risk Assessment						
Hazard	Cause/Mechanism	Outcome	Severity of Risk	Probability of Risk	Risk Level	Mitigation
Unstable launch platform	1. Unlevel ground	1. Unpredictable rocket path from launch	4	2	Low	1. It will be ensured that all personnel and individuals are at the minimum safe distance from the launch pad as established by the TRA and/or NAR. Prior to launch it will be ensured that the launch pad is stable and properly secured
Unlevel launch platform	1. Improperly leveled launch tower	1. Launch tower could tip during launch, making rocket flight path unpredictable	4	2	Low	1. Prior to launch, the launch tower will be tested on level ground to ensure that the launch tower is properly leveled
Rocket experiences high frictional forces on the launch rail and/or becomes stuck on launch rail	1. Improperly sized or flawed launch buttons on the rocket 2. Deflection or misalignment of launch rail	1. Rocket may not exit launch rail at correct velocity and/or may be damaged on launch 2. Rocket flight path may become unpredictable and/or rocket may not leave the launch rail	4	2	Low	1. Before attaching the rail buttons to the rocket they will be tested on the launch rail to ensure that they are properly sized and not flawed 2. Prior to launch the launch tower will be inspected to ensure proper fit. A spare portion of air frame will be tested with the launch rail to ensure that there is no undue friction between the launch rail and the rocket
Sharp edges on launch pad and/or rail	1. Manufacturing and fabrication	1. Minor cuts to personnel	4	2	Low	1. All sharp edges will be deburred and filed to reduce likelihood of cuts. When possible sharp edges will also be taped over

Brush fire during launch	1. Dry launch conditions	Small brush fire	3	4	Low	1. The range safety officer will determine if conditions are acceptable for launch. If a fire does occur the range safety officer will determine if and when personnel may approach the launch pad to extinguish the fire
Improper vehicle alignment	1. Incorrect loading of vehicle	1a. Payload may not be able to be inserted 1b. Vehicle instability 1c. Igniter can't install correctly	2	4	Low	1. A device has been constructed and added to the launch platform to ensure correct alignment of the rocket for payload retrieval. The motor retainer contains a bottom plate for proper alignment for the ignition and launch platform.

AGSE-Vehicle Erector Risk Assessment						
Hazard	Cause/Mechanism	Outcome	Severity of Risk	Probability of Risk	Risk Level	Mitigation
Sharp edges on the vehicle erector	1. Manufacturing and fabrication	1. Minor cuts to personnel	4	2	Low	1. Sharp edges of the vehicle erector will be filed down and deburred to reduce likelihood of cuts. When possible, sharp edges will also be taped over.
Carriage jams	1. Carriage tracks not square 2. Too much rail deflection under load 3. Uneven loading 4. Nylon guides dislodge 5. Buildup of foreign objects and debris (FOD) on tracks and/or carriage	1,2,3,4,5. Vehicle erector is incapable of raising the rocket. 2,3,4,5. May cause damage to rocket and/rocket components	2	3	Moderate	1. Tolerances of tracks will be noted during fabrication of the vehicle erector. 2. Deflection of the rail will be analyzed and corrected to be within the specified tolerances. 3. The geometry of the base was chosen for its ability to better distribute the load and reduce impact of uneven loading. 4. Appropriate fasteners and preload on installed fasteners will be in assembly process 5. Prior to launch and testing the tracks and carriage will be cleared of any debris and or buildup

AGSE-Ignition Installation Risk Assessment

Hazard	Cause/Mechanism	Outcome	Severity of Risk	Probability of Risk	Risk Level	Mitigation
Igniter is not fully installed inside the motor cavity	1. Igniter gets caught before installation 2. Initial misalignment of igniter causes it to miss the motor cavity.	1. Motor is not ignited.	2	3	Moderate	1,2. Igniter will be attached to a stiff object to ensure proper installation. Tests of installation system will be performed prior to competition
Motor Failure	1. Inconsistency in motor grain.	1. Catastrophic explosion resulting in major risk	1	4	Moderate	1. All motors will be purchased from reputable suppliers and inspected when possible.
Gear Mechanical Failure	1. Gear material failure	1. Igniter is not installed	2	3	Low	1. The use of high strength material will be used to ensure proper ignition installation.

AGSE-Ground Station Risk Assessment						
Hazard	Cause/Mechanism	Outcome	Severity of Risk	Probability of Risk	Risk Level	Mitigation
Sharp edges on tip of rail.	1. Manufacturing of the rail	1. Cuts of team members may occur.	4	2	Low	1. Sharp edges will be filed/sanded down.
Worm and gear system fails to lift rocket	1. System does not output enough torque.	1. Rocket does not reach 5 degrees from vertical	2	3	Moderate	1. Tests and calculations will confirm that the worm and gear system will lift our rocket properly.

AGSE-Payload Retrieval Arm Risk Assessment						
Hazard	Cause/Mechanism	Outcome	Severity of Risk	Probability of Risk	Risk Level	Mitigation
System Failure	1. Code does not work properly. 2. Servos	1,2. Arm fails to retrieve and place the payload in the rocket.	2	3	Moderate	1. Tests will be run to test all code and its operational ability 2. All servos will be tested to ensure they are in proper working order. All servos must deliver the

	aren't responsive.					required torque and will be tested accordingly
Robotic arm unable to pick up payload	1. Servos don't provide enough torque.	1. Arm fails retrieve and place the payload in the rocket.	2	3	Mode rate	1. Metal gear servos will be used to provide the required torque.
Robotic gripper unable to pick up payload	1. Coefficient of friction is too small. 2. Servo doesn't have the required torque to hold gripper closed.	1. Payload is not loaded into the rocket.	2	4	Low	1. Will use liquid rubber to coat the gripper appendages. 2. Will use karbonite gear servos to ensure a secure clasp on the payload.
Robotic arm drops payload in a random place	1. System failure 2. Loss of power 3. Failure of the servos	1. Challenge may not be completed in under 10 minutes. 2. Vision system may not be able to locate payload again.	2	3	Mode rate	1. Ensure that our robot can pick up the payload in under 20-30 seconds. We will also ensure that the gripping force is great enough to prevent the load from slipping out of the robot's grasp. 2. Ensure that the vision system is placed near the front of the robot so that it can sense where they payload will be in any direction.

Control Risk Assessment						
Hazard	Cause/Mechanism	Outcome	Severity of Risk	Probability of Risk	Risk Level	Mitigation
Pause function fails to activate	1. Mechanical failure in switch 2. Communication failure between switch and controller 3. Code error	1. Damage to AGSE. 2. Injury to personnel near AGSE.	2	3	Mode rate	1. All personnel are required to stand a specified distance away from the AGSE while it is operating. 2. Redundancies will be implemented to ensure pause function will perform properly. 2,3. All codes, systems and functions will be tested as it is written in addition to being tested and checked for errors prior to the competition
Pause function	1. Mechanical failure in switch	1. AGSE mission failure	2	3	Mode rate	1. Redundancies will be implemented to ensure pause function will perform properly.

fails to deactivate	2. Communication failure between switch and controller 3. Code error				High	2,3. All codes, systems and functions will be tested as it is written in addition to being tested and checked for errors prior to the competition
Boot function fails to activate	1. Mechanical failure in switch 2. Communication failure between switch and controller 3. Code error	1. AGSE mission failure	2	3	Mode rate	1. Redundancies will be implemented to ensure boot function will perform properly. 2,3. All codes, systems and functions will be tested as it is written in addition to being tested and checked for errors prior to the competition
Boot function activated at power up	1. Mechanical failure in switch 2. Communication failure between switch and controller 3. Code error	1. Unpredictable boot sequence	2	3	Mode rate	1. Redundancies will be implemented to ensure boot function will perform properly. 2. Reminder that boot function is disabled before powering on the AGSE will be included in pre-launch procedure list. 3. The code will be tested as it is written in addition to being tested and checked for errors prior to the competition
Failure to start and/or boot up	1. Error in code 2. No power or lose in power	1. AGSE mission failure.	2	4	Low	1. Testing will be done to ensure power is properly connected for the AGSE controllers.

Stability and Propulsion Risk Assessment						
Hazard	Cause/Mechanism	Outcome	Severity of Risk	Probability of Risk	Risk Level	Mitigation
Motor ignition failure	1. Damaged motor 2. Ignition delayed 3. Faulty e-match	1,3. Rocket unable to launch 2. Rocket fires at an unexpected time	1	3	Mode rate	1. Follow TRA safety code and wait a minimum of 60 seconds before approaching the rocket to ensure that the motor is not just delayed in launching. 2. If there is no activity after 60 seconds, the safety officer will check the ignition system for a lost connection or a bad igniter.

						3. In the event of a faulty ematch, the safety officer or project lead will remove the ignition system from the rocket motor, retrieve the motor from the launch pad and replace the motor with a spare.
Motor explodes upon ignition on the launch pad	1. Failure in the manufacturing of the motor.	1. Severely damaged or complete loss of rocket	1	4	Mode rate	1. Assure that all team members are a safe distance away from the launch pad upon ignition of the rocket. Wait a specified amount of time before approaching the pad after a catastrophe. All fires will be extinguished when it is safe to approach the pad.
Optimum velocity is not reached upon leaving the launch rail	1. Rocket has too much mass 2. Motor impulse is too low 3. Friction built up between rocket and launch rail	1,2,3. Unstable launch and may result in unpredictable flight path	2	3	Mode rate	1. Simulations have been run to confirm that the necessary velocity can be achieved by the motor selected. 2. Motor has been selected based on simulation data to meet lift off and flight requirements. 3. Prior to installation and launch, the launch buttons will be tested for fitting on the launch rail.
Internal bulkheads fail during ascent/flight	1. Forces during ascent are too much for the bulkheads to withstand	1. Components inside the rocket being held by the bulkheads will no longer be secure and could cause an anomaly 2. Parachutes attached to bulkheads will be left ineffective. 3. Rocket may pose a threat individuals at the field	1	4	Mode rate	1. All bulkheads will be secured with high strength 30 minute epoxy. 2. Bulkheads that have parachutes attached will have extra epoxy around eyebolts to ensure the bulkhead and eyebolts are secure within the rocket. 3. In the event that the rocket may pose a threat to any individual, all individuals at the launch will be notified immediately
Alignment of fins is not optimized	1. Geometry of mounted fins are not straight or not equally	1. Rocket becomes unstable or spins	2	2	Mode rate	1. All fin slots will have a specified tolerance that will devastate the rocket after launch.

	spaced around					
Fins fracture and/or shear off during flight	1. Epoxy fillets are not properly applied to edges of fins	1. Rocket flies in an unpredictable path 2. Fins fall completely off. 3. Rocket and or components pose a hazard to those at the launch field	1	4	Mode rate	2. Carbon fiber stands are mixed in with the epoxy fillets to increase the shear strength of the epoxy fillets along the fins. 1,2. Mentor, project lead, and safety officer will examine all epoxy fillets to ensure there are no cracks or deficiencies both during fabrication and after. 3. In the event that the rocket poses a hazard to any individual at the launch all individuals will be notified immediately
Motor Retainer Failure (falls off)	1. Improper preload or thread engagements	1. Motor and its casing release from rocket upon parachute deployment	1	4	Mode rate	1. Tests will be done to ensure proper motor retainment. Analysis will be done to ensure the current design is stable enough under the forces in flight.

Recovery and Recovery Systems Risk Assessment						
Hazard	Cause/Mechanism	Outcome	Severity of Risk	Probability of Risk	Risk Level	Mitigation
Separation of rocket at apogee and/or 500ft does not occur	1. Not enough pressurization to break shear pins 2. Coupling fit too tight	1,2. Rocket becomes ballistic	1	3	Mode rate	1. Separation sections of rocket will be designed to ensure that the black powder charges provide enough force to cause the pins to shear. Ground test will be done to ensure the correct amount of black powder is used 2. Couplings between components will be sanded to prevent components from sticking together. Fittings will be tested prior to launch to ensure that no components are sticking together In the event that the rocket does become ballistic, all individuals at the launch field will be notified immediately
Parachute does not deploy	1. Parachute is stuck in body tube	1, 2. Rocket becomes ballistic	1	3	Mode rate	1,2. The packing of each parachute will be checked by our mentor prior to launch to ensure proper packing. In addition the parachute

	2. Parachute lines are tangled					<p>size has been selected to fit within the body tube but not so tightly as to become stuck due to the size of the parachute.</p> <p>In the event that the rocket does become ballistic, all individuals at the launch field will be notified immediately</p>
Altimeter and/or e-match failure	1. Parachute does not deploy	1. Parachute becomes ballistic	1	4	Mode rate	<p>1. We will have a redundancy by including two altimeters each with their own e-matches and black powder charges, wired in series.</p> <p>In the event that the rocket does become ballistic, all individuals at the launch field will be notified immediately</p>
Rocket descent is too rapid despite parachute deployment	1. Parachute is not properly sized	1. Rocket poses hazard to those at launch field 2. Rocket and/or component parts are damaged in landing	2	4	Low	<p>1. In the event that the rocket is descending too quickly and may pose a hazard to those at the field, all individuals will be notified immediately.</p> <p>2. The parachutes have been selected according to load capacity size and coefficient of drag of the parachute. In addition several simulations were run to ensure the correct sizing of the parachute and descent of the rocket.</p>
Rocket descent is too slow	1. Parachute is improperly sized	1. Rocket may drift beyond desired range, and may damage surroundings or become unreachable	2	3	Mode rate	<p>1. Each parachute has been selected to fall within the desired coefficient of drag to prevent too great of a drift. Simulations were performed to ensure that the rocket does not descend too slowly with the chosen parachutes. In the event that the rocket does drift to prevent loss of the rocket it will be tracked both visually and by GPS.</p>
Parachute is torn or ripped	1. Parachute is less if not completely ineffective in controlling rocket descent	1a. Rocket may damage environment 1b. Rocket and/or components may become damaged upon landing 1c. rocket may pose a hazard	2	4	Low	<p>1. Prior to launch and packing, each parachute will be checked for tears or rips. In addition we will bring backup parachutes to replace any torn parachute.</p> <p>1c. In the event that the rocket does pose a hazard to individuals at the field, all individuals will be notified immediately.</p>

		to individuals at the field				
Parachute and/or cord is burnt	1. Parachute becomes less or entirely ineffective	1a. Rocket may damage environment 1b. Rocket and/or components may become damaged upon landing 1c. Rocket may pose a hazard to individuals at the field	2	3	Mode rate	1. To prevent damage to the cords and parachutes from black powder charges, rocket recovery wadding will be packed into the spaces containing the parachutes and cords. Each parachute will be packed in Nomex to aid in burn prevention. In the event that the parachutes separate from any rocket component, all individuals at the field will be notified immediately.
Parachutes separate from one or more rocket components	1. Bulkhead is dislodged 2. Parachute disconnect from eyebolt 3. Eyebolts shear through bulkhead	1,2,3. One or more components of the rocket become ballistic	1	4	Mode rate	1. Bulkheads will be secured by 30 minute epoxy and inspected by the mentor, project lead, and safety officer 2. Prior to launch the connection of the parachute to the eyebolts will be inspected by the mentor, project lead, and safety officer 3. Eyebolts will be epoxied to the bulkheads. In addition the bulkheads have been chosen to be baltic birch to meet shear and strength requirements. In the event that the rocket becomes ballistic all individuals at the field will be notified immediately.

Vehicle Assembly Risk Assessment						
Hazard	Cause/Mechanism	Outcome	Severity of Risk	Probability of Risk	Risk Level	Mitigation
Dropping of rocket	1. Mishandling of rocket in transit	1. Minimal damage to rocket components	3	4	Low	1. Careful handling will be executed while transporting the rocket. The rocket has been designed to withstand flight and landing conditions.

Environmental Hazards Assessment

Hazard	Cause/Mechanism	Outcome	Severity of Risk	Probability of Risk	Risk Level	Mitigation
Strong winds and/or rain	1. Disruption of rocket stability both on the platform and in flight	1a. rocket path may become unpredictable 1b. rocket may become damaged 1c. rocket may pose a hazard to those at the launch 1d. rocket systems may be damaged	2	2	Medium	1. If the winds are greater than 5 mph then the rocket will not be launched. If there is any rain then the rocket will not be launched. Weather conditions will be checked the day before and the morning of the launch Ultimately, the range safety officer of the field will determine whether conditions are acceptable for launch
Harmful substances contaminating water and/or ground	1. Improper disposal of batteries and/or chemicals	1. Reversible to irreversible damage to local environment	2	4	Low	1. All batteries and chemicals will be disposed of according to the associated MSDS. In the event of an accidental chemical spill then members are to follow the regulations of EHS for the given chemical spill.
Brush fire	1. Flames from ignition	1. reversible damage to local environment	2	4	Low	1. All required fire hazard equipment will be brought to the launch. The blast plate will be sized to minimize the risk of fire hazard. In the event of a fire the range safety officer will be to determine if the fire is small enough to be put out without the need of emergency service. All members will wait until signal from the range safety officer to approach the region in which the fire occurred.